

**An-Najah National University**  
**Faculty of Graduates Studies**

**The Effect of Various Patterns of Internal  
Partitions on the Fundamental Period of  
Reinforced Concrete Framed Buildings -  
Experimental and FE Modelling Study**

**By**

**Ola Mohsen Qarout**

**Supervisor**

**Dr. Monther Dwaikat**

**Co- Supervisor**

**Dr. Mahmoud Dwaikat**

**This Thesis is Submitted in Partial Fulfillment of the Requirements for  
the Degree of Master of Construction Engineering, Faculty of Graduate  
Studies, An-Najah National University, Nablus, Palestine.**

**2018**

**The Effect of Various Patterns of Internal Partitions  
on the Fundamental Period of Reinforced Concrete  
Framed Buildings -Experimental and FE Modelling  
Study**

**By**

**Ola Mohsen Qarout**

**This Thesis was defended successfully on 20/9/2018 and approved by**

**Defense Committee Members**

**Signature**

- |  |       |
|--|-------|
| <b>– Dr. Monther Dwaikat /Supervisor</b>         | ..... |
| <b>– Dr. Mahmoud Dwaikat / Co-Supervisor</b>     | ..... |
| <b>– Dr. Bilal Al-Masri / External Examiner</b>  | ..... |
| <b>– Dr. Mohamad Samaneh / Internal Examiner</b> | ..... |

III

**Dedication**

*I dedicate this success to everyone who paved my way*

*To the one who never tired of encouraging me, my  
beloved*

*husband*

*I dedicate most of my success to my children*

*I am thankful to my beloved family*

*I send my happy wishes to all my friends and whoever  
supported me*

## **Acknowledgment**

*Praise be to Allah, Lord of the World's, first of all*

*I would like to thank whoever participated in this effort*

*Many thanks and regards to Dr. Monther Dwaikat for his magnificent efforts in completing this work.*

*I would like to thank Dr. Mahmoud Dwaikat for his grand helpful supervision to finish this work.*

*Thanks to Dr. Mohamad Samanneh and Eng. Yazan Abu Thahnat for their great efforts and their special assistance.*

*I would like to thank the staff of the Building Materials Laboratory, represented by Eng. Sameer Halawa.*

*I really appreciate the faculty of Civil Engineering.*

*Finally, special thanks to my great university - An Najah National University*

## الإقرار

أنا الموقعة أدناه مقدمة الأطروحة التي تحمل عنوان:

# **The Effect of Various Patterns of Internal Partitions on the Fundamental Period of Reinforced Concrete Framed Buildings -Experimental and FE Modelling Study**

أقر بأن ما اشتملت عليه هذه الرسالة إنما هو نتاج جهدي الخاص, باستثناء ما تمت الإشارة إليه حيثما ورد, وأن هذه الرسالة ككل أو جزء منها لم يقدم من قبل لنيل أية درجة أو بحث علمي أو بحثي لدى أية مؤسسة تعليمية أو بحثية أخرى

## Declaration

**The work provided in this thesis, unless otherwise referenced, is the researcher's own work, and has not been submitted elsewhere for any other degree or qualification.**

**Student's name:**

اسم الطالبة : علا محسن قاروط

**Signature:**

التوقيع:

**Date**

التاريخ:

## Table of contents

Dedication .....	III
Acknowledgment .....	IV
Declaration .....	V
Table of contents .....	VI
Table of Figures .....	IX
Abstract .....	XVI
Chapter 1 Introduction.....	1
1.1 Overview .....	1
1.2 Problem Statement .....	3
1.2.1 Modelling of Brick Infill Wall.....	3
1.2.2 Parameters Affecting the Fundamental Period.....	5
1.3 Scope of the research .....	6
1.4 Research objectives.....	7
Chapter 2 Literature Review .....	9
2.1 Overview .....	9
2.2 Fundamental Period .....	10
2.3 RC frames with Infill Wall .....	18
2.4 Brick wall types and modeling .....	19
2.4.1 Brick wall types .....	19
2.4.2 Brick wall modelling .....	21
Chapter 3 Experimental Tests .....	28
3.1 General .....	28
3.2 Tested Specimens.....	28
3.3 Test Procedure.....	31
3.4 Tests Results .....	34
3.4.1 Results of brick tests .....	35
3.4.2 Mortar tests .....	37

3.4.3 Shear test.....	39
3.5 Summary .....	40
Chapter 4 Micro Modeling of Brick Wall.....	42
4.1 Overview .....	42
4.1.1 Definition of material.....	43
4.1.2 Model Geometry .....	56
4.1.3 Modeling of interfaces .....	58
4.1.4 Parameters for cohesive contact .....	59
4.1.5 Analysis type, loading and boundary conditions.....	61
4.2 Model verification.....	64
4.2.1 Overview.....	64
4.2.2 Methodology of calculating bare frame stiffness .....	67
4.2.3 Methodology of calculating the brick wall stiffness .....	72
4.3 Parametric studies .....	75
4.3.1 General.....	75
4.3.2 Parameters ranges .....	76
Chapter 5 Results of Micro Modeling and Discussion .....	78
5.1 General .....	78
5.2 Behavior of models .....	78
5.2.1 Effect of wall length .....	78
5.2.2 Effect of column size .....	80
5.2.3 Effect of brick wall .....	82
5.3 The end of linearity .....	87
5.4 Results and discussion .....	92
Equivalent strut model: .....	93
5.5 Verification of the results.....	101
Chapter 6 Macro Modeling and Results.....	104
6.1 General .....	104

VIII

6.2 Model description .....	104
6.2.1 Materials and sections.....	107
6.2.2 Loads and boundary conditions .....	110
6.2.3 Validation of the model .....	111
6.3 Parametric study.....	117
6.4 Final results and verification.....	119
6.4.1 Final results.....	119
6.4.2 Verification .....	120
6.6 Modification to Rayleigh method .....	127
Chapter 7 Conclusions and Recommendations .....	133
7.1 Overview .....	133
7.2 Conclusions .....	133
7.3 Proposed equations .....	134
7.4 Recommendations and Future studies .....	137
References .....	138
Appendix A .....	145
المخلص .....	ب

## Table of figures

<b>Figure (3. 1):</b> The brick specimens used in the experimental test of this thesis .....	30
<b>Figure (3. 2):</b> A mortar specimen used in the experimental test of this thesis .....	30
<b>Figure (3. 3):</b> The connected bricks which were used for the shear test ...	31
<b>Figure (3. 4):</b> MTS machine used for brick and mortar tests.....	33
<b>Figure (3. 5):</b> The shear test of a specimen of mortar-connected two bricks using the Tile Testing Machine .....	34
<b>Figure (3. 6):</b> The stress-strain curve and modulus of elasticity of the first specimen.....	<b>Error! Bookmark not defined.</b>
<b>Figure (3. 7):</b> The stress-strain curve and modulus of elasticity of the second specimen.....	35
<b>Figure (3. 8):</b> The stress-strain curve and modulus of elasticity of the third specimen.....	36
<b>Figure (3. 9):</b> The stress-strain curve and modulus of elasticity of the fourth specimen.....	36
<b>Figure (3. 10):</b> The stress-strain curve and modulus of elasticity of the first specimen.....	38
<b>Figure (3. 11):</b> The stress-strain curve and modulus of elasticity of the second specimen .....	38
<b>Figure (3. 12):</b> Load-slip curve obtained from the experimental shear test .....	39
<b>Figure (3. 13):</b> Failure of the specimen during the shear test .....	40
<b>Figure (4. 1):</b> Response of concrete to uniaxial loading in (a) compression and (b) tension (ABAQUS User Manual, 2013) .....	44
<b>Figure (4. 2):</b> Yield surface in plane stress (ABAQUS User Manual, 2013) .....	46

<b>Figure (4. 3):</b> Dilatation angle and eccentricity (ABAQUS User Manual, 2013). .....	50
<b>Figure (4. 4):</b> Deviatoric cross section of failure surface (ABAQUS User Manual, 2013) .....	51
<b>Figure (4. 5):</b> Curves needed to define CDP model in ABAQUS for testing by Clyde et al. (2000).....	52
<b>Figure (4. 6):</b> Uniaxial load cycle (tension-compression-tension), assuming the default values for the stiffness recovery factors as $\omega_t = 0$ and $\omega_c = 1$ (ABAQUS User Manual, 2013).....	53
<b>Figure (4. 7):</b> Typical stress-strain curve of steel .....	54
<b>Figure (4. 8):</b> Yield stress Vs. inelastic strain for brick material.....	55
<b>Figure (4. 9):</b> Yield stress Vs. inelastic strain for mortar material .....	56
<b>Figure (4. 10):</b> 3-D model of a frame without brick wall (bare frame) .....	57
<b>Figure (4. 11):</b> 3-D frame with a brick wall.....	58
<b>Figure (4. 12):</b> Force-slip curve obtained from analyzing ABAQUS model, and from experimental test .....	60
<b>Figure (4. 13):</b> Model of the shear test in ABAQUS for two bricks connected with mortar .....	61
<b>Figure (4. 14):</b> Finite element mesh types used for modeling the frames .	63
<b>Figure (4. 15):</b> Load-deflection curves for several type of meshes, as used for the sensitivity study .....	63
<b>Figure (4. 16):</b> The bare frame of model (W5 C50) that is used for verification by the virtual work method, as appears in SAP2000 .....	68
<b>Figure (4. 17):</b> Virtual shear and moment diagrams of the beam in the bare frame of model (W5 C50) used for verification by the virtual work method, as obtained from SAP2000 .....	68

**Figure (4. 18):** Virtual shear and moment diagrams for the right column in the bare frame of model (W5 C50) used for verification by the virtual work method, as obtained from SAP2000 .....69

**Figure (4. 19):** Virtual shear and moment diagrams for the left column in the bare frame of model (W5 C50) used for verification by the virtual work method, as obtained from SAP2000 .....70

**Figure (4. 20):** Virtual axial force diagram for the bare frame of model (W5 C50) used for verification by the virtual work method, as obtained from SAP2000.....71

**Figure (5. 1):** Load-deflection curves of three frame models, all having (0.3x0.3) columns cross sections, with three different wall lengths, as obtained from ABAQUS .....79

**Figure (5. 2):** Load-deflection curves of three frame models, all having (0.5x0.5) columns cross sections, with three different wall lengths, as obtained from ABAQUS .....79

**Figure (5. 3):** Load-deflection curves of three frame models, all having (0.75x0.75) columns cross sections, with three different wall lengths, as obtained from ABAQUS .....80

**Figure (5. 4):** Load-deflection curves of three frame models, all having 4m long brick walls, with three different column cross sections, as obtained from ABAQUS .....81

**Figure (5. 5):** Load-deflection curves of three frame models, all having 5m long brick walls, with three different column cross sections, as obtained from ABAQUS .....81

**Figure (5. 6):** Load-deflection curves of three frame models, all having 7m long brick walls, with three different column cross sections, as obtained from ABAQUS .....82

<b>Figure (5. 7):</b> Load-deflection curves for frame W4 C30 with and without bricks, as obtained from ABAQUS .....	83
<b>Figure (5. 8):</b> Load- deflection curves for frame W5 C30 with and without bricks, as obtained from ABAQUS .....	83
<b>Figure (5. 9):</b> Load- deflection curves for frame W7 C30 with and without bricks, as obtained from ABAQUS .....	84
<b>Figure (5. 10):</b> Load- deflection curves for frame W4 C50 with and without bricks, as obtained from ABAQUS .....	84
<b>Figure (5. 11):</b> Load- deflection curves for frame W5 C50 with and without bricks, as obtained from ABAQUS .....	85
<b>Figure (5. 12):</b> Load - deflection curves for frame W7 C50 with and without bricks, as obtained from ABAQUS .....	85
<b>Figure (5. 13):</b> Load- deflection curves for frame W4 C75 with and without bricks, as obtained from ABAQUS .....	86
<b>Figure (5. 14):</b> Load- deflection curves for frame W5 C75 with and without bricks, as obtained from ABAQUS .....	86
<b>Figure (5. 15):</b> Load- deflection curves for frame W7 C75 with and without bricks, as obtained from ABAQUS .....	87
<b>Figure (5. 16):</b> Tensile stress distribution in frame W4 C50, as obtained from ABAQUS .....	89
<b>Figure (5. 17):</b> Horizontal displacement contour for brick wall W4 C30, as obtained from ABAQUS .....	90
<b>Figure (5. 18):</b> First yield occurred in frame W4 C30, as obtained from ABAQUS .....	91
<b>Figure (5. 19):</b> Simple representation of a frame with a brick-wall-equivalent strut.....	93
<b>Figure (5. 20):</b> Error distribution with respect to column size ( $A_c$ ) for the bilinear equation.....	98

<b>Figure (5. 21):</b> Error distribution with respect to wall length (L) for the bilinear equation.....	99
<b>Figure (5. 22):</b> Error distribution with respect to column size ( $A_c$ ) for the linear equation.....	100
<b>Figure (5. 23):</b> Error distribution with respect to wall length (L) for the linear equation.....	100
<b>Figure (6. 1):</b> SAP2000 Model of the RC framed structure, prepared for macro modeling analysis .....	105
<b>Figure (6. 2):</b> Plan of the RC frames structure showing the different partitions dimensions .....	106
<b>Figure (6. 3):</b> Section in a slab showing some components of the super imposed dead load .....	110
<b>Figure (6. 4):</b> Deformed shape of the structure showing compatibility of the structure, as taken from SAP2000 .....	112
<b>Figure (6. 5):</b> MS and CS Definition .....	114
<b>Figure (6. 6):</b> Fitting of the fundamental period values in cases of variation in the amount of partitions .....	125
<b>Figure (6. 7):</b> Error distribution that results from using the proposed equation of determining the fundamental period of partitioned structure (Equation (6.5)).....	126

## List of Table

<b>Table (3. 1):</b> Brick requirements according to the Palestinian specification .....	29
<b>Table (3. 2):</b> Dimensions and properties of the first specimen of mortar ..	30
<b>Table (3. 3):</b> The moduli of elasticity values for all brick specimens as obtained from tests .....	37
<b>Table (3. 4):</b> Properties of the first and second mortar specimens.....	37
<b>Table (4. 1):</b> Geometric characteristics and loads for all models .....	76
 <b>Table (5. 1):</b> Stiffness values for all models, obtained by means of ABAQUS .....	 92
<b>Table (5. 2):</b> Equivalent strut width values for all models.....	95
<b>Table (5. 3):</b> List of the models data used to fit the equivalent strut dimensions equation.....	97
<b>Table (5. 4):</b> Characteristics of the verified models and equivalent strut, with their stiffness values.....	101
<b>Table (6. 1):</b> General properties of the RC framed structure used in macro modeling.....	105
<b>Table (6. 2):</b> Properties of the struts used in the RC framed structure.....	108
<b>Table (6. 3):</b> Dead loads calculation both by hand and by SAP2000 .....	113
<b>Table (6. 4):</b> Live loads and superimposed dead loads calculations both by hand and by SAP2000.....	113
<b>Table (6. 5):</b> Model types used in the parametric study.....	118
<b>Table (6. 6):</b> Seismic dead load of stories for the frame taken from Model type (1), and used for time period verification .....	121
<b>Table (6. 7):</b> Values of the terms used in Rayleigh method to compute time periods.....	122
<b>Table (A. 1):</b> Fundamental period, in Y-direction, for Model type (1) ...	145

<b>Table (A. 2):</b> Fundamental period, in X-direction, for Model type (1) ...	150
<b>Table (A. 3):</b> Fundamental period of the structure, in each X and Y-directions, for Model type (2) .....	157
<b>Table (A. 4):</b> Fundamental period of the structure, in each X and Y-directions, for Model type (3) .....	158
<b>Table (A. 5):</b> Fundamental period of the structure in Y-direction for Model type (4) .....	158

**The Effect of Various Patterns of Partitions on the Fundamental  
Period of RC Framed Structure**

**By**

**Ola Mohsen Qarout**

**Supervisor**

**Dr. Monther Dwaikat**

**Co- Supervisor**

**Dr. Mahmoud Dwaikat**

**Abstract**

Reinforced concrete (RC) with infill wall partitions are common structures in Palestine. The presence of infill walls can definitely influence the seismic behavior of the structure, as they contribute to the total mass and stiffness of the structure. Specifically, the fundamental period of the structure, which depends mainly on the stiffness and mass of the structure, can be influenced by the existence of brick walls.

Several models were proposed by different researchers to predict the seismic behavior of infill wall structures, and also to study their effect on the fundamental period of the whole structure. However, one obvious shortcoming of these models is that their properties do not match those of the brick walls commonly used in Palestine. Therefore, this thesis involves a study to predict the stiffness of brick walls used in Palestine based on 3-D nonlinear F.E. analysis. Some needed parameters in this modeling are taken from experimental tests which were conducted as a part of the work of this thesis. The results of this study were used to develop strut models equivalent to real brick walls. This, in turn, would facilitate modeling and analysis of buildings by using struts as substitutes to brick wall partitions. After that, the effect of these partitions on the fundamental period of the structure was

studied. For this goal, macro modeling of RC framed structure was carried out with several patterns of partitions. The results of this study were simplified into two simple, reasonable and practical equations. One of these equations is used for predicting the equivalent strut width as a function of wall length and the column size of the surrounding frame. The other equation is used for predicting the fundamental period of the structure with infill wall partition as a function of the density of partitions distribution in the structure.

# Chapter 1

## Introduction

### 1.1 Overview

Reinforced concrete (R.C.) frames with brick infill walls are common elements of structures in Palestine, and all over the world. Brick infill walls are generally designed as nonstructural elements. The seismic behavior of such elements is ignored including their expected effect on stiffness and fundamental period of framed structure (Holmes 1961). It should be noted that the fundamental period of a structure significantly affects its seismic behavior (Chopra 2012). In general, the fundamental period of building can be evaluated using two approaches, namely; theoretical and empirical approaches. Several empirical formulae are proposed to estimate the fundamental periods of all kinds of structures by many seismic design codes all over the world. For instance, ATC-3 and FEMA450 adopt empirical formulae of the fundamental period derived from seismic response records. In these codes, the empirical formulae are mainly obtained based on the measurements of 1971 San Fernando seismic response records. Goel and Chopra (2012) provided empirical formulae of the fundamental periods for shear wall and moment-resisting frame buildings based on the buildings' earthquake response data in several earthquakes. Their formulae provide better agreement with the fundamental period measured from building motion during earthquake compared to those adopted in codes.

In addition to the empirical formula of fundamental period, there are different approaches can be used to investigate the behavior of structures including analytical, experimental, and numerical approaches. Analytical approaches provide accurate results but usually tend to be complex to the extent that, in some complicated problems, they can no more be followed. Experimental approaches, on the other side, provide more proper visualizations of problems. However, experiments are expensive, and need high technical lab facilities. Numerical approach provides attractive solution for solving structural problems. The FE method adapts great visualization, and proper accuracy of predicting structural behavior. ABAQUS computer program is one of the professional FE software that has many material models needed to provide acceptable agreement with real behavior of structures (ABAQUS user manual (2013)).

In this research, three-dimensional (3-D) nonlinear FE approach using the commercial software ABAQUS is used to predict the structural behavior of brick infill walls under the effect of lateral load. This simulates the behavior of brick walls and overall structural behavior under seismic lateral loads.

The model is used to predict the additional stiffness from bricks to the overall RC frame. Results are used to construct a 3-D frame linear model using the structural analysis software SAP2000 to evaluate effect of stiffness on fundamental period of buildings. The effect of different parameters such as, frame span length, and size of columns are investigated.

## **1.2 Problem Statement**

Brick infill walls are used in RC structures. Generally, traditional design ignores the influence of partition walls on the overall stiffness and the fundamental period of buildings. The literature review (Chapter 2), showed limited published research that identifies and quantifies effect of such walls on the response of structures to lateral seismic loads. However, the availability of such research is more locally oriented because it considers brick properties specific to the countries where research was conducted. These properties hardly match those of the bricks commonly used in Palestine. For this reason and for the insufficient knowledge exhibited by previous research regarding the effect of interior partitions on the fundamental period of structures, this thesis undertakes a research that addresses these issues, reaching finally to some useful recommendations by which current and future engineers can be guided.

### **1.2.1 Modelling of Brick Infill Wall**

Brick walls are generally composed of solid bricks (blocks) or hollow ones. Solid brick wall partition is constructed as reinforced bricks, plain bricks or nogged bricks. Hollow bricks are molded from clay, terracotta or concrete (Juan Rodriguez 2017). They are commonly used for the construction of partition walls. Such walls are rigid, light, strong, economical and provide fire resistant. In addition, walls have good sound insulating properties. The thickness of this type of partition wall varies between 6 cm to 20 cm. These walls are constructed in a similar manner as structural load bearing walls.

Hollow brick walls are much more common in Palestine and are the focus of this research.

Due to the importance of infill wall modeling, various analytical methods have been proposed to evaluate the seismic performance of masonry infill in framed structures. These methods ranged from classical replacement of the infill with a single strut or multi-strut diagonal, to modern computational techniques (Holmes (1961), Smith and Carter (1969) and Mainstone (1971)). Such techniques can be used for block infill walls. However, these approaches focused on solid brick infill walls and may not be suitable for hollow brick infill walls which are the most common in Palestine. In our study, nonlinear FE model (micro-modeling) is used to evaluate stiffness properties of frames with and without bricks. Then, the results are used as an equivalent strut model (macro-modeling) to study the effect of brick stiffness on building fundamental period. The reason for preferring macro-modeling to micro-modeling in the second case despite the high accuracy of micro-modeling, is that micro-modeling is much more complex, and it requires very long completion time. These restrictions limit the ability of using a complete building micro-model. This micro-modeling can provide an accurate computational representation of both geometrical and material nonlinearities. At the same time, macro-modeling has computational simplicity and can make use of the simple material properties. However, infill material is heterogeneous and it is difficult to predict the distribution of material properties of its constituent elements. Therefore, both micro and macro modeling are employed to obtain strut and tie properties which is be

used as a representative element of the infill wall in the structure. These properties are employed to analyze a framed structure of several partitions in order to study the effect of infill partitions on the fundamental period of the structure.

### **1.2.2 Parameters Affecting the Fundamental Period**

Natural period ( $T_n$ ) is defined as the time taken by un-damped system to complete one cycle during free vibration (Chopra 2012). The fundamental period of the structure is influenced by many factors, such as: building height, number of bays, area of shear walls, the amount of infill panels and type of frame. The fundamental period depends mainly on the distribution of mass and rigidity of the structure. The presence of non-structural elements may affect the distribution of mass and rigidity of the structure. Many of code formulae focus on the mass and rigidity of the structure to determine the fundamental period. Therefore, the presence of infill wall should be carefully considered.

Each of the mentioned parameters has an influence on the actual value of the fundamental period of a building. It should be noted that some of these parameters have more effect than the others. Frame span length and size of column (stiffness) are among the main factors that differs in the structures in this research. These factors are studied to illustrate their effect on the fundamental period.

### **1.3 Scope of the research**

According to various design codes, the presence of non-structural elements should be properly considered in the seismic design of structures (IBC 2006). However, limited published models properly represent the hollow brick infill walls, whereas no models are found related to the common bricks in Palestine (Paulay and Priestley 1992, Al-Dakhakhni et al. 2003 and Mediawati 2016). Therefore, the main focus of this research is to investigate the effect of several patterns of interior infill wall partitions on the fundamental period of framed buildings. Three-dimensional (3-D) non-linear finite element (F.E.) models are built using the commercial software, ABAQUS. To obtain the material properties of bricks, mortar and bond, test were done using universal compressive testing machines( MTS machine and Tiles Testing Machine). The models are used to conduct parametric study to investigate the effect of the main parameters that affect the stiffness of the brick wall. Afterwards, macro-modeling of a framed structure is conducted to study the influence of partitioning on the fundamental period.

Due to time limitations: the scope of this research is limited to interior brick wall. Also, the analysis of the fundamental period is conducted for a typical moment resisting frame (MRF). The level of details for the brick wall models and partitions is assumed to be consistent and typical to common frames used in Palestine.

## 1.4 Research objectives

The main objective of this study is to quantify the effect of several patterns of brick wall partitions on the fundamental period of R.C. framed structures. To achieve this main objective, the following tasks are performed:

- 1- Testing mechanical properties of different samples of mortar and bricks used for the interior partitions to obtain the constitutive relationships needed for modeling. This task is explained in details in the methodology chapter, the experimental tests section.
- 2- Developing a 3-D non-linear F.E. models for the typical brick wall. The commercial (F.E.) software (ABAQUS) is used to create a general parametric frame model with and without brick wall. The models include material and geometrical nonlinearities. The interaction properties between brick and mortar are calibrated to fit the experimental test. The modeling process and related assumptions are explained in details in the chapter of micro-modeling of brick wall.
- 3- Correlating the results obtained from the F.E. micro models into a usable equation. This equation is used to predict the dimensions of the strut representing the brick wall in a macro-modeling process.
- 4- Conducting parametric study. Developing a 3-D linear macro model for (MRF) with several cases of interior partitions and characteristics obtained from the brick wall modeling to study the effect of these cases on the fundamental period of the structure.

- 5- Correlating the results obtained from the macro frame model into a simple equation to predict the fundamental period of the framed structure, in terms of the intensity of brick wall partitions in this structure.
- 6- Summarizing the results and drawing conclusions and recommendations for engineers.

## Chapter 2

### Literature Review

#### 2.1 Overview

In the perspective of structural engineers, infill walls are considered nonstructural elements, and thereby their effects on the seismic performance of buildings and on their fundamental periods are usually underestimated (Smith and Carter 1969). Therefore, imprecise estimations may influence the strength, ductility and lateral stiffness of buildings. For this reason, a great attention should be paid to the influence of infill walls on the structural behavior of structures.

Studying the structural effects of infill wall brought many researchers to propose models, such as diagonal struts, whose behavior and characteristics are equivalent to the real infill walls (Smith 1967, Smith and Carter 1969 and Paulay and Priestly 1992). Using these models enabled the researchers to study the influence of infill walls on the seismic behavior of buildings. More specifically, the researchers tried to evaluate the effective width of the diagonal struts so that it can simulate the behavior of real infill walls. Some researchers examined the relationship between the equivalent strut width and the length of the contact between infill and frame (Yasushi Sanada et al. (2011)), which drew them to understand the interactions between both components. However, these studies did not consider the hollow brick infill walls.

This chapter addresses relevant research and information, collected from the literature, that show the significant influence of the brick infill walls on the structural behavior of buildings. The main considered behavior is the fundamental period of the structure that is influenced by the structural stiffness and mass. Some shortcomings of previous research is represented by its inadequacy to reflect the nature of the common hollow-brick walls in Palestine, were observed. This led to serve the objective of this research which is to propose, verify, and apply a strut and tie model equivalent to hollow-brick walls and to investigate its effects, mainly on the fundamental period of RC frame buildings.

In the following subsections, research and information are presented regarding the fundamental period of structures, types of RC frames. Finally, types of brick walls used around the world and in Palestine are presented along with the methods adopted by previous researchers to model them.

## **2.2 Fundamental Period**

The natural period ( $T_n$ ) is a dynamic characteristic of structures, defined as the time taken by a structure during oscillation to complete one cycle. For a single-degree-of-freedom structure (SDOF structure), it exhibits only one natural time period. It depends on natural characteristics inherent in the structure which are its mass( $m$ ) and stiffness( $k$ ). Taking these two parameters, the natural period can be theoretically expressed for an SDOF structure by Equation (2.1) (Murty et al. 2012).

$$T_n = 2\pi \sqrt{\frac{m}{k}} \quad (2.1)$$

It can be inferred from Equation (2.1) that heavier and more flexible buildings are longer their natural periods (Murty et al. 2012).

While an SDOF structure has only one time period as explained above, a multi-degree-of-freedom structure (MDOF structure), has a number of natural time periods (or frequencies) equal to the number of its degrees of freedom. When such a structure is shaken at its natural frequencies, it exhibits the least resistance and its oscillations become very large, leading ultimately to the failure of the structure. This phenomenon is known as resonance (Murty et al. 2012).

Every structure possesses a large number of natural frequencies. The least of these frequencies is called the fundamental natural frequency, and its associated time period is called the fundamental time period. Every natural time period of a structure is associated with a unique form of motion. Both the natural period and the corresponding form of motion define together a Natural Mode of the structure. As one structure has a large number of natural periods, it consequently has a large number of natural modes (Murty et al. 2012).

When a building is subjected to ground seismic motion, it responds in different manners according to its different natural modes. The responses of a structure to a specific earthquake ground motion can be represented by a graph called the response spectrum. This graph plots the maximum responses

of the structure at its different natural periods. When this graph considers the acceleration response of the building, it is referred to as the Acceleration Response Spectrum (Murty et al. 2012). Such a graph is shown in Figure (2.1).

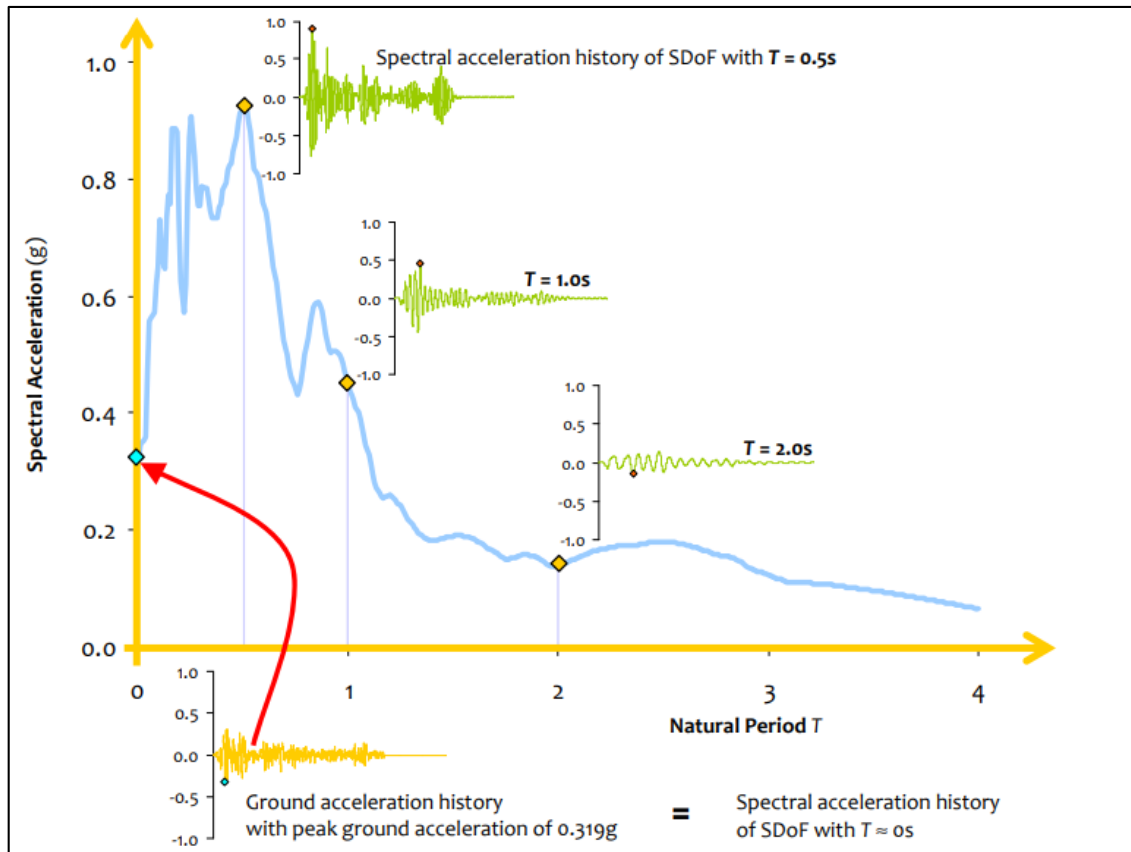


**Figure (2.1):** Acceleration response spectrum for a SDOF subjected to a seismic record (murly et al.2012).

For design purposes, it is necessary to find the seismic lateral force that develops in a building during earthquake action. Obtaining this force requires estimating the natural time periods of the building which are associated with each mode of oscillation. Then by referring to the “Acceleration Response Spectrum” introduced by seismic design codes, one

can determine the corresponding acceleration response spectrum value, which can in turn be used to determine the seismic force in the building. This force obtained therein is called the design seismic base shear of the building (Murty et al. 2012).

The above discussion emphasizes the importance of calculating the natural periods of structures for both analysis and design. For this reason, huge efforts have been put into developing empirical equations to be used in calculating the fundamental period of structures. These equations have been developed based on regression analysis on the periods of vibration measured during earthquakes. One prominent formula that is found in design codes, such as the IBC (2013), is given by Equation (2.2).

$$T = C_t H^x \quad (2.2)$$

Where:

X and  $C_t$ : Factors depend on the type of frames used in the building.

H: is the height of the building in (ft) or (m). Values of  $C_t$  are scaled according to the selected unit of H.

Naturally, having infill walls would affect the stiffness of the frames, thus leading to changes in the fundamental period of the frames compared to bare frames, i.e. those with no partitions. In fact, there are other equations for estimating the vibration period of buildings, developed by Crowley and Pinho (2006), which can be used for the case of reinforced concrete (RC)

buildings with moment resisting frames and infill panels. One of these equations is for uncracked infill frames, and the other is for cracked infill ones. Their research involved 11 existing buildings with the total height of the frames varying between 2 and 24m. The materials used to construct these buildings were of diverse properties. For example, the used concrete compressive strength ( $f'_c$ ) ranged from (15 – 29) MPa, while the yield strength ( $F_y$ ) of the reinforcement ranged from (200 – 380) MPa. The buildings considered in the research consisted of frames of three types – bare frames, fully infill frames and infill frames with openings. The weighted average was calculated for the vibration periods of these types of frames based on their number of occurrences within a sample of buildings.

As for the equation pertaining to uncracked infill frames, eigenvalue analyses were applied to the three types of frames, taking into account their gross stiffness section properties. Afterwards, the vibration period versus the building height were plotted and subjected to regression analysis to determine the best fitting line equations for the three types of frames. These results are shown separately for each frame in Figure (2.2). The mean period was then determined as shown in Figure (2.3).

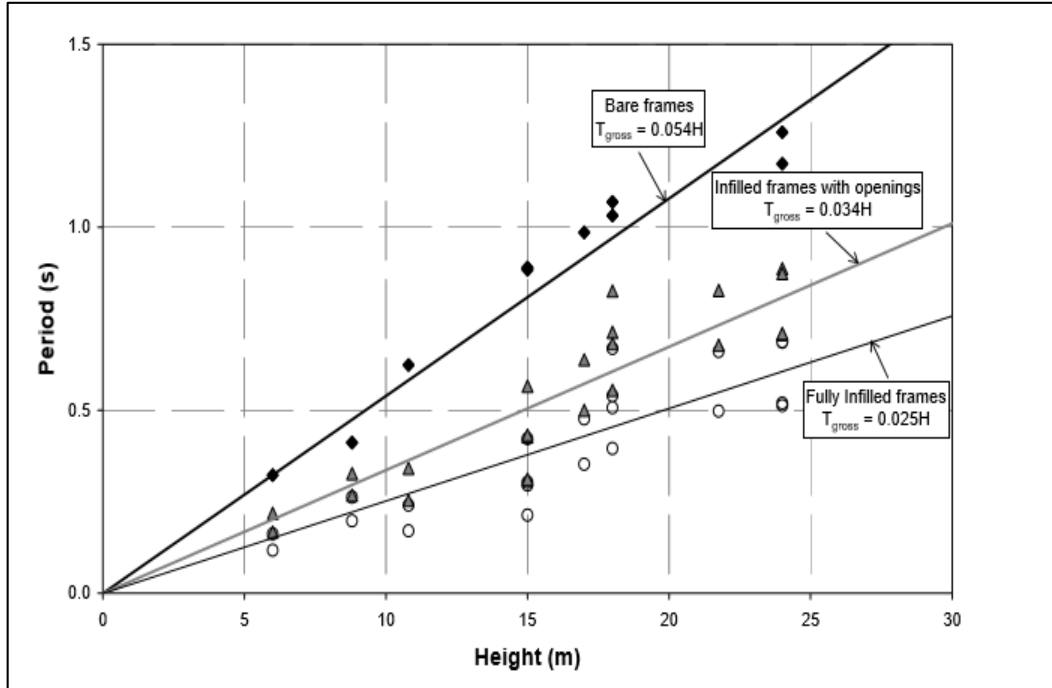


**Figure (2.2):** Period-height relationships for uncracked RC frames obtained with gross stiffness eigenvalue analyses for bare frames, fully infilled frames and frames with openings (Crowley and Pinho (2006))

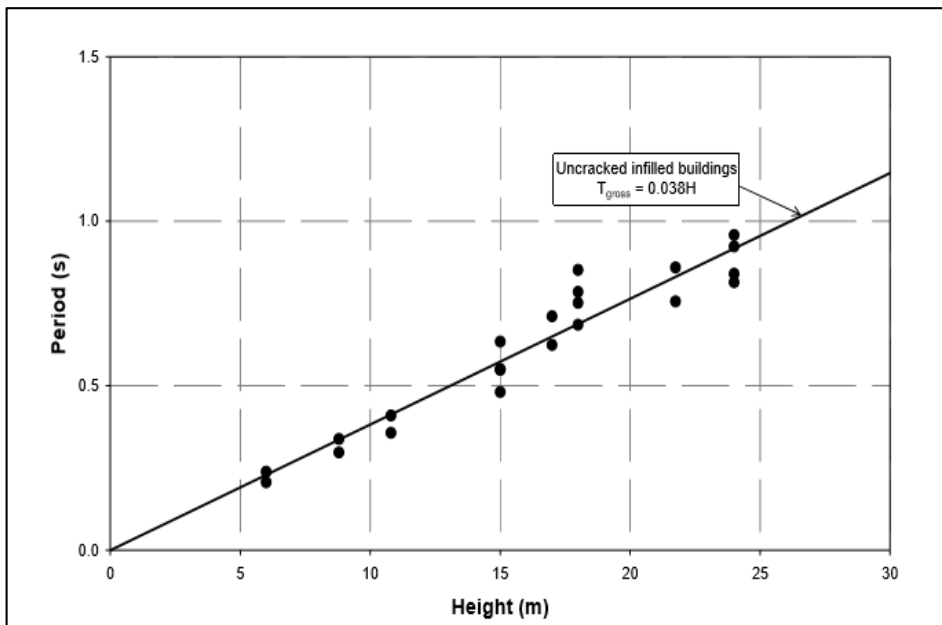


**Figure (2.3):** Period-height relationship for uncracked infilled RC buildings obtained by calculating a weighted average of the results in Figure (2.2)

As it appears in Figure (2.3), the equation of period for uncracked infill frames is given by Equation (2.3).

$$T_{uncracked} = 0.038 H \quad (2.3)$$

To obtain the time period equation for the cracked infill frames, it is required to use the reduced member stiffness to construct the infill frames. Cracking of the masonry was considered by finding the residual strut area using the reduced strut width. Afterwards, time period of the cracked infill frames was estimated based on the same approach followed to find time period of the uncracked infill frames. The obtained data as well as the results of regression analysis are plotted in the graph shown in Figure (2.4). The mean period of cracked infill frames was then determined as shown in Figure (2.5) and is given by Equation (2.4).

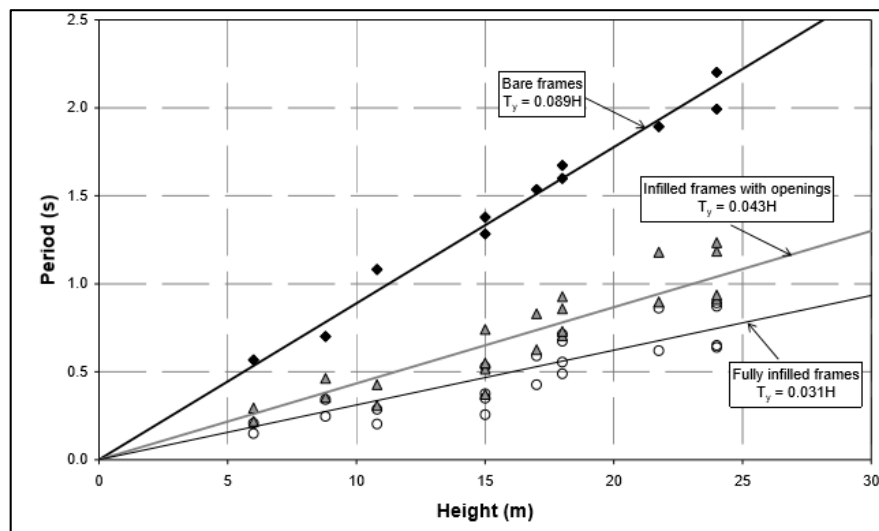


**Figure (2.4):** Analytical yield period-height relationships for cracked RC buildings obtained with yield stiffness eigenvalue analyses for bare frames, fully infilled frames and frames with openings (Crowley and Pinho (2006))

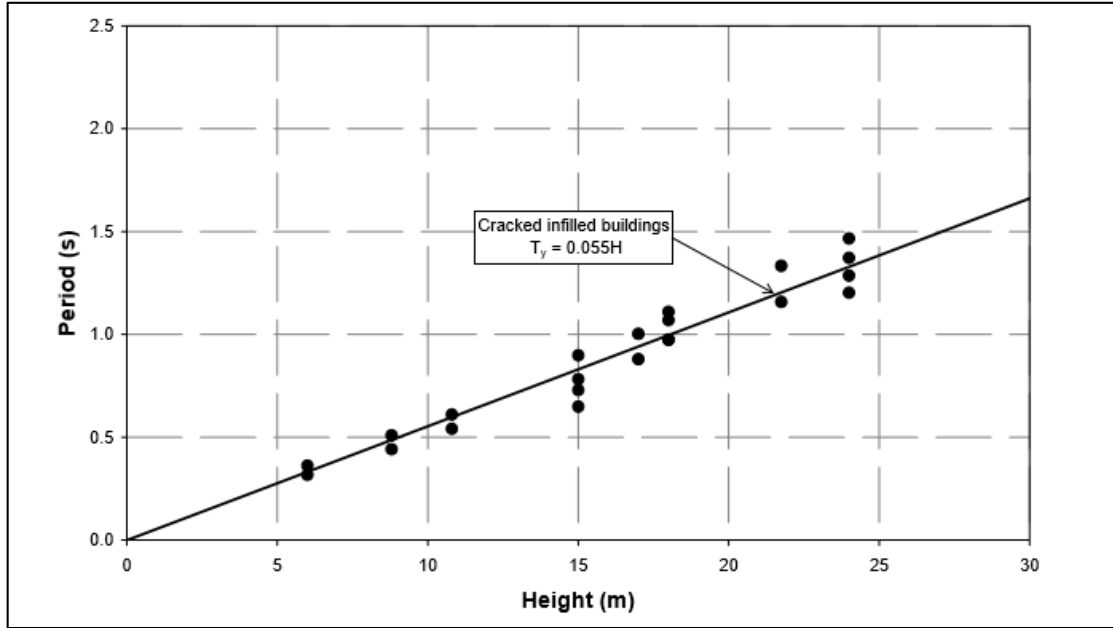


**Figure (2.5):** Analytical yield period-height relationship for cracked infilled RC buildings obtained by calculating a weighted average of the results in Figure (2.8)

As it appears in Figure (2.5), the equation of vibration time period for cracked infill frames is given by Equation (2.4).

$$T_{cracked} = 0.055 H \quad (2.4)$$

By comparing between Equations (2.3) and (2.4), it can be clearly observed that RC frames with cracked members have natural time periods longer than those with uncracked members. This can be owed to the reduction in the total stiffness of the RC frames when their members crack.

Guler et al. (2008) studied the effects of infill walls on the fundamental period of RC buildings. Their research was based on an experimental approach. They derived an equation (Equation (2.5)) to calculate the fundamental time period for fully elastic condition.

$$T = 0.026 H^{0.9} \quad (2.5)$$

Although huge efforts have been devoted to reach good estimations of the natural time period of infill frames, these estimations are only applicable to the frames with infill characteristics which are popular in the countries of researchers. Specifically saying, the types of infill bricks that have been studied so far are different from those usually used in Palestine, namely, the hollow brick infill walls. In our research, modal analysis of a framed structure is conducted in order to investigate the effect of interior infill partitions commonly used in Palestine, on the fundamental period of buildings. The fundamental period is aimed to be derived for such frames under several conditions depending on the distribution of the interior infill partitions in the frame. See more details in the methodology in Chapter (6).

### **2.3 RC frames with Infill Wall**

The work of this research is focused on frames used in Palestine. The type of frames most commonly used in Palestine is the RC frame. Most often these frames are built and filled with specific types of infill walls, with the hollow block infill walls being the mostly used type as is mentioned in the next section. Generally, RC frames consist of two main components – beams and columns, connected by rigid joints. They are designed to resist both gravity and lateral loads by transferring moments and shear through members of the frame. The following types of RC frames construction are observed in practice (Juan Rodriguez (2017)):

- Non-ductile RC frames with/without infill walls.
- Non-ductile RC frames with reinforced infill walls.
- Ductile RC frames with/without infill walls.

## **2.4 Brick wall types and modeling**

A summary of the widely known brick wall types is presented in this section. Their properties are mentioned along with brief descriptions. Methods of modeling of these partitions are found in research findings collected from the literature and introduced in the subsection that follows.

### **2.4.1 Brick wall types**

Generally, there are two classifications of infill partition walls used within RC frames: solid brick walls and hollow brick walls. The latter is the most commonly used in Palestine. Solid brick wall may be constructed with plain bricks, reinforced bricks or nogged bricks. Details on these types are given below Juan Rodriguez (2017):

**Plain brick wall:** Construction of this type of walls involves layering bricks using cement mortar. Thickness of the wall is 10 cm and overlaid with two thick side layers of plaster, one over each edge. It is known for its great strength and fire resistance, provided it is properly constructed.

**Reinforced brick wall:** This type of wall is similar to plain brick partition wall. However, bricks in this type are provided with reinforcement by using iron straps 25 to 28 mm wide and 1.6 mm thick. When iron straps are

unavailable, mild steel bars of 6 mm diameter spaced at every third course of the wall can be used.

**Nogged brick wall:** brickwork in this type is built within a framework of wooden members. The framework is established using vertical studs held at 60 to 90cm apart by horizontal members called nogging pieces. These nogging pieces pass through studs at 60 cm to 90cm apart vertically. A nogging brick wall is shown in Figure (2.6).



**Figure (2. 6):** Nogged brick wall

- **Hollow brick wall:** This type is made of materials such as concrete, clay or terracotta that is cast in moulds. Several advantages are obtained from using hollow brick walls such as lightness, rigidity, strength, and fire resistance. They are also economical and provide good sound insulation. These walls are usually used with thicknesses ranging from 7 to 20cm. Bricks of this type are shown in Figure (2.7).



Figure (2.7): Hollow brick samples

The shape, material texture and geometry of the hollow brick walls used in this research are presented in details in Section 3.2 (Tested specimens).

#### 2.4.2 Brick wall modelling

For its great importance in structures, modeling of brick walls has been a subject of interest for many researchers. Most of the models proposed by researchers replaced real brick walls with diagonal struts. Two compression struts were usually used in place of a panel along its diagonals.

Some studies, that used the approach of equivalent struts, suggested an equivalent strut cross section. One of these suggestion was put forward by Holmes (1961) who tried to investigate the effect of wall panels, built inside steel frames, on the strength and stiffness of these frames.

Holmes (1961) adopted an analytical approach to study the deflection of a wall panel built inside a steel frame (ABCD) as shown in Figure (2.8). In this figure the frame is subjected to a horizontal shear force ( $H$ ) that causes a vertical force ( $H \tan \alpha$ ) to arise. The resultant diagonal force ( $\frac{H}{\cos \alpha}$ ) tends to

compress the wall panel. If the wall panel is represented by a strut, it will show a reaction of (F) against the horizontal and vertical shear forces acting on the frame. This is clearly shown in Figure (2.9-a). As a result, the shear forces acting on the frame alone are shown in Figure (2.9-b). These shear forces tend to shorten the frame diagonal by some distance. If this distance is set to equal the distance compressed in an equivalent strut made out of concrete, then the cross sectional area of the strut can be determined. The obtained strut equivalent cross section as  $(t \frac{d}{3})$ , where (t) denotes the actual thickness of the infilling wall; and (d) denotes the diagonal length of the frame before lateral deformation, Holmes (1961).

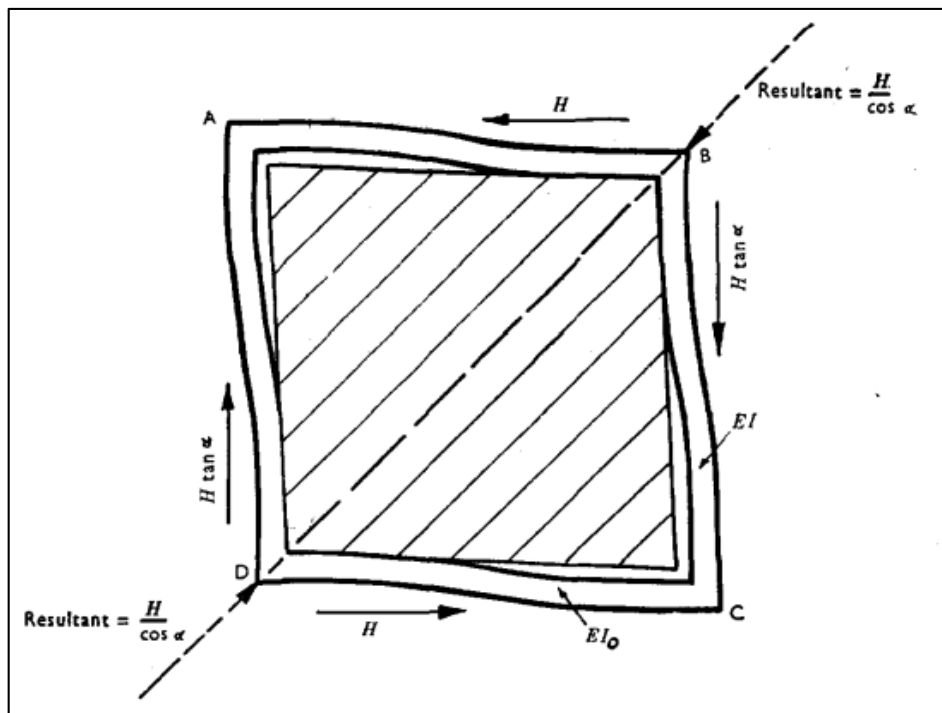


**Figure (2. 8):** Panel of steel frame with concrete infill wall, (Holmes (1961))

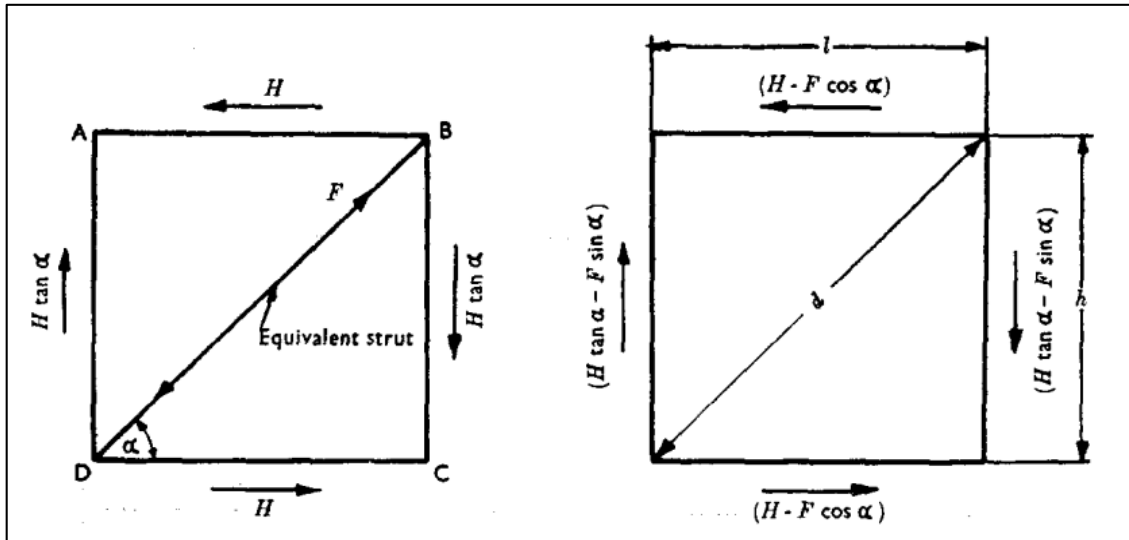


**Figure (2.9):** (a) Equivalent structure, (b) shear force on steel frame alone, (Holmes (1961))

In addition to Holmes's study, Smith and Carter (1969) also proposed a design method based on an equivalent strut method to predict the lateral stiffness of the composite frame. Their study was based on the case of non-linear infill material. The main observations and assumptions of their model were:

- 1- Infill and frame are neither monolithically constructed nor intentionally bonded together.
- 2- Infill and frame, if separated, remain in contact adjacent to the corners at the ends of the compression diagonal (Figure (2.10-a)). This entails the suggestion that partition can be represented by diagonal struts. The analogous structure shown in Figure (2.10-b) may be adopted, with equivalent struts replacing the infills.

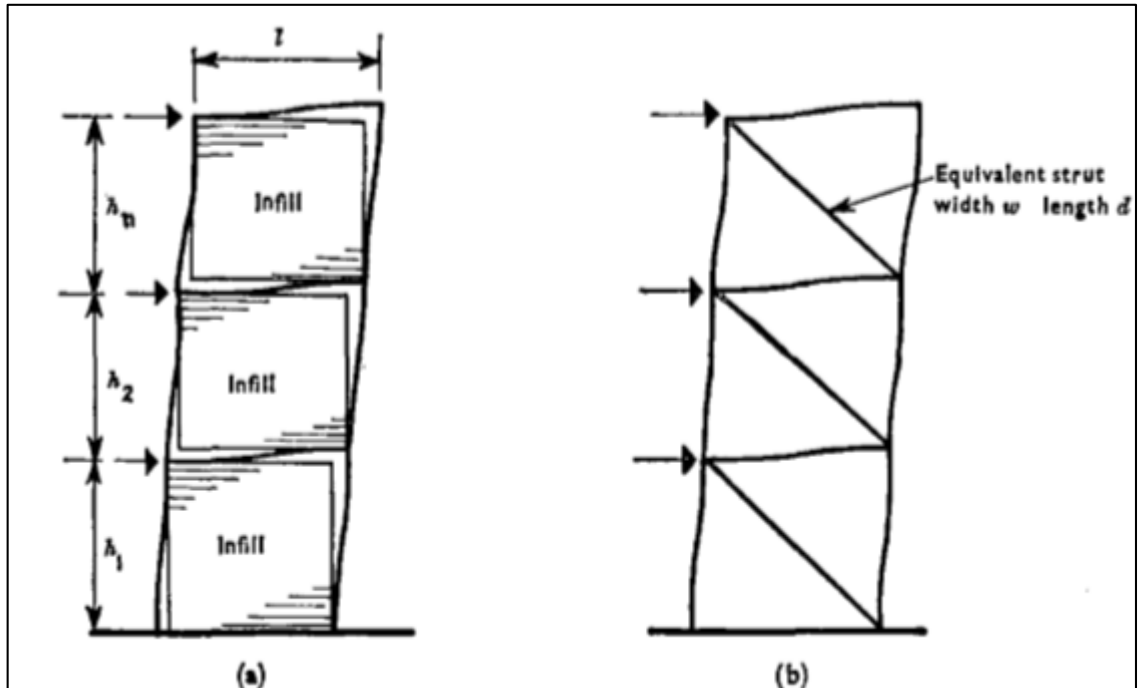


**Figure (2. 1):** (a) Laterally loaded infilled frame, (b) Equivalent frame (Smith and Carter 1969)

- 3- Concrete modulus of elasticity decreases as stress increases and, therefore, it is not constant.
- 4- For the frame and infill wall behaving compositely, the lateral stiffness of the frame as well as its strength depend separately on each of the frame and infill, and at the same time, on the relative stiffness of both components.
- 5- Factors affecting the effective width related to the infill when it is to be represented as a diagonal strut are: (a) column-infill relative stiffness, (b) length-height proportions of the infill, (c) the stress-strain relationship related to the infill material; and (d) value of the load acting diagonally on the infill.

- 6- The frame is pin-jointed and includes the infill represented as diagonal struts. Therefore, lateral stiffness can be evaluated based on static analysis of the frame.
- 7- The infill frame can collapse when failure takes place in the frame or in the infill wall. High tension and shear in columns or high shear in the beams or joints can cause the frame itself to fail. Otherwise, failure ultimately will take place in the infill wall.
- 8- Infill panels may fail in two modes: tensile cracking that extends along the diagonal in the direction of loading, and failure due to compression at the loaded corners. In some cases, the compressive mode of failure may be forerun by the tensile cracking, but in other cases it occurs alone.

Smith and Carter's [8] research reported that the equivalent strut width varied according to the applied loading and the relative properties of the frame and its infill. However, results of this research are still inadequate to be adopted for buildings in Palestine because the researchers did not specifically address the hollow brick walls as the infill of the frames.

The above mentioned models were applied to the results of several experiments conducted by Yasushi Sanada et al. (2011) in Indonesia. Their experiments involved brick infill RC frames. The researchers proposed another diagonal compression strut equivalent to the infill wall. The width of this strut was expressed by a function of the contact length between the frame and the infill. The contact length was evaluated based on the static principles through compression balance and compatibility of the lateral

displacement at the frame–infill interfaces. Verification of this model was then conducted by running comparisons with results from experimental tests. These tests considered several brick-infill RC frames representing a typical RC building in Indonesia.

Yasushi Sanada et al. (2011) applied their proposed model for two existing RC structures which had been struck by natural earthquakes and, as a result, they experienced damages of various degrees. These structures included infill walls within their frames. The model was used to evaluate the effect of infill walls on the seismic performance exhibited by the frame. The results led to the conclusion that brick infill walls impose apparent changes to the seismic behavior of the frames by affecting their seismic resistance, leading to varying damage levels, as similarly was apparent from the real damaged structures. The results, therefore, emphasized the efficiency of the model proposed by Yasushi Sanada et al. (2011) in accurately predicting the vulnerability of existing RC structures in Indonesia.

As a result, the experimental results for Sanada et al. showed good congruence with the analytical results of the lateral strength and ductility of the infill frames. Furthermore, a comparison between the proposed model and other models is shown in Figure (2.11). It should be noted that the proposed model and Mainstone (1971) model were close to the experimental test. In contrast, the coefficient of variance for Holmes model has the largest value, that means Holmes model and Smith and Carter model do not match the experimental test that was conducted by Sanada et al (2011).

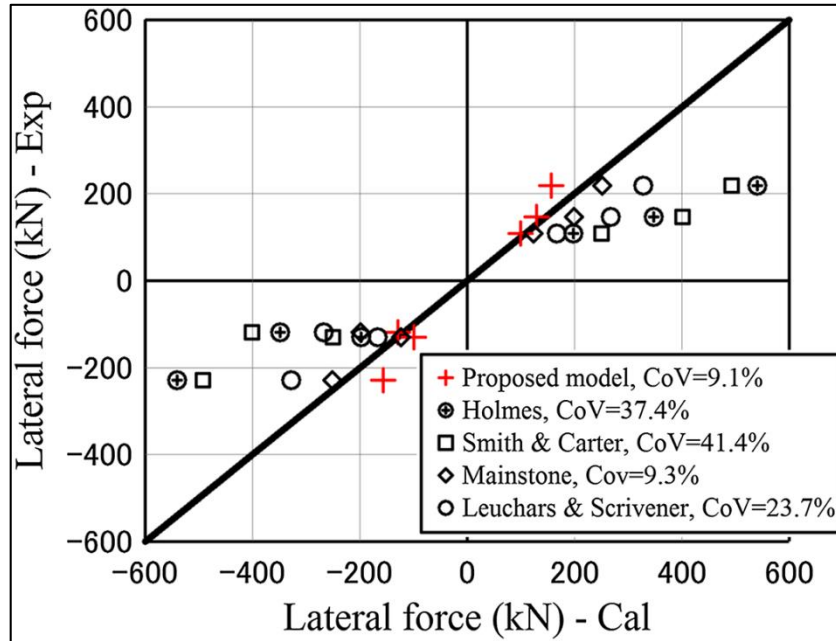


**Figure (2.2):** Comparison between the Yasushi Sanada et al model and other previous models

It can be noted from the above proposed models that they all dealt with RC frames that include solid brick walls. None has addressed those frames that include hollow brick walls. As the latter type of walls is more commonly used in Palestine, therefore, researcher's efforts were extended through this study to include frames with hollow-brick walls.

## **Chapter 3**

### **Experimental Tests**

#### **3.1 General**

The literature review presented in Chapter (2) indicates that most of the experimental studies were carried out under conditions that did not cover important factors such as modulus of elasticity for hollow brick, Poisson ratio and load slip curve for the contact between brick and mortar. For these reasons, part of the work of this thesis involves experiments that were carried out on several specimens of brick and mortar under realistic loading conditions. Four specimens of brick, two specimens of mortar, and a specimen of two bricks connected to each other with mortar were tested according to specifications. A useful amount of data was collected from these experiments to be used for validating the numerical model. Full details of the experiments, including specimen's preparation, testing procedure and results are discussed in this chapter.

#### **3.2 Tested Specimens**

The experiment program consists of conducting compressive strength tests on four specimens of hollow bricks, two cubic specimens of mortar and a formation of two bricks connected to each other with mortar.

Bricks commonly used in Palestine, along with their specifications are categorized under three types (Type (1), Type (2) and Type (3)) as listed in

Table (3.1). In this research, all tests are focused on bricks of Type (1) because they are used in interior partitions. Bricks of Type (1) are 400mm long, 200mm high and 100mm wide. The bricks specimens were prepared and capped with small layer of cement- water, in order to level the surface, as shown in Figure (3.1).

**Table (3. 1): Brick requirements according to the Palestinian specification**

<b>Requirements</b>	<b>Type (1)</b>	<b>Type (2)</b>	<b>Type (3)</b>
<b>Dimensions (mm)</b>	400x200x100	400x200x150	400x200x200
<b>Number of openings</b>	3 (2 minimum)	3 or 4 (2 minimum)	3 or 4(2 minimum)
<b>Shape of texture and finishing</b>	Good	Good	Good
<b>Length (mm)</b>	400±3	400±3	400±3
<b>Width (mm)</b>	100±3	150±3	200±3
<b>Height (mm)</b>	200±4	200±4	200±4
<b>Thickness of large face (mm)</b>	27 minimum	30 minimum	30 minimum
<b>Thickness of small face (mm)</b>	18 minimum	25 minimum	25 minimum
<b>Density (kg/m<sup>3</sup>)</b>	1650	1400	1400



**Figure (3.1):** The brick specimens used in the experimental test of this thesis

The mortar specimens were casted in cubes of the dimensions and properties summarized in Table (3.2), and shown in Figure (3.2).

**Table (3.2): Dimensions and properties of the first specimen of mortar**

	Length (mm)	Width (mm)	Height (mm)	Weight (kg)	Density (kg/mm <sup>3</sup> )	Poisson's ratio
<b>First specimen</b>	93	100	100	1.884	2.0 E-06	0.2
<b>Second specimen</b>	100	100	100	1.857	1.8 E-06	0.2



**Figure (3.2):** A mortar specimen used in the experimental test of this thesis

Finally, a formation of two bricks were prepared by connecting them to each other with 5mm layer of mortar, and left for curing, in order to test the connection between bricks, as shown in Figure (3.3). This test is intended to investigate the failure mode, and to obtain the load- slip curve for the interaction between bricks.



**Figure (3.3):** The connected bricks which were used for the shear test

### **3.3 Test Procedure**

One of the main purposes of this research is to determine the stiffness of the brick wall. Due to lack of information on some parameters needed to find the stiffness of brick wall, it was necessary to test several specimens of the bricks. The modulus of elasticity and stress-strain values were the main needed parameters that had to be taken from the brick testing.

Brick walls consist not only of bricks, but also mortar is used to connect bricks together. Therefore, testing includes, brick test, mortar test, and shear test of the contact between mortar and brick.

The brick and mortar specimens were tested by using a universal testing machine (MTS) as shown in Figure (3.4). This machine is a hydraulic machine, whose principle is based on compressing the sample with a uniform load. The machine is connected with a personal computer that provides it with the load – deflection curve from the beginning of loading up to failure. The machine applies this curve to the specimen. The loading rate used in the test, according to ASTM C-652, ranged from 0.04 to 0.09 N/mm/sec.

The procedure of testing was the same for both the brick and mortar specimens. However, the shear test of the connected bricks was performed by using the Tiles Testing Machine. This machine was connected with two dial gauges, the first gave the reading of the load on one of the two bricks, and the second gave the reading of the slip between mortar and brick. The specimen was loaded until mortar failed by a crack developed between mortar and brick. It should be noted that the load was applied to one brick while the other was held fixed, as shown in Figure (3.5).

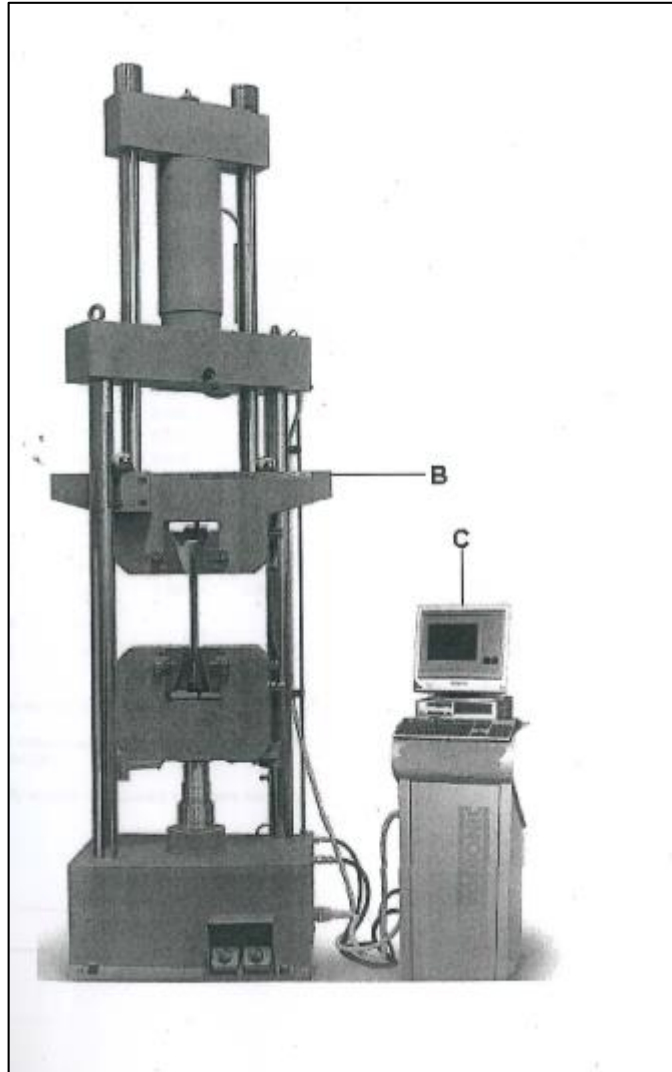


**Figure (3.4):** MTS machine used for brick and mortar tests

Where point B is the location at where the specimen is put to be tested, and point C is the computerized results



**Figure (3.5):** The shear test of a specimen of mortar-connected two bricks using the Tile Testing Machine

### **3.4 Tests Results**

The results of the previously described tests are presented in this section. They are divided into three groups of results – brick tests results, mortar tests results and shear test results. Every group is presented in the following subsections.

### 3.4.1 Results of brick tests

The main parameter that was taken from the compression test of the four specimens of bricks, is the modulus of elasticity and crushing strength.

The first, second, and third specimens were tested with loading rates of 0.08 MPa/sec.

The results were extracted as load-deflection values from the MTS machine. They were then transformed into stress-strain values which were subjected to regression analysis to produce line equations. The slopes of these equations are the modulus of elasticity of the brick specimens. The stress-strain curves produced for the four specimens are shown in Figures (3.6 – 3.8).

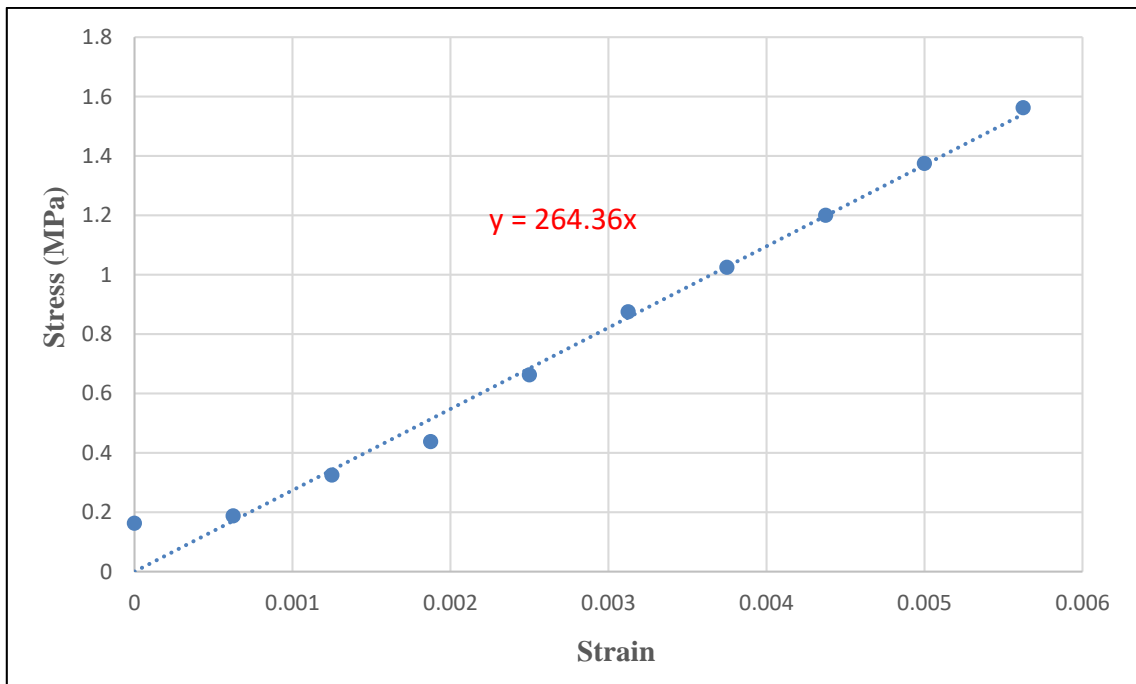


**Figure (3. 6):** The stress-strain curve and modulus of elasticity of the first specimen

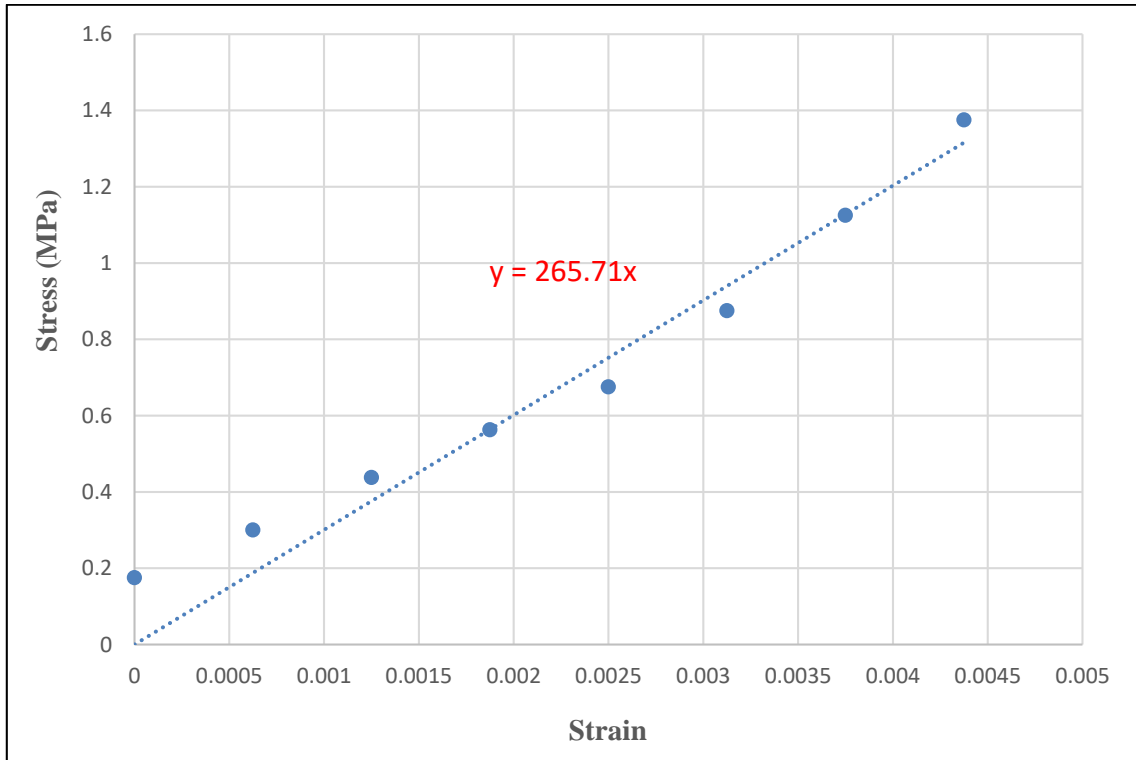


**Figure (3. 7):** The stress-strain curve and modulus of elasticity of the second specimen

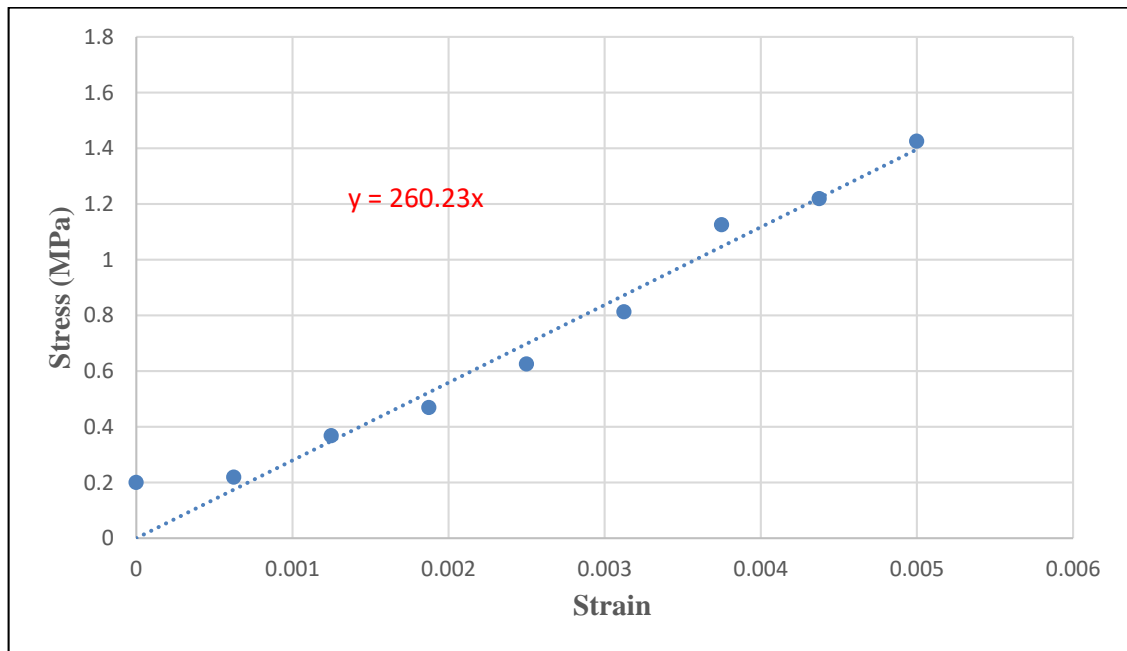


**Figure (3. 8):** The stress-strain curve and modulus of elasticity of the third specimen

The summary of the previous results is shown in Table (3.3). This table lists the modulus of elasticity of each of the four specimens. The used value of the modulus of elasticity can be taken as the average value.

**Table (3. 3): The moduli of elasticity values for all brick specimens as obtained from tests**

<b>Test</b>	<b>E (MPa)</b>
1	264.36
2	265.71
3	260.23
<b>Average (E)</b>	<b>263.4</b>

### 3.4.2 Mortar tests

The main parameter obtained from the compression test of the two specimens of mortar, is the modulus of elasticity.

The first and second specimens had the properties shown in Table (3.4).

**Table (3. 4): Properties of the first and second mortar specimens**

	<b>Length (mm)</b>	<b>Width (mm)</b>	<b>Height (mm)</b>	<b>Weight (kg)</b>	<b>Density (kg/mm<sup>3</sup>)</b>	<b>Poisson's ratio</b>
<b>First specimen</b>	93	100	100	1.884	2.02581E-06	0.2
<b>Second specimen</b>	100	100	100	1.857	1.857E-06	0.2

The stress-strain curves, resulted from the mortar tests, are shown Figures (3.10) and (3.11).

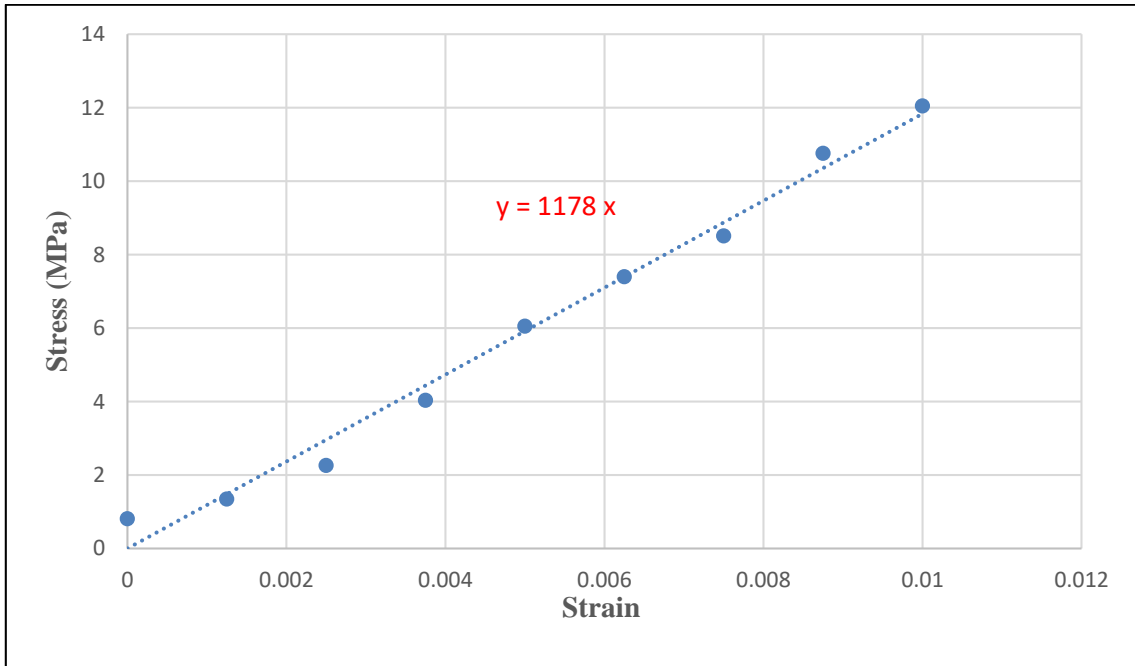


**Figure (3. 6):** The stress-strain curve and modulus of elasticity of the first specimen

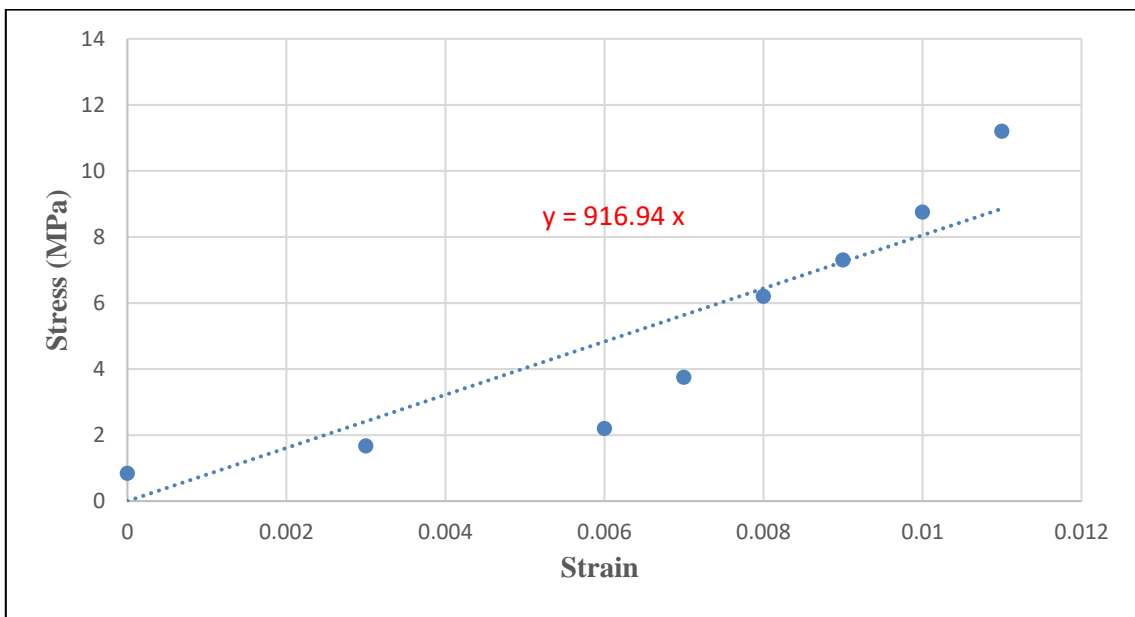


**Figure (3. 7):** The stress-strain curve and modulus of elasticity of the second specimen

The regressions shown in Figures (3.10) and (3.11) imply that the obtained moduli of elasticity of the tested specimens of mortar are 1178 MPa and

916.94 MPa. Therefore, the modulus of elasticity of mortar can be taken as the average of these values which is equal to 1047.47 Mpa.

### 3.4.3 Shear test

This test aimed to illustrate the failure mode in a sample of two bricks connected by a layer of mortar. The resulted load slip curve is shown in Figure (3.12).

Figure (3.13) is a picture caught for the specimen upon failure.

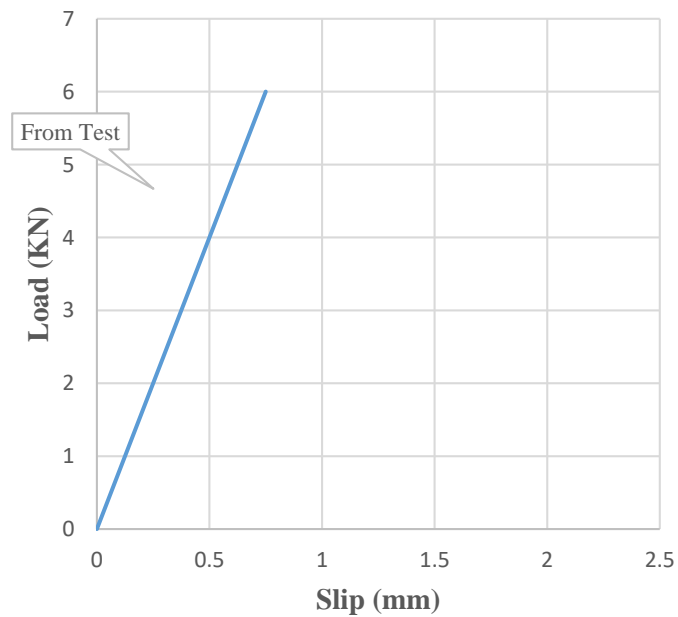


**Figure (3.8):** Load-slip curve obtained from the experimental shear test



**Figure (3.9):** Failure of the specimen during the shear test

The obtained load-slip curve continues linearly until the failure point (load = 6 kN) after which it is immediately cut. This curve is used in the micro modeling stage (Chapter 4) to define the interaction between brick and mortar.

### **3.5 Summary**

Details of brick, mortar and shear testing are presented in this chapter, the main parameters needed for brick wall modeling are the modulus of elasticity (E) and the stress-strain relationship.

The brick is found to have a modulus of elasticity of around 260MPa according to the test, which is about 1% of the modulus of elasticity of

concrete. This can be justified by the weakness of the brick material and the voids contained by the hollow brick.

The stress-strain relationships of brick and mortar as well as the load-slip curve of the contact between brick and mortar are also presented in this chapter.

## Chapter 4

### Micro Modeling of Brick Wall

#### 4.1 Overview

Structural analysis based on numerical methods such as the Finite Element Method (FEM) is regarded as a very useful technique for that it yields quick results with relatively little costs. It also makes possible to study several variables in depth. In this study, the commercial FE software ABAQUS is, therefore, used to build and analyze brick wall models based on a three-dimensional non-linear finite element.

In this chapter, nine models of brick walls are described. They are assigned properties that vary according to two main variables – length of the brick wall and cross sectional area of the columns of the surrounding frame. Other variables such as frame height and wall depth are assumed constant. Defining the stiffness of brick walls requires modeling of two versions of frame models – frames without a brick wall which are named bare frames, and frames with brick walls.

Modeling of each of the bare frame and frame with brick wall in ABAQUS is done by following several steps which include definition of materials, creation of parts, modeling of interfaces, definition of interaction between parts, selection of analysis type, application of loading, boundary conditions and meshing; all of which are discussed in the following subsections.

#### **4.1.1 Definition of material**

In this subsection, constitutive models for concrete and steel under compression and tension loads are presented. Furthermore, a constitutive model for brick and mortar are included.

##### ***Concrete***

Concrete material is hard to be accurately modeled due to its non-homogeneity and because of the change in its response at different loading stages under both compression and tension. Effects of cracking and crushing effects on strength and stiffness of concrete can be modeled in different ways, among of which is a method called “Concrete Damaged Plasticity” model (CDP). It involves the inclusion of cracking and crushing effects in the stress-strain behavior of concrete model.

ABAQUS software provides the CPD model that enables modeling of complex nonlinear behavior of concrete. In this model, two main failure criteria are considered: compressive crushing and tensile cracking of concrete. Compression and tension behavior of concrete under uniaxial loading is shown in Figure (4.1).

Stiffness and strength degradation can be defined using the CDP through the tension and compression parameters ( $d_t$ ,  $d_c$ ). This is clearly shown in Figure (4.1) (ABAQUS User Manual, 2013).

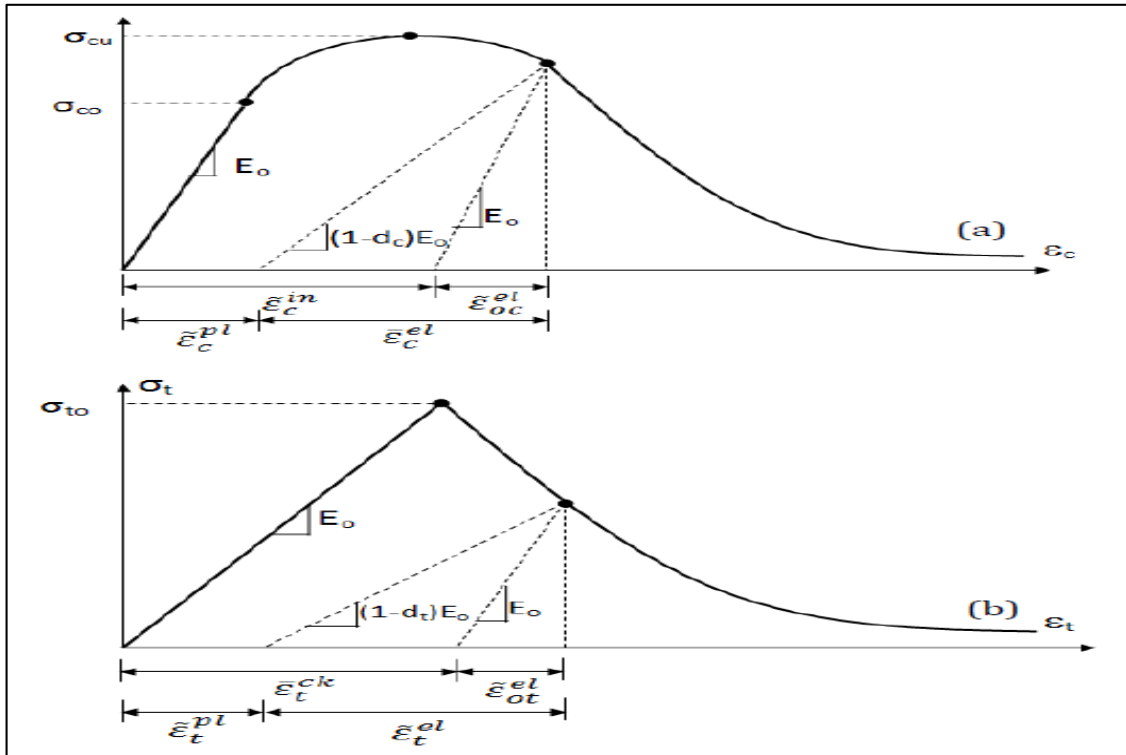


**Figure (4. 1):** Response of concrete to uniaxial loading in (a) compression and (b) tension (ABAQUS User Manual, 2013)

Figure (4.1) depicts how elastic stiffness changes in a concrete specimen in case it is unloaded. It declines or may even be damaged due to developed cracks. This is why the unloaded response of the specimen seems weakened. The decline of the elastic stiffness that appears on the strain softening part of the stress-strain curve is characterized by two damage variables,  $d_t$  and  $d_c$ ; whose values range from zero to one. A zero value indicates undamaged material condition, while a value of 1 represents total loss of strength.  $E_0$  in the diagram denotes the initial (undamaged) elastic stiffness of the material and  $\tilde{\epsilon}_t^{pl}$ ,  $\tilde{\epsilon}_c^{pl}$ ,  $\tilde{\epsilon}_t^{in}$ ,  $\tilde{\epsilon}_c^{in}$  denote the compressive plastic strain, tensile plastic strain, compressive inelastic strain and tensile inelastic strain, respectively.

Equations (4.1) and (4.2) give the elastic relations under uniaxial tension ( $\sigma_t$ ) and compression ( $\sigma_c$ ).

$$\sigma_t = (1 - d_t) \cdot E_0 \cdot (\varepsilon_t - \varepsilon_t^{\sim pl}) \quad (4.1)$$

$$\sigma_c = (1 - d_c) \cdot E_0 \cdot (\varepsilon_c - \varepsilon_c^{\sim pl}) \quad (4.2)$$

The uniaxial tension ( $\sigma_t$ ) and compression ( $\sigma_c$ ), along with the parameters ( $d_t$ ,  $d_c$ ,  $E_0$ ,  $\varepsilon_c^{\sim pl}$ ,  $\varepsilon_t^{\sim pl}$ ) are input into ABAQUS so that it can compute the effective tensile and compressive cohesion stresses, as shown in Figure (4.2). These stresses, in turn, are needed by ABAQUS to construct the yield function. It is possible to make use of the yield function to assess strength of concrete for tension and compression when it is subjected to multi-axial loading. This argument is proved according to Lubliner et al. (1989), taking into account the modifications proposed by Lee and Fenves (1998). The yield function in 2-D plane stress (bi-axial) conditions is shown in Figure (4.2).

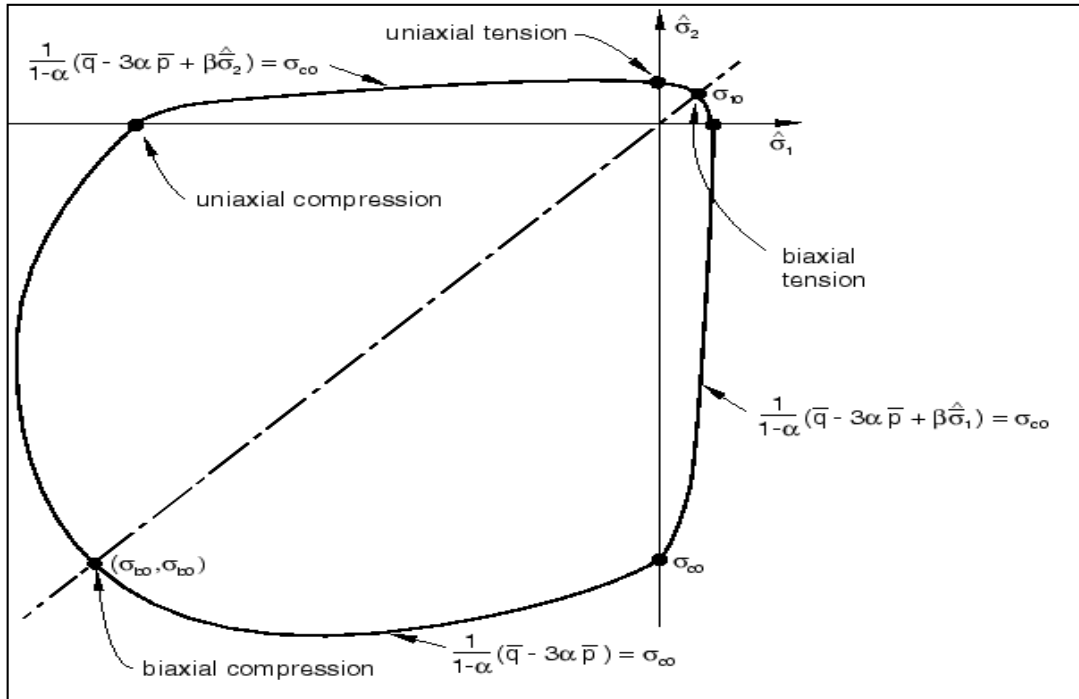


**Figure (4. 2):** Yield surface in plane stress (ABAQUS User Manual, 2013)

Since ABAQUS is able to assess concrete strength under multi-axial loading, the confinement effect which results from tri-axial stress in concrete can be detected by the material model. Based on that, improvements can be imposed to the compressive capacity in the case of hydrostatic stress state.

### ***Uniaxial compression behavior***

According to literature, several researchers developed equations that describe the behavior of concrete subjected to uniaxial compression stress. Despite the fact that these equations as well as the models proposed by Mander et al. (1988) and Yong et al. (1988) do not yield the full stress-strain curve of concrete, the behavior of concrete can still be fully described by the stress-strain equation (Equation (4.3)) proposed by Saenz (1964) which was

validated by Asran et al. (2016). Terms and factors used in this equation are given in Equations (4.4 – 4.9).

$$\sigma_c = \frac{E_c \varepsilon_c}{1 + (R + R_E - 2) \frac{\varepsilon_c}{\varepsilon_0} - (2R - 1) \left(\frac{\varepsilon_c}{\varepsilon_0}\right)^2 + R \left(\frac{\varepsilon_c}{\varepsilon_0}\right)^3} \quad (4.3)$$

$$E_c = 4700 \sqrt{f'_c} \quad (4.4)$$

$$R = \frac{R_E (R_\sigma - 1)}{(R_\varepsilon - 1)^2} - \frac{1}{R_\varepsilon} \quad (4.5)$$

$$R_E = \frac{E_c}{E_0} \quad (4.6)$$

$$R_\sigma = \frac{f'_c}{\sigma_f} \quad (4.7)$$

$$R_\varepsilon = \frac{\varepsilon_f}{\varepsilon_0} \quad (4.8)$$

$$E_0 = \frac{f'_c}{\varepsilon_0} \quad (4.9)$$

Where:

$\sigma_c$ : Concrete compressive stress (MPa).

$E_c$ : Modulus of elasticity of concrete (MPa).

$E_0$ : Secant modulus of concrete (MPa).

$f'_c$ : Maximum compressive strength of concrete (MPa).

$\varepsilon_c$ : Compression strain.

$\varepsilon_0$ : Strain corresponding to  $f'_c$  which equals approximately 0.0025 as reported by Hu (1989).

$\varepsilon_f$ : Maximum strain.

$\sigma_f$ : Stress at maximum strain (MPa).

$R$  : Ratio relation.

$R_E$ : Modular ratio.

$R_\sigma$ : Stress ratio, which equals 4 as reported by Hu (1989).

$R_\varepsilon$ : Strain ratio, which equals 4 as reported by Hu (1989).

### ***Tension behavior***

Concrete stress-strain curve under tension was constructed based on an experimental test made by Sharif et al. (2015) for concrete of 23 MPa compressive strength. The maximum tensile stress observed is 2.9 MPa which relates to the modulus of rupture of concrete ( $0.62\sqrt{f'_c}$  according to ACI 318). Tensile stress is observed decreasing just beyond the peak value up to a strain of 0.003. Asran et al. (2016) used this equation to define the tension behavior of concrete in ABAQUS. They assumed the curve decreasing in a linear manner after the peak. Due to insufficient experimental information on the ultimate strain of concrete under tension, it is assumed equal to 0.003 in this model under flexural test for all types of concrete.

According to the CDP, the following parameters are required to model concrete and define its behavior accurately:

1. Young's Modulus ( $E_c = 23000$  MPa): Modulus of elasticity of concrete computed using Equation (4.4).
2. Poisson's Ratio ( $\nu = 0.2$ ): The ratio of transversal elongation to the axial elongation.
3. Dilation angle (internal friction angle) ( $\psi$ ), defined as the angle measured in the p–q plane (hydrostatic pressure stress - Mises equivalent effective stress) at high confining pressure as shown in Figure (4.3) (ABAQUS User Manual, 2013). The reasonable values of ( $\psi$ ) lie between  $36^\circ$  and  $40^\circ$  as suggested by Kmiecik and Kaminski (2011). In this research, a value of  $36^\circ$  is used.
4. Eccentricity: It is defined as the rate at which the flow potential function approaches the asymptote in p–q plane. An eccentricity value of 0.1 is recommended by the CDP model (ABAQUS User Manual, 2013). As this value approaches 0, the surface in the meridian plan becomes a straight line and consistent with the classic Drucker-Prager hypothesis as shown in Figure (4.3) (ABAQUS User Manual, 2013).

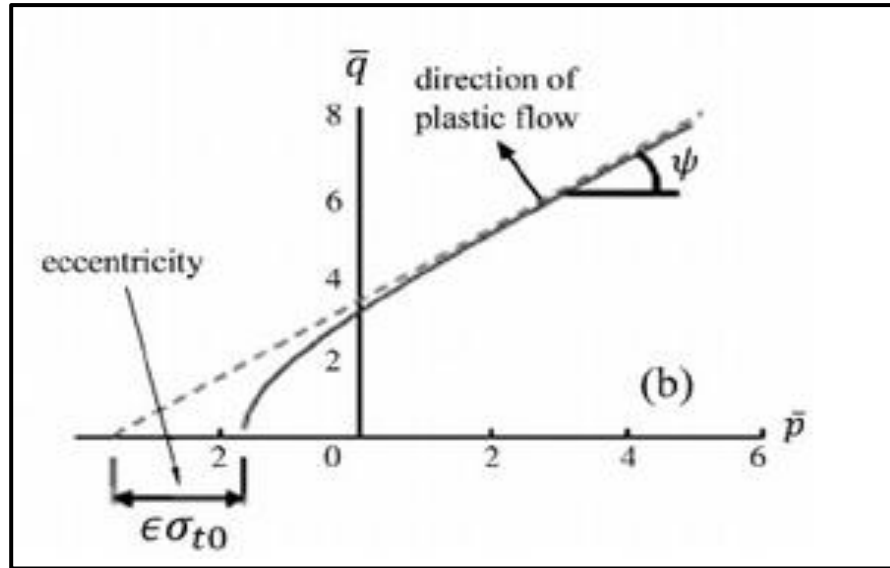


**Figure (4.3):** Dilatation angle and eccentricity (ABAQUS User Manual, 2013).

5.  $f_{b0}/f_{c0}$ : The ratio of bi-axial compression stress to uni-axial compression stress. This ratio is determined experimentally by Kupfer (1969) and it is found equal to 1.16.
6.  $K$ : This factor equals the ratio of the distances measured between the hydrostatic axis and both the compression and the tension meridians in the deviatoric cross section. A value of  $2/3$  is recommended by ABAQUS User Manual (2013). The purpose of this factor is to be used for converting the shape of cross section of failure surface from circle to combination of three mutually tangent ellipses as shown in Figure (4.4) (ABAQUS User Manual, 2013). This shape was formulated by William and Warkne (1975).



concrete, compression damage parameter Vs. inelastic strain curve, and tension damage parameter Vs. cracking strain curve, respectively.

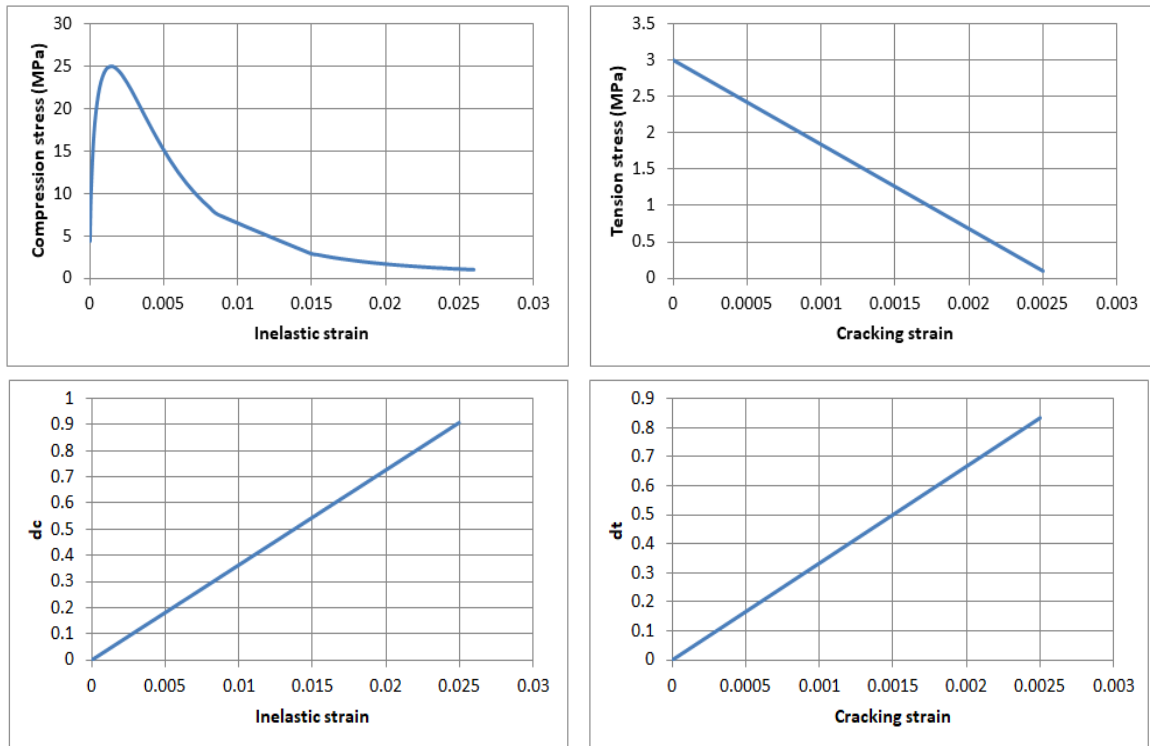


**Figure (4.5):** Curves needed to define CDP model in ABAQUS for testing by Clyde et al. (2000)

11. Tension recovery ( $\omega_t$ ) and compression recovery ( $\omega_c$ ): These are material properties used to reflect the recovery of the tensile and compressive stiffness upon load reversal. It was observed in experimental tests for most quasi-brittle materials, including concrete, that the compressive stiffness is recovered upon crack closure as the load reverses from tension to compression. However, this is not the case for the tensile stiffness as compression reverses to tension. In this case, crushing micro-cracks that have developed prevent the recovery

of tensile stiffness. This behavior, which corresponds to  $\omega_t = 0$  and  $\omega_c = 1$ , is the default used by ABAQUS. Uniaxial load cycle (tension-compression-tension) is shown in Figure (4.6), where the default values for the stiffness recovery factors ( $\omega_t = 0$  and  $\omega_c = 1$ ) are indicated (ABAQUS User Manual, 2013).

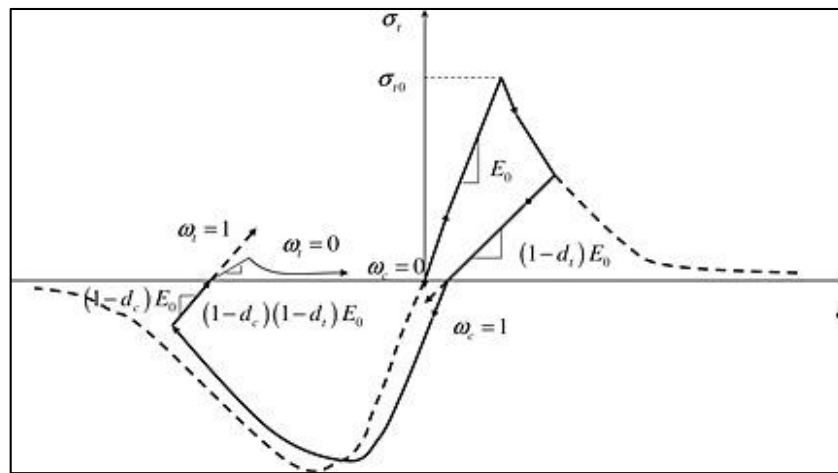


**Figure (4.6):** Uniaxial load cycle (tension-compression-tension), assuming the default values for the stiffness recovery factors as  $\omega_t = 0$  and  $\omega_c = 1$  (ABAQUS User Manual, 2013)

### ***Reinforcing Steel Model***

Generally, stresses less than the initial yield stress in steel are regarded linear-elastic. When ultimate tensile strain is reached, reinforcement starts to neck and strength is reduced. At the maximum strain, steel reinforcement fractures, causing loss of load capacity. These loading stages are displayed in Figure (4.7).

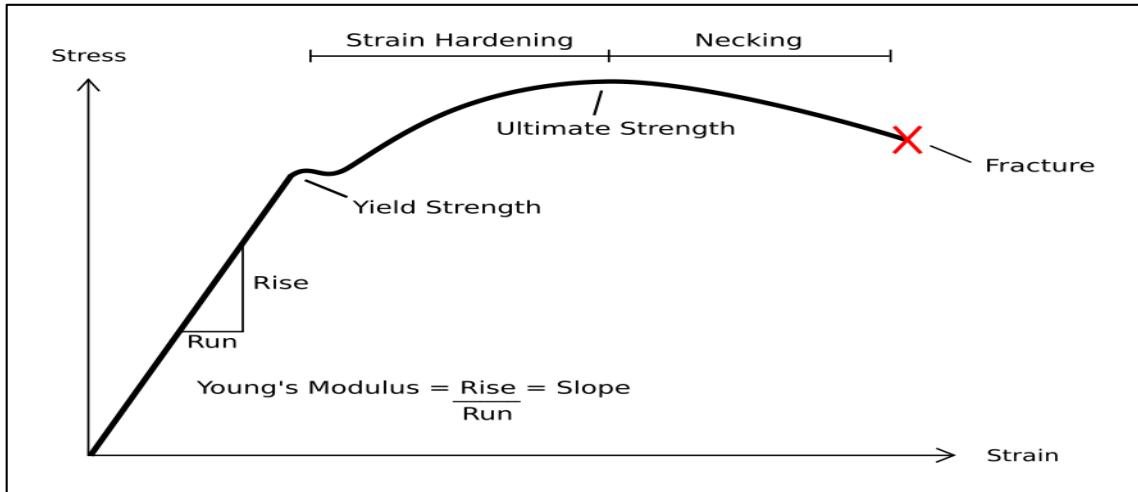


**Figure (4.7):** Typical stress-strain curve of steel

The reinforcement and loading plate materials are chosen to be isotropic in the model. This indicates a uniform change in the size of the yield surface in all directions such that when plastic straining occurs, the yield stress increases (or decreases) in all stress directions. The main parameters used in defining steel are the modulus of elasticity ( $E$ ) = 205000 MPa for steel reinforcement, yield stress ( $F_y$ ) = 420 MPa, density ( $\rho$ ) = 7800 kg/m<sup>3</sup> and Poisson ratio ( $\nu$ ) = 0.3.

### ***Brick Model***

Based on the tests and results as presented in chapter 3, the hollow bricks used in Palestine have the following elastic and plastic properties:

- 1- Modulus of elasticity ( $E$ ): Based on research findings,  $E = 260$  MPa  
and
- 2- Bricks' density ( $\rho$ ) = 1650 kg/m<sup>3</sup>.

- 3- Plastic properties (including CDP model): They are assumed to be the same as those in concrete. The compressive stress is as shown in Figure (4.8). while the tensile stress is assumed to be 10% of compressive stress=0.15 MPa, and cracking strain=0

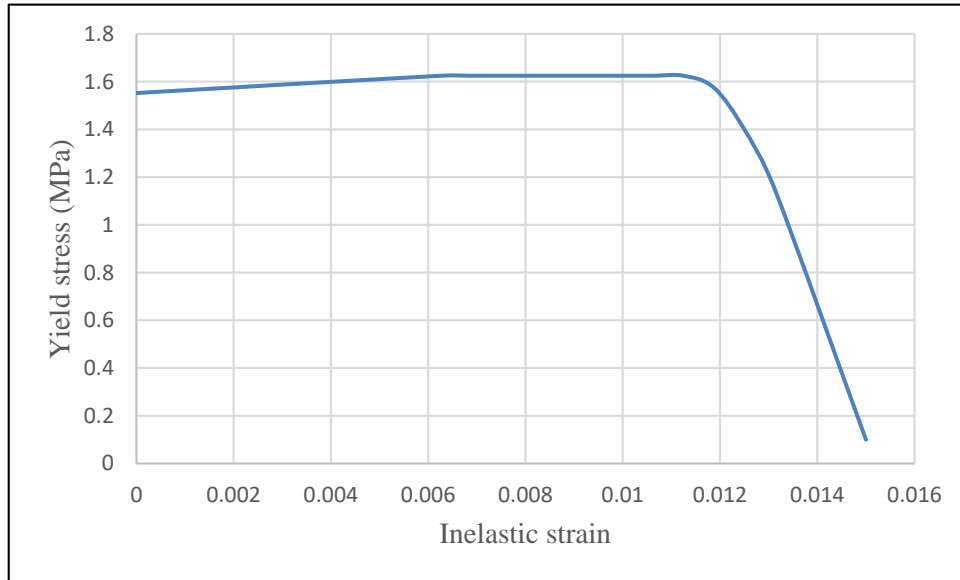


**Figure (4.8):** Yield stress Vs. inelastic strain for brick material

### ***Mortar Model***

Mortar is a mixture of water, cement and sand. It is used as a construction material to bind bricks firmly and adhere them to the surrounding frame. Based on experiments for chapter 3, it has the following elastic and plastic properties:

- 1- Modulus of elasticity (E) and Poisson's ratio ( $\nu$ ): Based on research results,  $E = 1047$  MPa, and Poisson's ratio ( $\nu$ ) is assumed 0.2.
- 2- Mortar's density =  $1940$  kg/m<sup>3</sup>.

- 3- Plastic properties CDP: including CDP model that was assumed as for concrete, compressive behavior as shown in figure 4.9, tensile stress is assumed to be 10% of compressive stress= 1.2 MPa, and cracking strain =0).

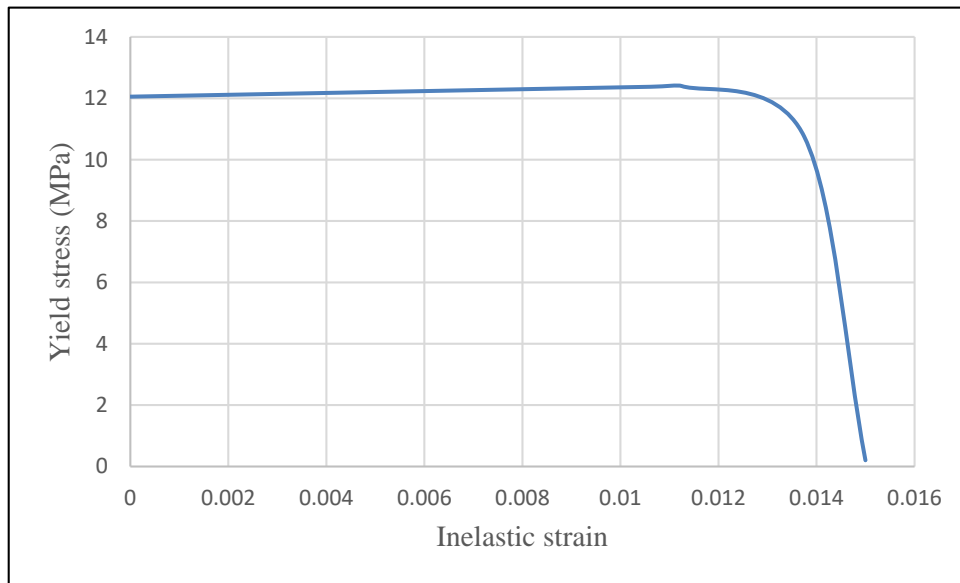


**Figure (4. 9):** Yield stress Vs. inelastic strain for mortar material

#### 4.1.2 Model Geometry

In this step, the whole set of parts needed for each model are built. These parts include brick, mortar, column, main beam, stiffener beam, loading plate, steel reinforcement and stirrups for beams and columns. At their definition, parts are all chosen to be 3-D homogenous. However, two parts including steel reinforcement and stirrups are chosen to be of the type 2-D wire. After creation of the parts, they are assigned suitable sections. In order to construct the models, parts are assembled together, ending up with building two versions of frames to be studied – bare frame and frame with bricks, as shown in Figures (4.10) and (4.11), respectively.

These parts have the following geometric characteristics:

- Brick dimensions: (length = 400 mm, width = 200 mm and depth = 100 mm).
- Mortar dimensions: (suitable to neighboring bricks with thickness = 5 mm).
- Stiffening beam: (width = 200 mm, depth = 100 mm).
- Loading plate: (thickness = 30 mm, length and width are equal to column size).

Main beam, columns and steel reinforcement are given variable dimensions as dictated by the parametric study which is illustrated later in this chapter.

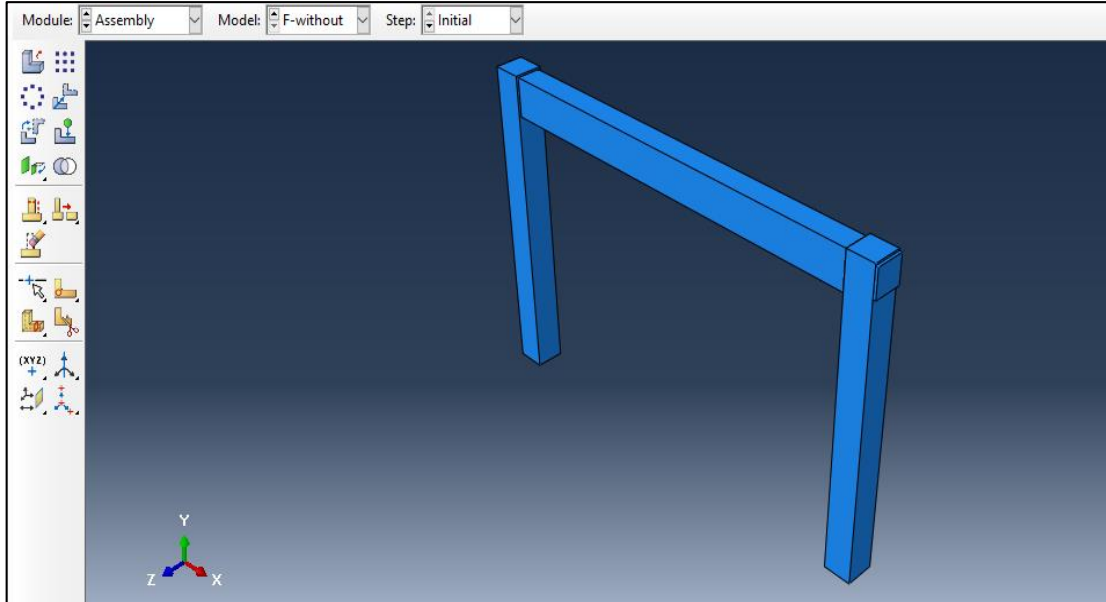


**Figure (4.10):** 3-D model of a frame without brick wall (bare frame)

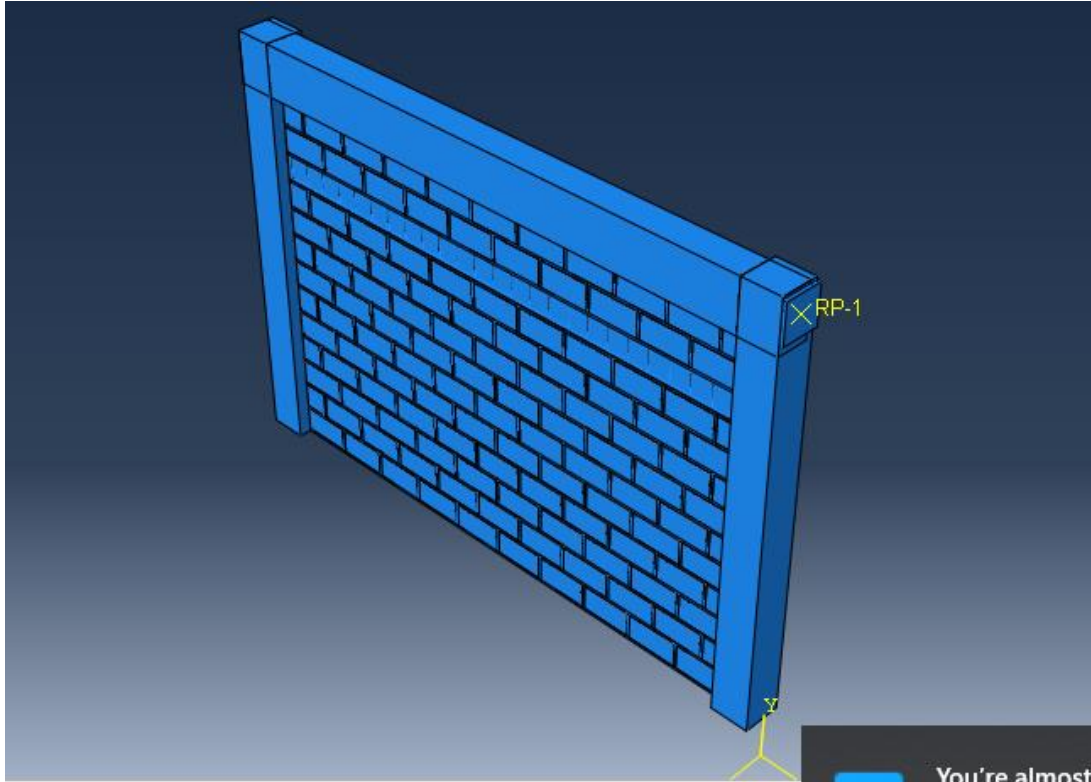


**Figure (4.11):** 3-D frame with a brick wall

### 4.1.3 Modeling of interfaces

There are some parameters that govern the selection of a suitable model for the interfacial regions. They mainly include the actual behavior and degree of accuracy. First, one of the types is the tie contact which is used to connect beam and columns parts, and to connect columns and loading plates as well. This contact is a perfect bond that is when placed between a pair of surfaces, it keeps their translational and rotational displacements as well as all other active degrees of freedom equal. At the same time, embedded region contact represents a perfect bond, allowing no slip of reinforcement in the concrete. In reality this can be justified by the enough development length provided for rebar and the available friction that naturally exists between them. In this

type of contact, the translational degrees of freedom of the embedded body are contained in the host elements. Secondly, cohesive contact is used to simulate the behavior of adhesive interaction between brick and mortar as discussed in the following section. Using this contact, delamination as well as slip can be modeled at interfaces in terms of traction versus. separation.

#### **4.1.4 Parameters for cohesive contact**

In order to model the cohesive behavior, two constitutive curves are needed – the force-slip and separation-traction curves. In fact, several models are available with different complexity levels. For example, the linear-brittle model, developed by Neubauer and Rostasy (1999), ignores the softening behavior, while Nakaba et al. (2001) and Savioa et al. (2003) make use of the ascending and descending branches of bond-slip curve to consider the softening behavior. Monti et al. (2003), on the other hand, presented a bilinear bond-slip curve. A “Precise model” was presented by Lu et al. (2005). It is regarded as a very complicated model. However, in this research an experimental shear test is conducted, and verified by simulating the test in ABAQUS as shown in Figure (4.12).

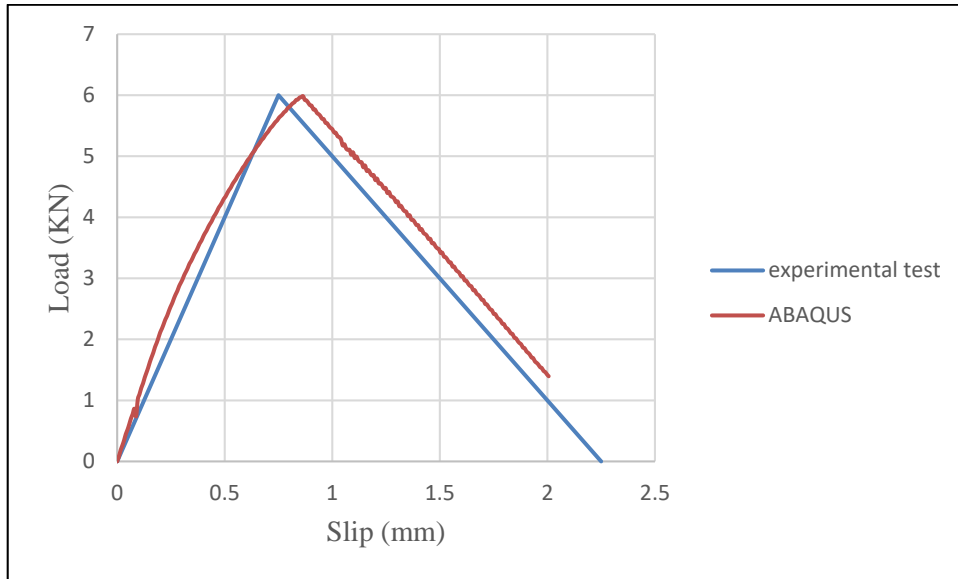


**Figure (4. 12):** Force-slip curve obtained from analyzing ABAQUS model, and from experimental test

The shear test is simulated by modeling two specimens of bricks, connected by a mortar layer, with the contact defined as a cohesive contact with calibrated parameters to fit the experimental test as shown in Figure (4.12). The main value that needs to be obtained from the model is the maximum shear stress beyond which the sample is immediately damaged. Figure (4.12) clearly shows that the maximum shear force reached is 6 kN. Shear is resisted by the area separating between bricks that is shown in Figure (4.13). This area equals  $400 \times 100 \text{ mm}^2$ , therefore, the maximum shear stress is 0.15 MPa according to Equation (4.10).

$$\begin{aligned}
 \text{Shear stress} &= \frac{\text{Shear force}}{\text{Area}} = \frac{6000}{400 \times 100} \\
 &= 0.15 \text{ MPa}
 \end{aligned}
 \tag{4.10}$$

The post peak force-slip curve was assumed to be linearly decaying up to twice the displacement corresponding to the peak force, the slip that corresponds to the maximum shear force (6 KN) is 0.75 mm. Therefore, the final displacement reached by the force–slip curve is  $0.75+(2 \times 0.75) = 2.25$  mm.

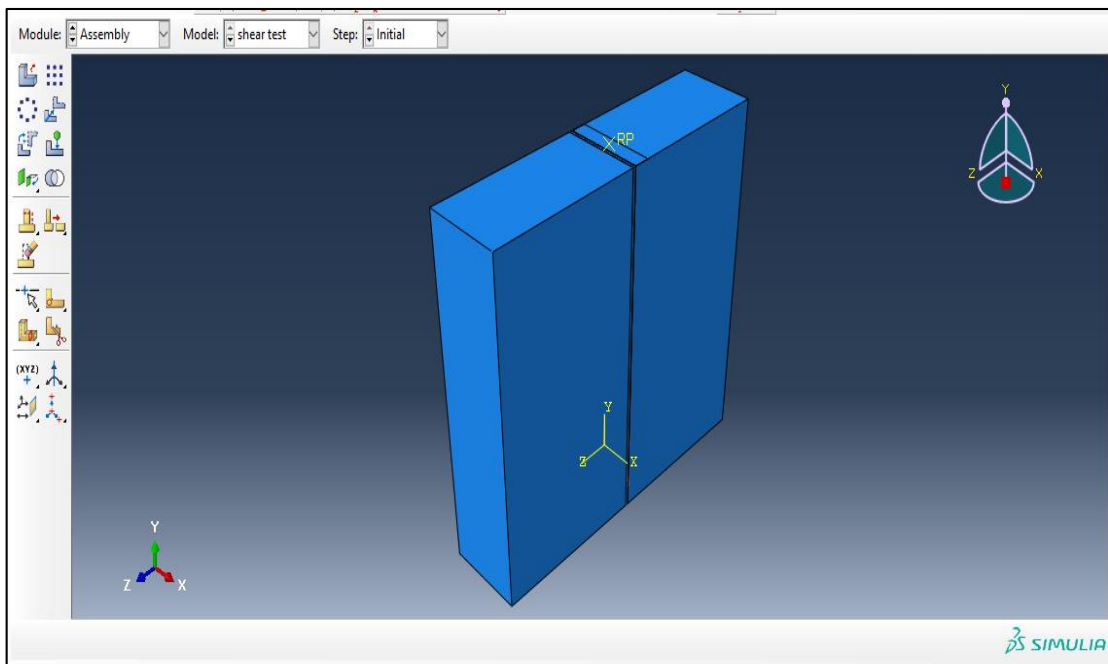


**Figure (4.13):** Model of the shear test in ABAQUS for two bricks connected with mortar

#### 4.1.5 Analysis type, loading and boundary conditions

For the purpose of obtaining the full behavior of the model and to prevent emergence of convergence problems in ABAQUS, Pseudo-dynamic analysis is utilized. This requires the load to be applied very slowly with very long time steps in order to converge to the static condition. The advantage of dynamic analysis over static analysis is that it helps solution to converge in ABAQUS in the case of highly non-linear behavior of cohesive contact.

Translational and rotational movements are prevented at the bottom ends of the frame by attaching them to fixed supports. Furthermore, the center point of loading plate is applied through displacement control. A uniform load is also applied to the main beam, with different load values used in each model. On the other hand, columns in each model are assigned a compression axial load with a value of  $0.25A_g f'_c$ , Where  $A_g$  is the gross area of the column, and  $f'_c$  is the compressive strength of concrete used to build the column.

### ***Meshing type and sensitivity study***

Meshing for all components of the brick wall and bare frame is implemented on part-by-part basis instead of using global or sweep mesh. The solid elements including bricks, mortar, main beams, stiffener beams, columns and loading plates; are modeled using 8-noded linear brick element (C3D8R). On the other hand, main reinforcement and stirrups are modeled using 2-noded linear 3-D truss element (T3D2). This is shown in Figure (4.14).

Selection of a suitable mesh size depends on how accurate the results are desired within an acceptable run time of the model. In fact, the smaller the mesh size is the more accurate the results become, and the longer takes the runtime. For this purpose, a sensitivity study is conducted in order to determine the most proper mesh size for the model. Four mesh sizes (40mm, 50mm, 70mm and 90mm) are considered in the sensitivity study. Results of the sensitivity study are represented by the curves in Figure (4.15). It can be

observed that, for all models, a mesh size of 50mm provides suitable accuracy. Selecting this size makes it possible to fit two elements within the wall thickness (100mm).

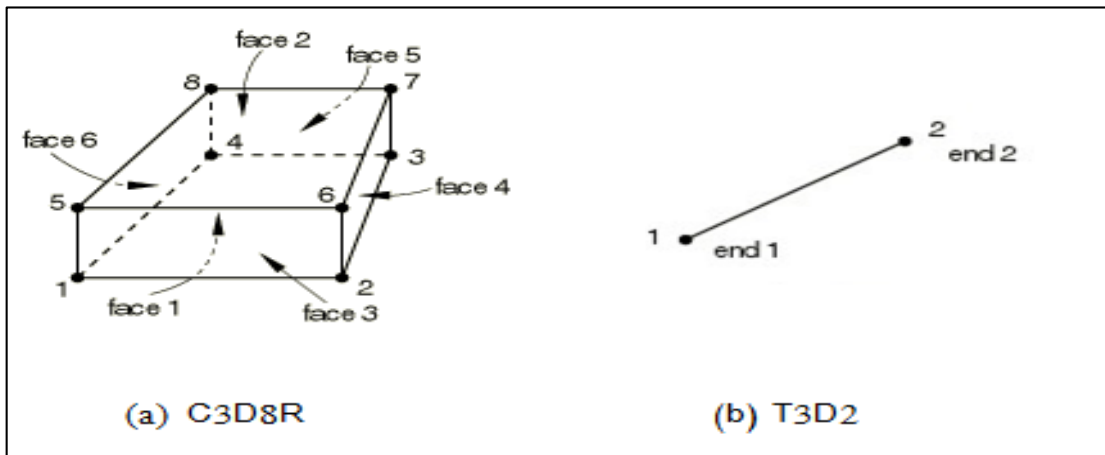


**Figure (4.14):** Finite element types used for modeling the frames

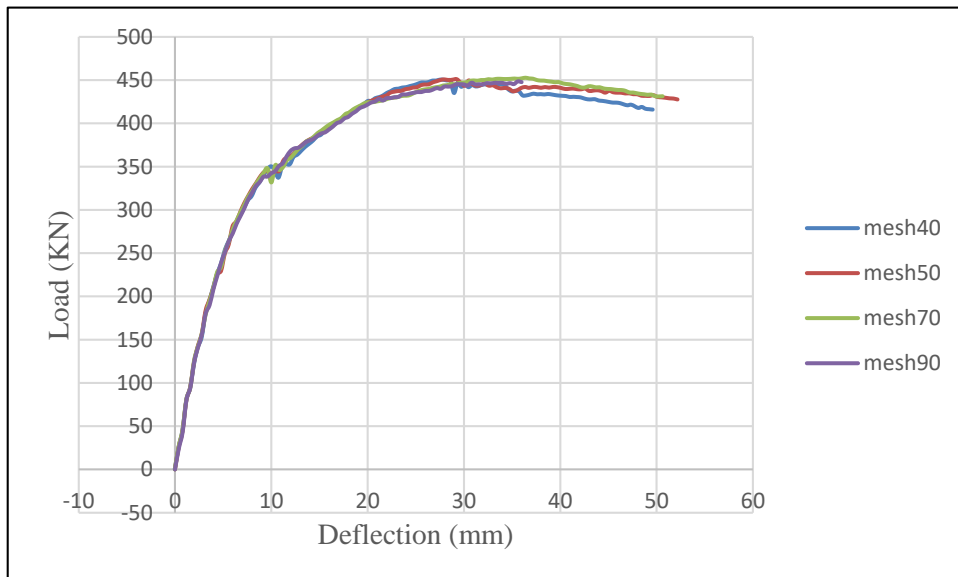


**Figure (4.15):** Load-deflection curves for several type of meshes, as used for the sensitivity study

## 4.2 Model verification

### 4.2.1 Overview

To validate the results from the finite element model, the analytical solution is found by using the virtual work method, this method is used to verify the results of the bare frame. Furthermore, additional verification is conducted for the brick wall.

The virtual work method is used to find the deflection for each bare frame and brick wall at the linear stage (before cracking) in order to compare their stiffness with the stiffness computed based on ABAQUS results. The analytical solution is assumed to be at the linear stage to avoid the complexity in finding the nonlinear properties for the brick wall such as the cracked moment of inertia.

The bare frame of model W5 C50 and brick wall of 5m length are used to be verified under the following assumptions:

- 1- For model verifications, flexure, shear and axial deformations are considered according to virtual work method.
- 2- The bare frame is assumed to have uncracked sections for beam and columns. Therefore, the gross moment of inertia is used in calculation.
- 3- Modulus of elasticity for beam and column sections in the bare frame is assumed to be equal to the concrete modulus of elasticity.
- 4- SAP2000 software is used to find moment, shear and axial diagram for the bare frame.

- 5- The brick wall section is also assumed to be uncracked.
- 6- The modulus of elasticity of brick wall is calculated twice, one by assuming it equal to brick modulus of elasticity, which is 260 MPa; and the other by assuming the modulus of elasticity of brick wall equal to the mortar modulus of elasticity, which is 1047 MPa. Therefore, there are upper and lower limits of brick wall stiffness.
- 7- Axial deflection is neglected in the brick wall only. However, it is considered in the bare frame.
- 8- In the brick wall model, it is assumed that the stiffness of the brick wall in the linear stage (before cracking) is not affected by the surrounding frame. This means that models (W5 C30, W5 C50 and W5 C75), in the linear stage, have stiffness values between lower and upper limit that are computed using the virtual work method, this is explained in the following subsection.

$$\Delta_f = \int_0^l m_v k dx = \frac{1}{E_c I_g} \int_0^l m_v M_r dx \quad (4.11)$$

$$\Delta_s = \frac{\mathcal{F}}{G_c A} \int_0^l v_v V_r dx \quad (4.12)$$

$$\Delta_a = \frac{1}{E_c A} \int_0^l n_v N_r dx \quad (4.13)$$

$$\mathcal{F} = \frac{6}{5} \quad \text{for rectangular cross section} \quad (4.14)$$

$$I_e = \left( \frac{M_{cr}}{M_y} \right)^3 I_g \quad (ACI - 318) \quad (4.15)$$

$$M_{cr} = \frac{f_r I_g}{y_b} \quad (4.16)$$

$$f_r = 0.62 \sqrt{f_c'} \quad (4.17)$$

$$I_g = \frac{BH^3}{12} \quad (4.18)$$

Where:

$\Delta_f$  : Flexural deflection

$l$ : Length of element

$m_v$  : Virtual moment

$k$ : Curvature

$M_r$ : Real moment

$I_e$ : Effective moment of inertia of cross section

$\Delta_s$ : Shear deflection

$\mathcal{F}$  : Shear shape factor

$A$ : Area of cross section

$v_v$ : Virtual shear force

$V_r$  : Real shear force

$\Delta_a$ : Axial deflection

$n_v$ : Virtual axial force

$N_r$ : Real axial force

$I_g$ : Gross moment of inertia

$f_r$ : Modulus of rupture

$y_b$ : Depth of natural axis before cracking which is equal approximately  $(\frac{H}{2})$  for rectangular cross section.

$B$ : Width of cross section

$H$ : Depth of cross section

#### **4.2.2 Methodology of calculating bare frame stiffness**

As mentioned earlier. Model W5 C50 is used to be verified, this model has the following characteristics:

- 1- Beam length is equal to 5270mm, and its cross section has dimensions of 400mm x 250mm.
- 2- Columns height is equal to 3300mm, and their cross section have dimensions of 500mm x 500mm.
- 3- Modulus of elasticity for beam and columns is equal to 23000 MPa, and Poisson ratio is equal to 0.2.
- 4- Columns are restrained with fixed supports.

A lateral load of 1000N is applied to the bare frame as shown in Figure (4.16). The resulting axial, shear and moment diagrams are shown in Figures (4.17 – 4.20).

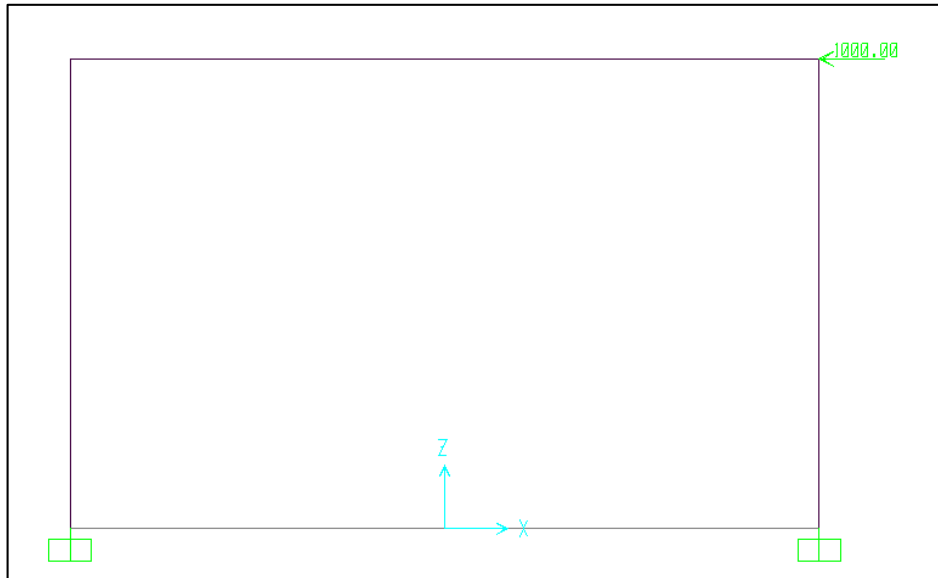


**Figure (4.16):** The bare frame of model (W5 C50) that is used for verification by the virtual work method, as appears in SAP2000

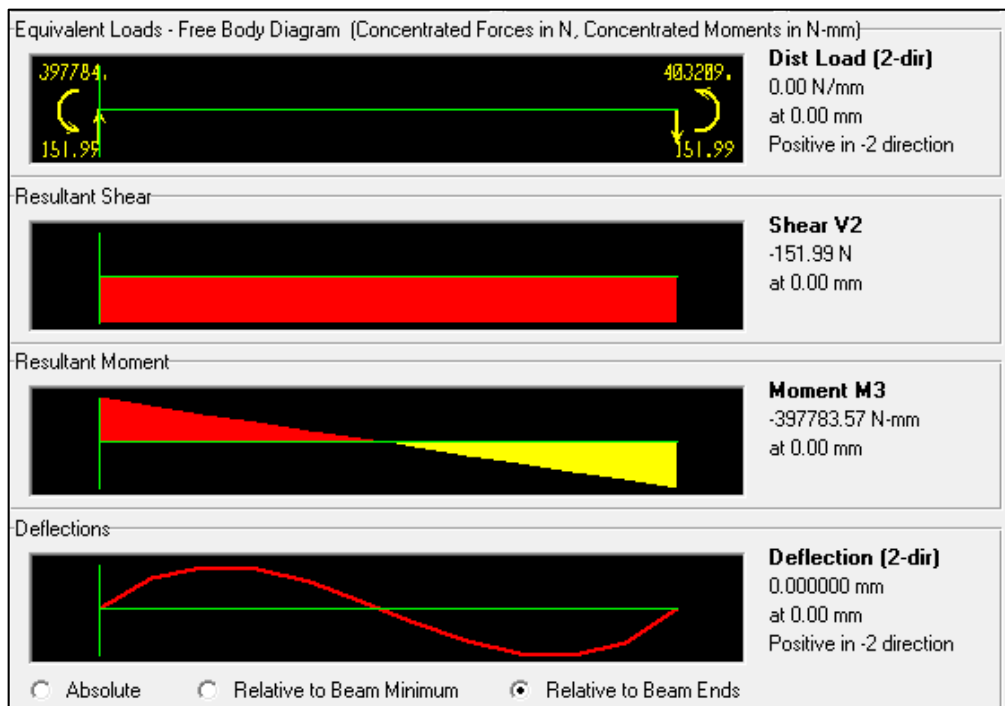


**Figure (4.17):** Virtual shear and moment diagrams of the beam in the bare frame of model (W5 C50) used for verification by the virtual work method, as obtained from SAP2000

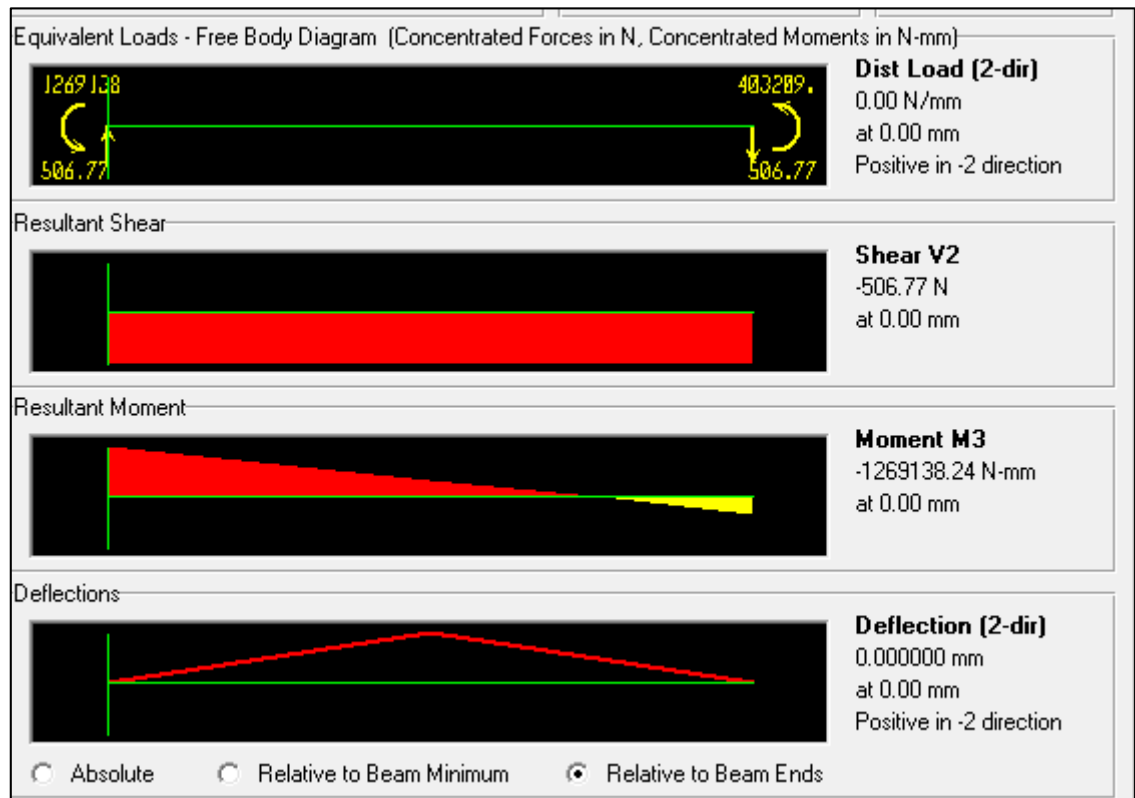


**Figure (4.18):** Virtual shear and moment diagrams for the right column in the bare frame of model (W5 C50) used for verification by the virtual work method, as obtained from SAP2000



**Figure (4.19):** Virtual shear and moment diagrams for the left column in the bare frame of model (W5 C50) used for verification by the virtual work method, as obtained from SAP2000

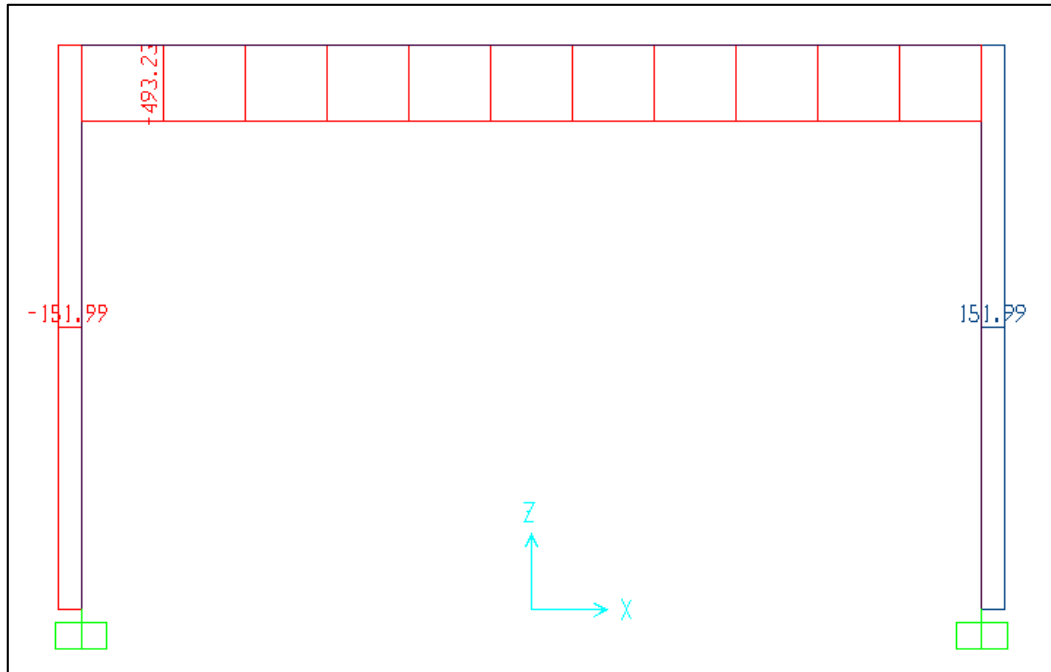


**Figure (4.20):** Virtual axial force diagram for the bare frame of model (W5 C50) used for verification by the virtual work method, as obtained from SAP2000

It should be noted that the units in the previous Figures (4.16 – 4.20) are in (N and mm).

The real axial, shear and moment diagrams resemble those in Figures (4.17 – 4.20). On the other hand, the virtual axial, shear and moment diagrams are the same of figures (4.17– 4.20) but the values divided by 1000 kN.

After finding the real and virtual axial, shear and moment diagrams for the bare frame, and by using Equations (4.11 – 4.19), it becomes possible to calculate the total deformation of the bare frame under lateral load. The axial, shear and flexural deformations are found as below:

$$\delta_{axial} = 0.00057mm$$

$$\delta_{shear} = 0.00095mm$$

$$\delta_{flexure} = 0.0345mm$$

The total deformation of the bare frame under the lateral load (1000 N) as well as the stiffness of the bare frame are given by Equations (4.20) and (4.21), respectively.

$$\delta_{total} = 0.00057 + 0.00095 + 0.0345 = 0.0359 \text{ mm} \quad (4.19)$$

$$K = \frac{P}{\delta_{total}} = \frac{1}{0.0395} = 25.316 \text{ kN/mm} \quad (4.20)$$

It appears later in the next chapter that the bare frame of model (W5 C50) exhibits a stiffness of 24.6 KN/mm in ABAQUS during the linear stage. Therefore, an error of 2.85% results between the two values (the one obtained by Equation (4.21) and that obtained by ABAQUS).

### 4.2.3 Methodology of calculating the brick wall stiffness

The brick wall consists of two components – brick and mortar. This makes it complex to find its stiffness accurately. Therefore, the brick wall is simplified as 1-D model restrained by fixed support and subjected to lateral load. Furthermore, the methodology of calculating the brick wall stiffness is done into two stages; the modulus of elasticity of the brick wall is assumed to be equal to the brick modulus of elasticity, and then it is assumed to be equal to the mortar modulus of elasticity. This model is analyzed with neglecting the surrounding frame. Based on this assumption, it may be

predicted that the stiffness of brick walls for different surrounding frames are closer in value to each other in the linear stage. The brick wall of model W5 that is analyzed using the virtual work method has the following characteristics:

- 1- Brick wall height is equal to 2900mm, with cross section dimensions of 5270mm x 100mm.
- 2- The brick wall is analyzed as a 1-D model restrained by fixed support and subjected to a lateral load equal to 1000 N.
- 3- The brick model is analyzed twice. In the first step, it is assumed that the modulus of elasticity of the brick wall is equal to 260MPa. On the other hand, in the second step, the brick wall modulus is assumed to be equal to 1047 MPa.
- 4- Axial deformation is neglected.

By using the virtual work method, the same method followed in the previous subsection, the deformation and stiffness of the brick wall is computed for the first step based on Equations (4.22) and (4.23), taking into account the following values:

$$E = E_{brick} = 260 \text{ MPa}$$

$$\delta_{shear} = 0.061 \text{ mm}$$

$$\delta_{flexure} = 0.025 \text{ mm}$$

$$\delta_{total} = 0.061 + 0.025 = 0.0866 \text{ mm} \quad (4.21)$$

$$K = \frac{P}{\delta_{total}} = \frac{1}{0.0866} = 11.55 \text{ kN/mm} \quad (4.22)$$

For the second step, the deformation and stiffness of the brick wall is computed based on Equations (4.24) and (4.25), taking into account the following values:

$$E = E_{mortar} = 1047 \text{ MPa}$$

$$\delta_{shear} = 0.0025 \text{ mm}$$

$$\delta_{flexure} = 0.005 \text{ mm}$$

$$\delta_{total} = 0.0025 + 0.005 = 0.007 \text{ mm} \quad (4.23)$$

$$K = \frac{P}{\delta_{total}} = \frac{1}{0.007} = 142.8 \text{ kN/mm} \quad (4.24)$$

Finally, the stiffness of the brick wall in the linear stage, can be predicted falling within the following range:

$$11.5 \text{ kN/mm} < K_{brick\ wall} < 142.8 \text{ kN/mm}$$

In fact, the stiffness of brick wall for models (W5 C30, W5 C50, and W5 C75), as shown in the next chapter, have the following values (as found from the micro modeling):

$$\text{W5 C30:} \quad K_{brick\ wall} = 19.07\ kN/mm$$

$$\text{W5 C50:} \quad K_{brick\ wall} = 21.8\ kN/mm$$

$$\text{W5 C75:} \quad K_{brick\ wall} = 18.9\ kN/mm$$

It should be noted that the above values are found at the linear stage.

From the above stiffness values of the three models of brick walls, it can be noted that all of them fall within the lower and upper limits of brick wall stiffness that is found previously based on the virtual work method.

### **4.3 Parametric studies**

#### **4.3.1 General**

Based on the above verifications, the F.E. model is able to predict the behavior of frame with and without brick wall. Therefore, a parametric study is conducted to investigate the effect of two main parameters that are mainly varying in the structures in Palestine, these parameters are: the wall length; and the relative stiffness of the surrounding frame in which the columns parts are mainly considered – on the behavior of the brick wall. Therefore, nine models of brick walls as well as nine models of bare frames are analyzed, with varying the two parameters in each model, using ABAQUS software.

### 4.3.2 Parameters ranges

The validated model was used to conduct a parametric study, where nine models of different properties were analyzed. The models had the characteristics shown in Table (4.1).

**Table (4. 1): Geometric characteristics and loads for all models**

Designation	$W_B$ (m)	$D_B$ (m)	$L_B$ (m)	$H_C$ (m)	$W_C$ (m)	$D_C$ (m)	$As_c$ (mm <sup>2</sup> )	$As_t$ (mm <sup>2</sup> )	$As_b$ (mm <sup>2</sup> )	$W_s$ (kN/m)
W4 C30	0.25	0.4	4.18	3.3	0.3	0.3	4 $\phi$ 18	2 $\phi$ 14	3 $\phi$ 14	0.094
W4 C50	0.25	0.4	4.18	3.3	0.5	0.5	8 $\phi$ 20	3 $\phi$ 14	2 $\phi$ 14	0.094
W4 C75	0.25	0.4	4.18	3.3	0.75	0.75	12 $\phi$ 25	4 $\phi$ 14	2 $\phi$ 14	0.094
W5 C30	0.25	0.4	5.27	3.3	0.3	0.3	4 $\phi$ 18	3 $\phi$ 14	2 $\phi$ 16	0.094
W5 C50	0.25	0.4	5.27	3.3	0.5	0.5	8 $\phi$ 20	2 $\phi$ 14	2 $\phi$ 16	0.094
W5 C75	0.25	0.4	5.27	3.3	0.75	0.75	12 $\phi$ 25	2 $\phi$ 14	4 $\phi$ 16	0.094
W7 C30	0.3	0.6	7.12	3.3	0.3	0.3	4 $\phi$ 18	3 $\phi$ 14	4 $\phi$ 25	0.085
W7 C50	0.3	0.6	7.12	3.3	0.5	0.5	8 $\phi$ 20	4 $\phi$ 16	4 $\phi$ 16	0.085
W7 C75	0.3	0.6	7.12	3.3	0.75	0.75	12 $\phi$ 25	4 $\phi$ 18	2 $\phi$ 18	0.085

Symbols and terms used in Table (4.2) are illustrated below:

- 1- W4 C30: Name of the model that consists of a 4m long wall and columns of 0.3x0.3m cross section.
- 2-  $W_B$ : Main beam width in (m).
- 3-  $D_B$ : Main beam depth in (m).
- 4-  $L_B$ : Main beam length in (m).
- 5-  $H_C$ : Column height in (m).
- 6-  $W_C$ : Column width in (m).

- 7-  $D_C$ : Column depth in (m).
- 8-  $A_{s_c}$ : Area of steel in column in ( $\text{mm}^2$ ).
- 9-  $A_{s_t}$ : Top reinforcement in main beam in ( $\text{mm}^2$ ).
- 10-  $A_{s_b}$ : Bottom reinforcement in main beam in ( $\text{mm}^2$ ).
- 11-  $W_s$ : Uniform service load on main beam in ( $\text{kN/m}$ ).

The beams and columns in the nine models are designed according to ACI-318. Ratios (or modifiers) of effective moments of inertia for columns and beams were taken as 0.7 and 0.35, respectively. On the other hand, a uniform service load (dead load (DL) + live load (LL)) is applied to the main beam, where the dead load is computed as (cross section area x concrete density + superimposed dead load (SIDL)). Superimposed dead load is found to be  $0.48 \text{ kN/m}^2$  as calculated by adding the weights of the layers indicated in Figure (6.3) in Chapter 6. Live load is taken to be  $4.8 \text{ kN/m}^2$  as recommended by ASCE for the case of commercial buildings.

## **Chapter 5**

### **Results of Micro Modeling and Discussion**

#### **5.1 General**

The parametric study resulted in load-deflection curves for all cases, which are used later to estimate the stiffness of brick wall. The stiffness values are used to develop an equivalent strut model. Afterwards, regression analysis is conducted to obtain a simplified practical equation for the width of the equivalent strut which is used for the next macro modeling step.

#### **5.2 Behavior of models**

Load-deflection curves for each of the bare frame and frame with brick wall models of the nine cases are presented herein. In order to understand the behavior of the models, the effects of the most influencing parameters on each frame are discussed in the subsequent subsections.

##### **5.2.1 Effect of wall length**

The frames are modeled by keeping the column section factor constant, and each model has different wall length. The resulting load-deflection curves for different wall lengths are obtained for column cross section of (0.3 x 0.3), (0.5 x 0.5) and (0.75 x 0.75) as shown in Figures (5.1), (5.2) and (5.3).

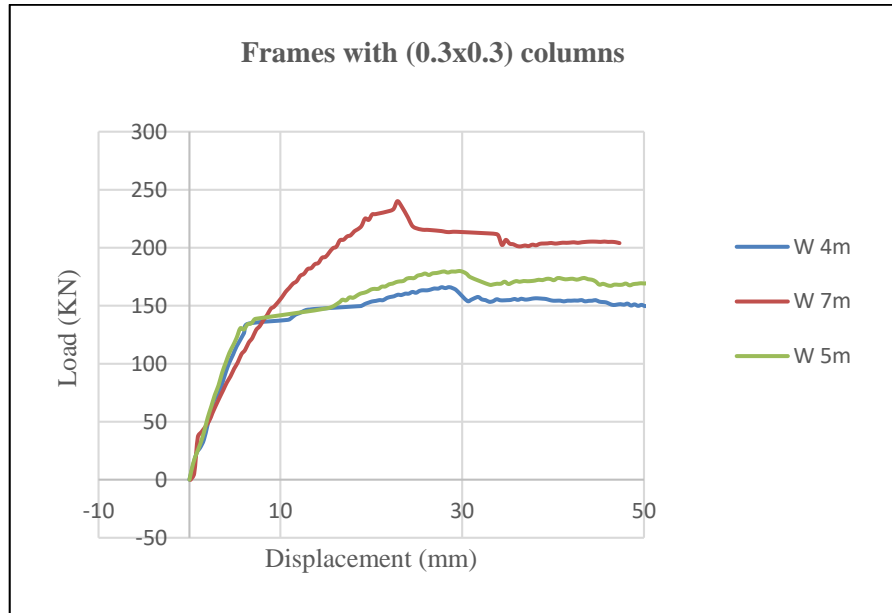


**Figure (5.1):** Load-deflection curves of three frame models, all having (0.3x0.3) columns cross sections, with three different wall lengths, as obtained from ABAQUS

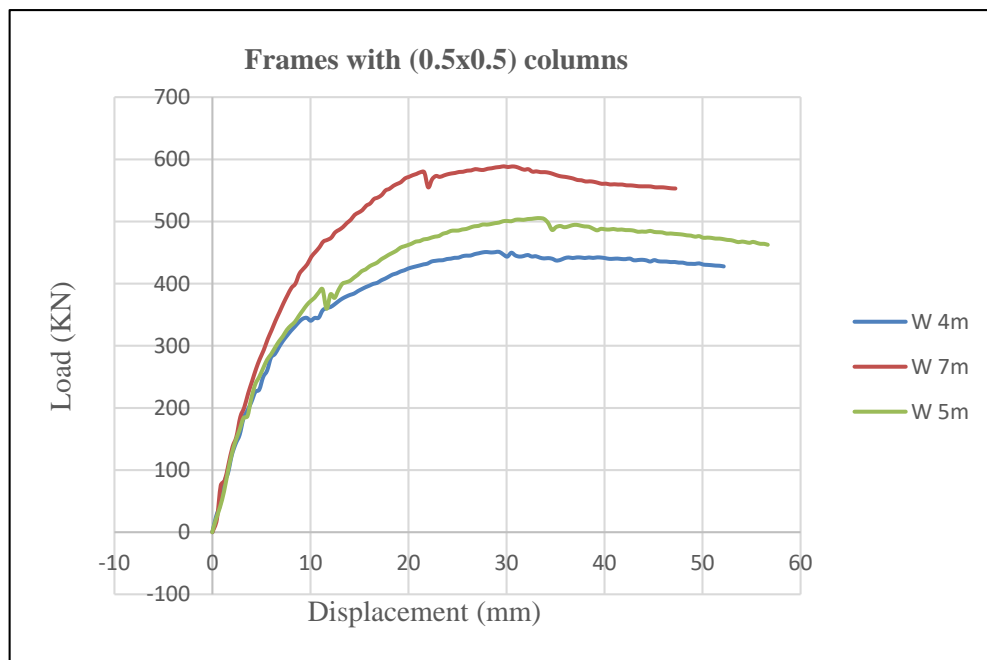


**Figure (5.2):** Load-deflection curves of three frame models, all having (0.5x0.5) columns cross sections, with three different wall lengths, as obtained from ABAQUS

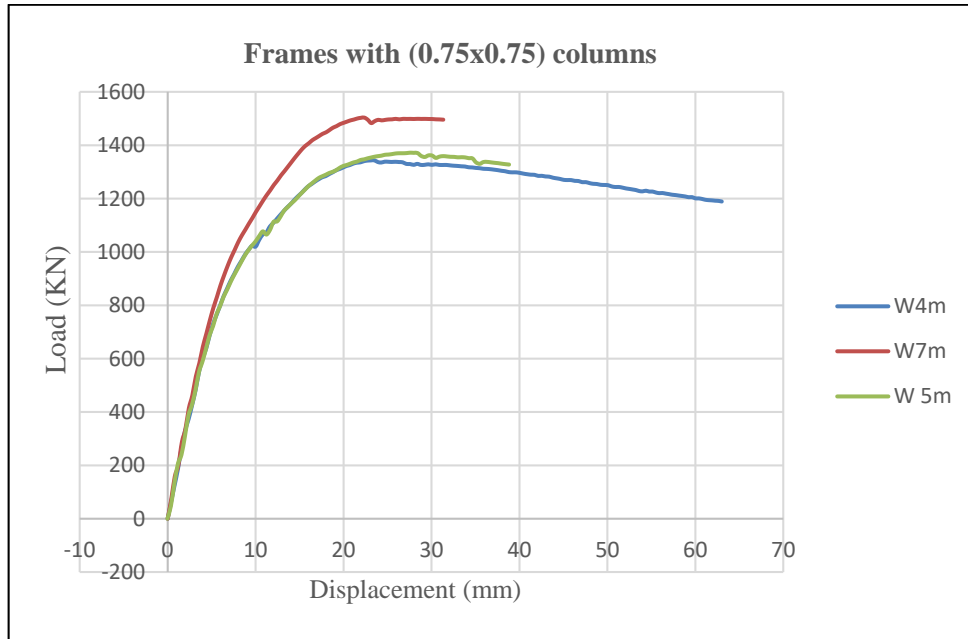


**Figure (5.3):** Load-deflection curves of three frame models, all having (0.75x0.75) columns cross sections, with three different wall lengths, as obtained from ABAQUS

From the load-deflection curves shown in Figures (5.1 – 5.3), it can be concluded that wall stiffness increases by increasing wall length, because of the additional stiffness that is resulted from the increase in wall length. However, it should be noted in Figure 5.1 that the stiffness of frame W5m and W4m have larger stiffness value than frame W7m at the beginning of load-deflection curve, because of shear slipping that occurred in the frame W7m as will be discussed later.

### 5.2.2 Effect of column size

The frames are modeled by keeping the wall length factor constant, and each model has different column size. The resulting load-deflection curves for different column sizes are shown in Figures (5.4), (5.5) and (5.6).

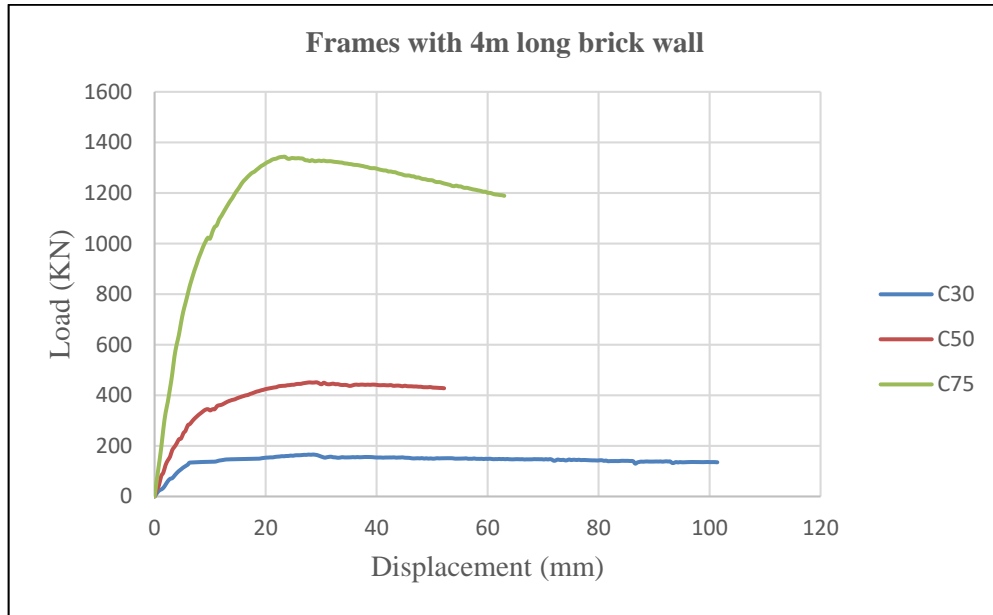


**Figure (5.4):** Load-deflection curves of three frame models, all having 4m long brick walls, with three different column cross sections, as obtained from ABAQUS

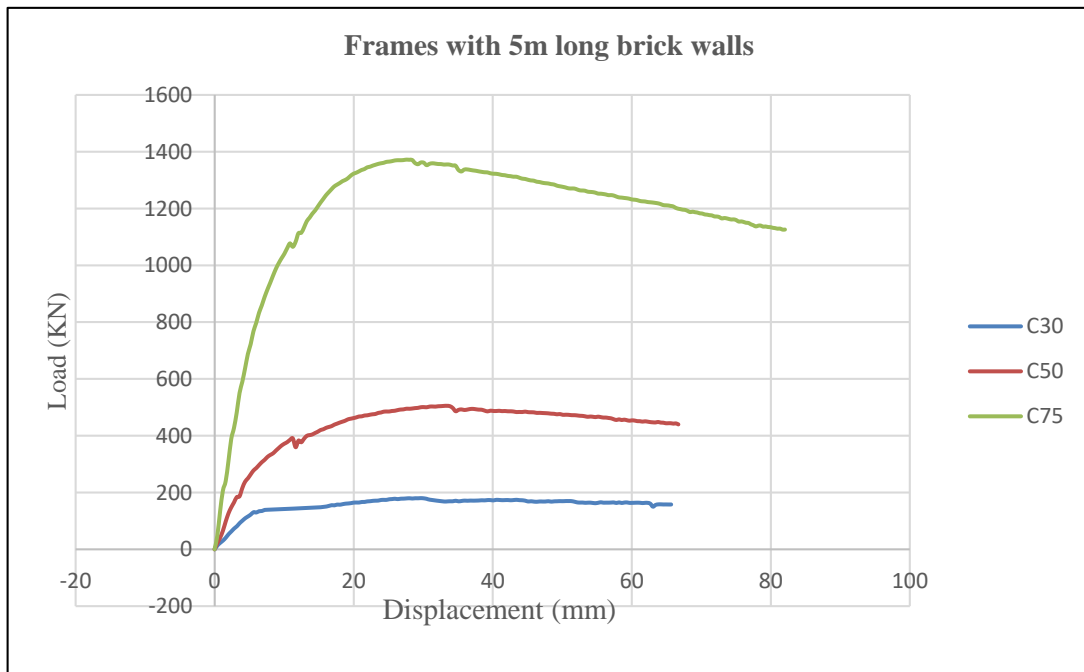


**Figure (5.5):** Load-deflection curves of three frame models, all having 5m long brick walls, with three different column cross sections, as obtained from ABAQUS

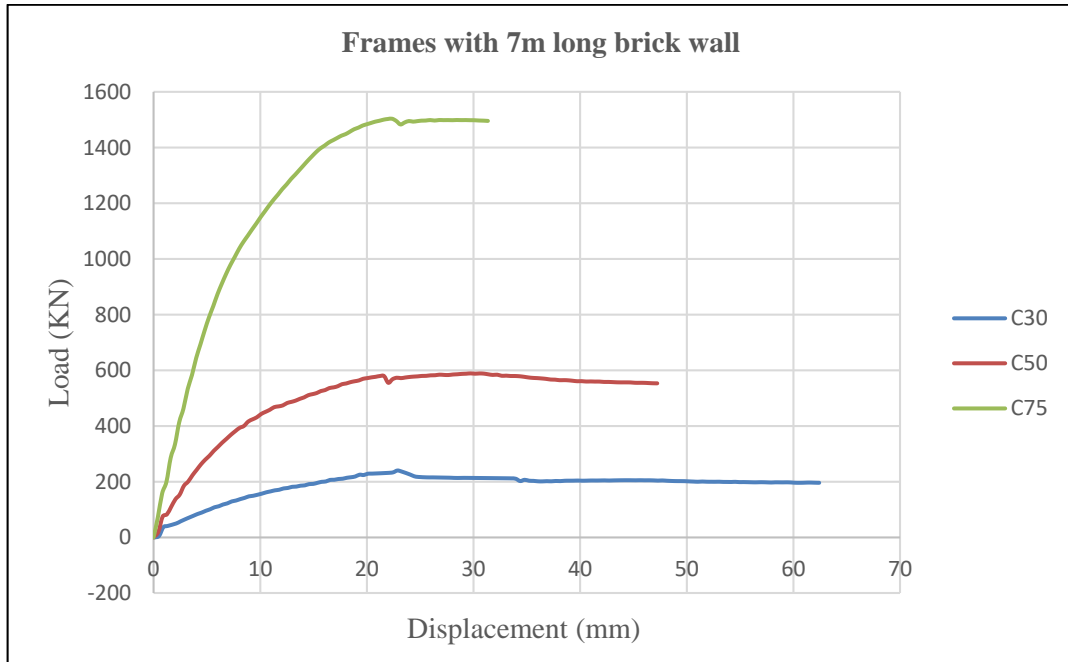


**Figure (5.6):** Load-deflection curves of three frame models, all having 7m long brick walls, with three different column cross sections, as obtained from ABAQUS

From the load-deflection curves shown in Figures (5.4 – 5.6), it can be concluded that frame stiffness increases by increasing column size. In contrast, the increasing of column size is found that decreases the stiffness of brick wall in the frame because of shear slipping that occurred in the bricks, this will be discussed later in the subsequent section.

### 5.2.3 Effect of brick wall

The effect of brick wall existence within the surrounding frame is reflected by Figures (5.7 - 5.15). Each figure shows the load – deflection curve for two frames: the frame with brick wall, and the frame without brick wall, in order to find the stiffness of brick wall.

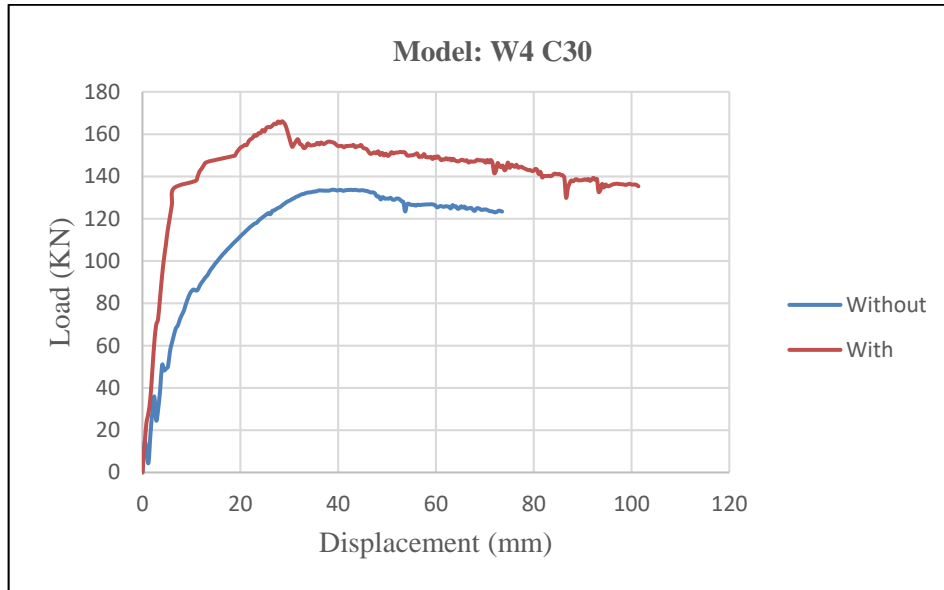


**Figure (5.7):** Load-deflection curves for frame W4 C30 with and without bricks, as obtained from ABAQUS

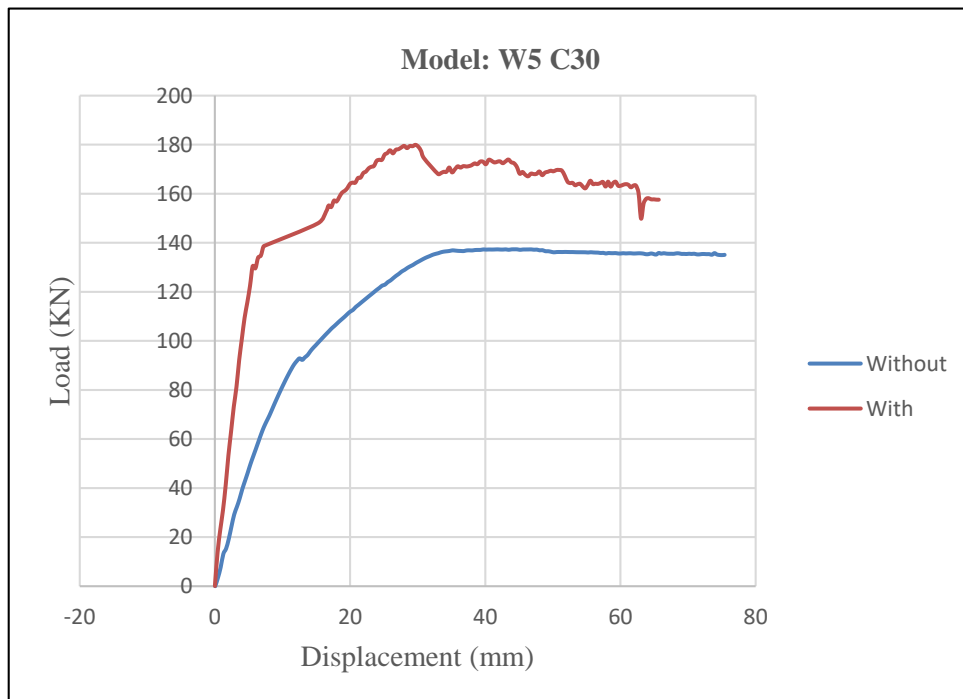


**Figure (5.8):** Load-deflection curves for frame W5 C30 with and without bricks, as obtained from ABAQUS

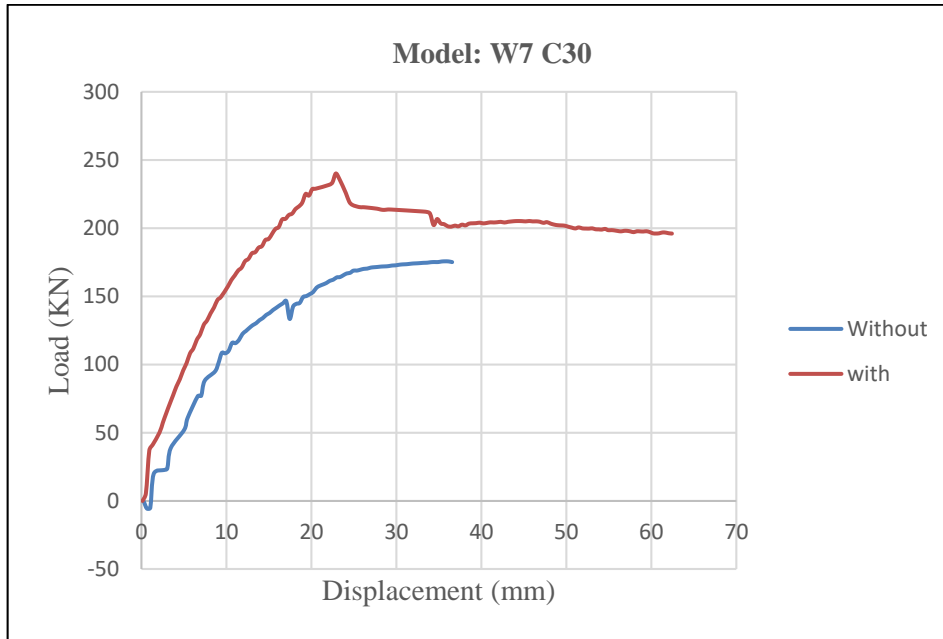


**Figure (5.9):** Load- deflection curves for frame W7 C30 with and without bricks, as obtained from ABAQUS

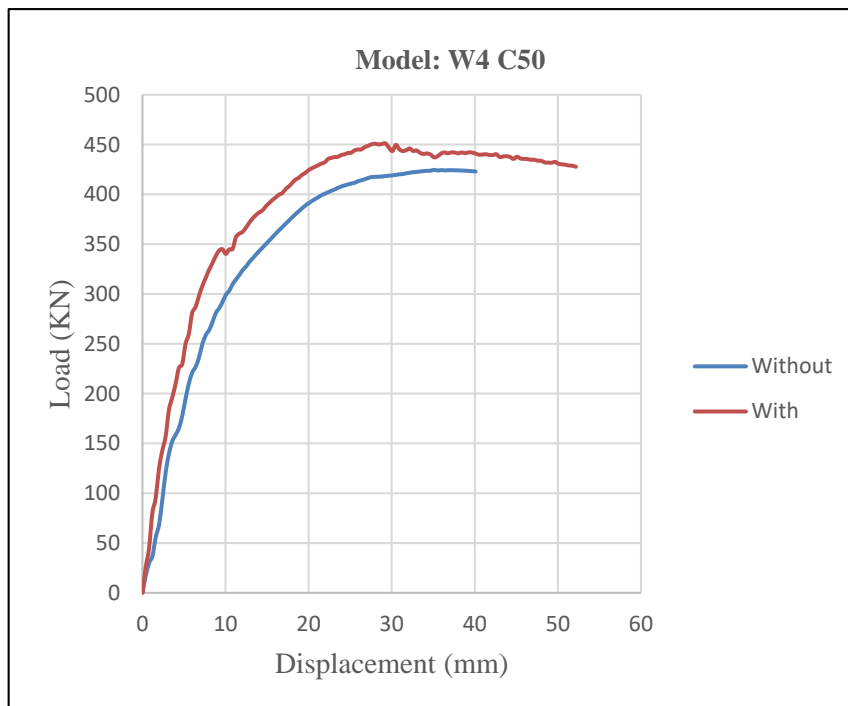


**Figure (5.10):** Load- deflection curves for frame W4 C50 with and without bricks, as obtained from ABAQUS

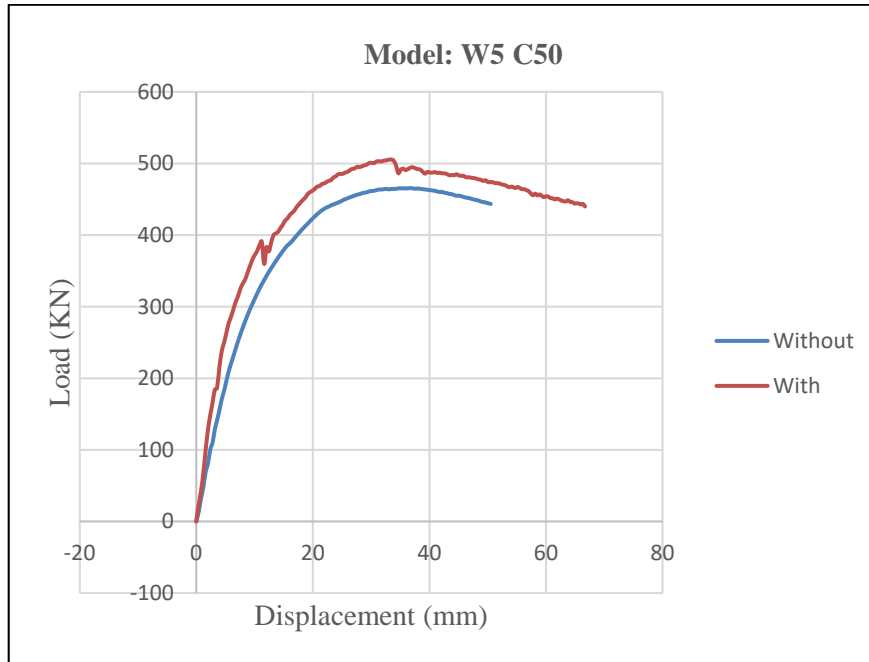


**Figure (5.11):** Load- deflection curves for frame W5 C50 with and without bricks, as obtained from ABAQUS

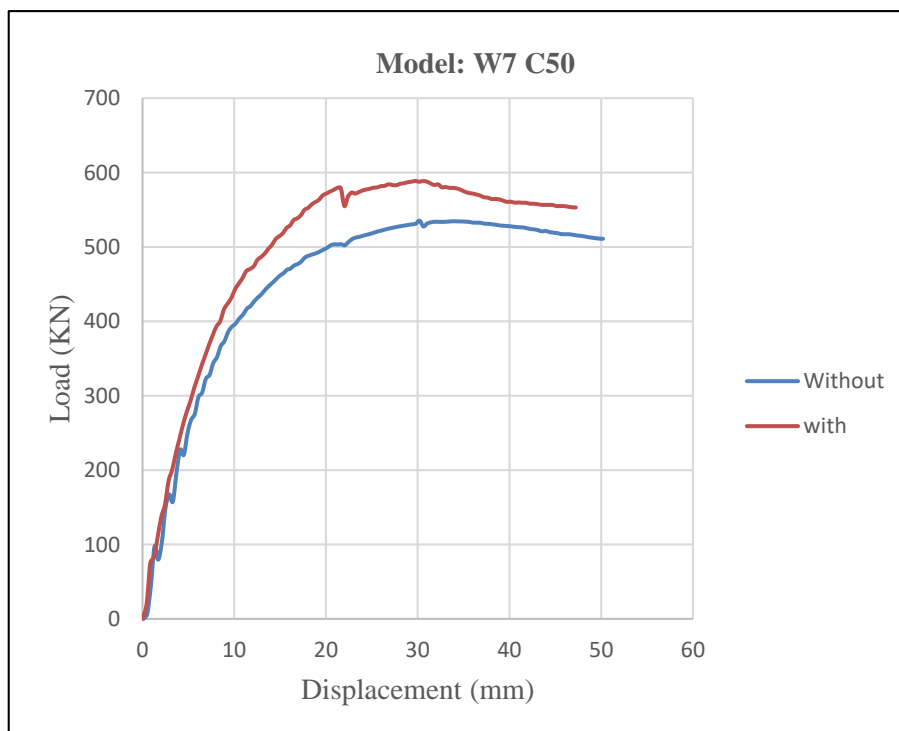


**Figure (5.12):** Load - deflection curves for frame W7 C50 with and without bricks, as obtained from ABAQUS

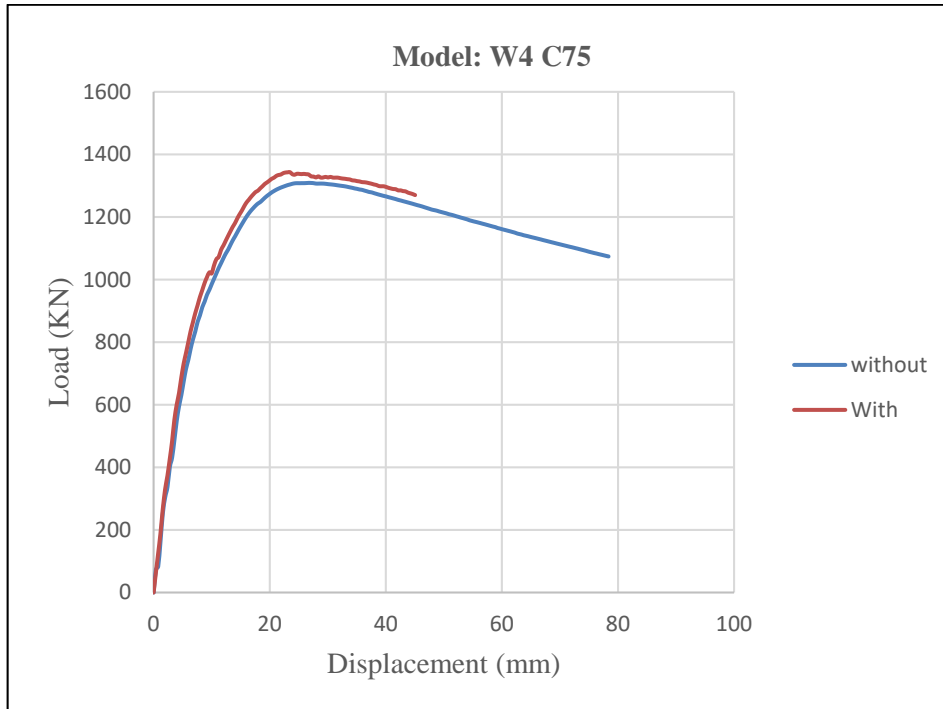


**Figure (5.13):** Load- deflection curves for frame W4 C75 with and without bricks, as obtained from ABAQUS

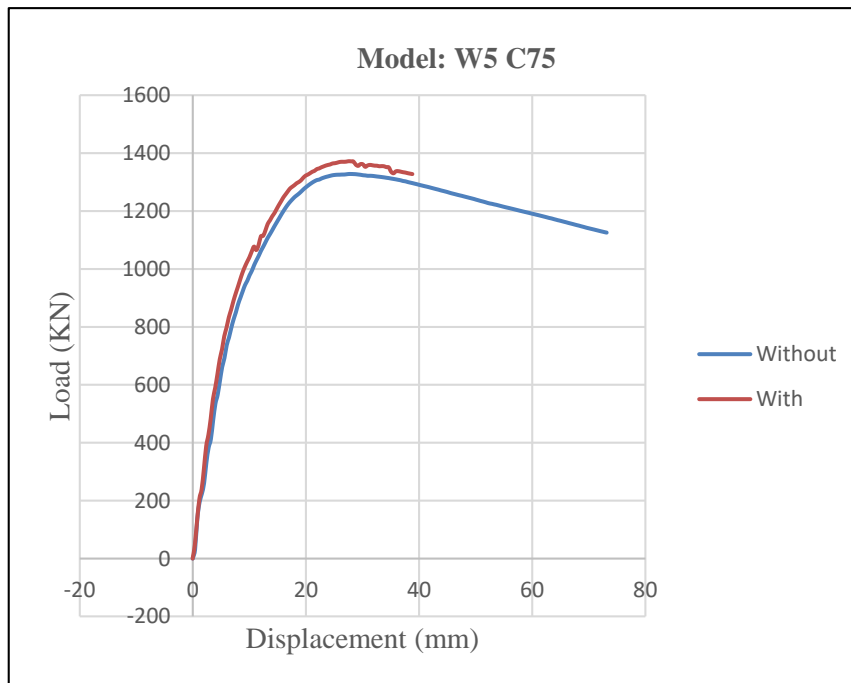


**Figure (5.14):** Load- deflection curves for frame W5 C75 with and without bricks, as obtained from ABAQUS

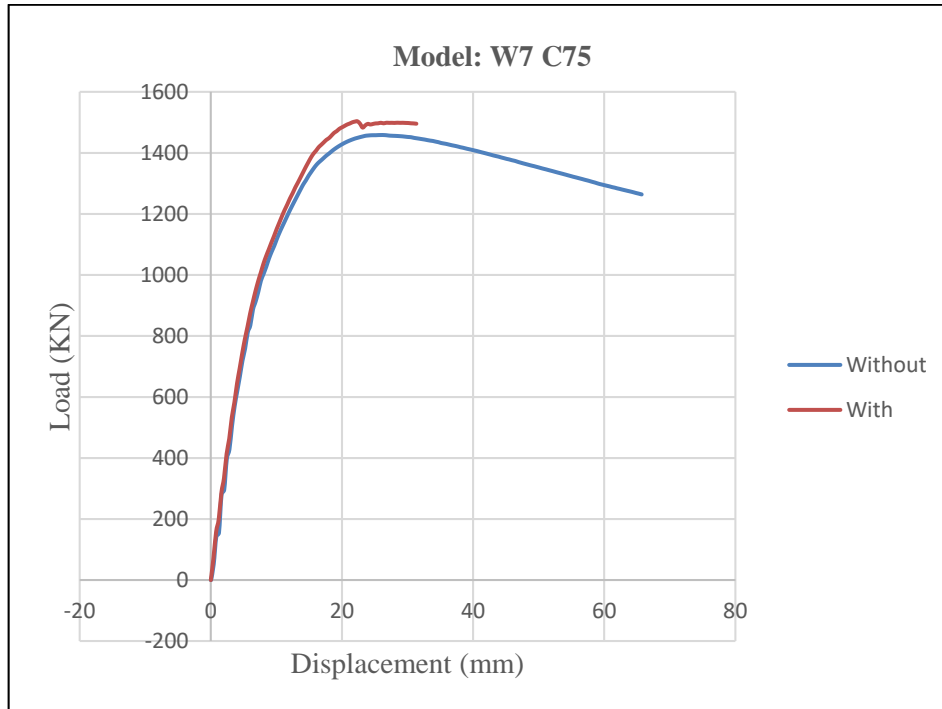


**Figure (5.15):** Load- deflection curves for frame W7 C75 with and without bricks, as obtained from ABAQUS

From Figures (5.7 to 5.15) it can be observed that the existence of bricks increases the stiffness of the surrounding frame by increasing the length of the frame and by decreasing column size. For example, it is found from figures of W4 C50 and W7 C50 that the stiffness of brick wall in frame W7 C50 is more than the stiffness of brick wall in frame W4 C50. In contrast, it is found from figures of W7 C50 and W7 C75 that the stiffness of brick wall in frame W7 C50 is more than the stiffness of brick wall in frame W7 C75. This fact is illustrated in details in the subsequent sections.

### 5.3 The end of linearity

In order to calculate the stiffness of brick wall from the resulting load-deflection curves, a criterion is needed to specify the end of linearity in the

behavior. The first portion in the load- deflection curves is used to find the stiffness of brick wall, because the main purpose of the research is to find the fundamental period of the frames with brick wall and for this, the stiffness is our main concern. Therefore, the point at which the first yield in either beam or column reinforcement occurs, this point is assumed as the end of linearity in behavior, and the secant stiffness of the brick wall is calculated at this point as  $\frac{P}{\delta}$ . This criterion is applied for all curves.

**Failure stages:**

The previous load-deflection curves consist of three stages, namely, cracking, slipping and yielding which is considered in this research as the end of linearity.

**Cracking:**

The stage at which cracking occurred was when the tensile stress reached 2.9 MP in either beam or column as shown in Figure (5.16).

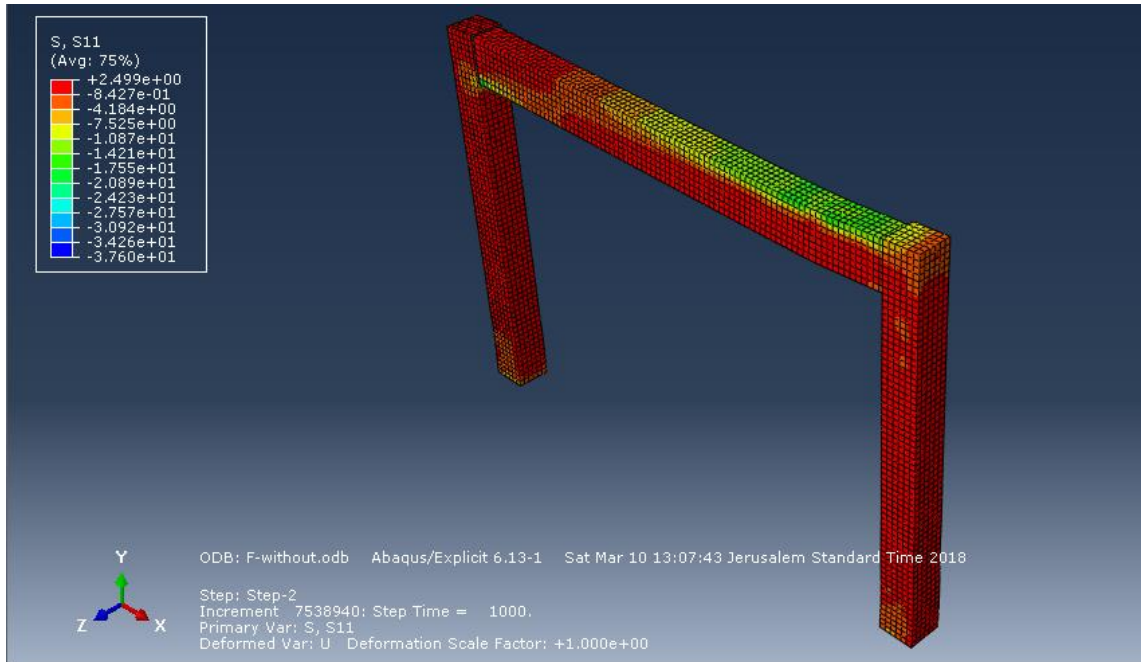


**Figure (5. 16):** Tensile stress distribution in frame W4 C50, as obtained from ABAQUS

### Slipping:

The shear slipping that occurred between bricks is shown in Figure (5.17). The figure shows the horizontal displacement distribution in the brick wall. The maximum value of deformation is at the top of the wall and equals 13.8 mm.

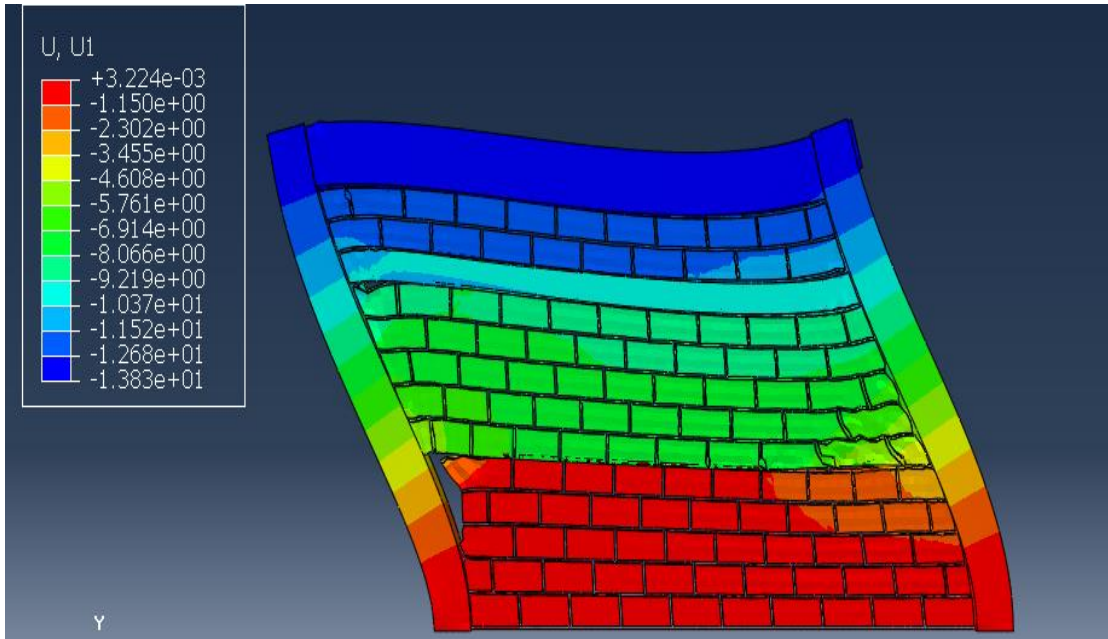


**Figure (5. 17):** Exaggerated horizontal displacement contour for brick wall W4 C30, as obtained from ABAQUS

### **Yielding:**

This stage is considered the end of linearity point in all models. It is the point at which yielding occurs either in beam or column reinforcement as shown in Figure (5.18).

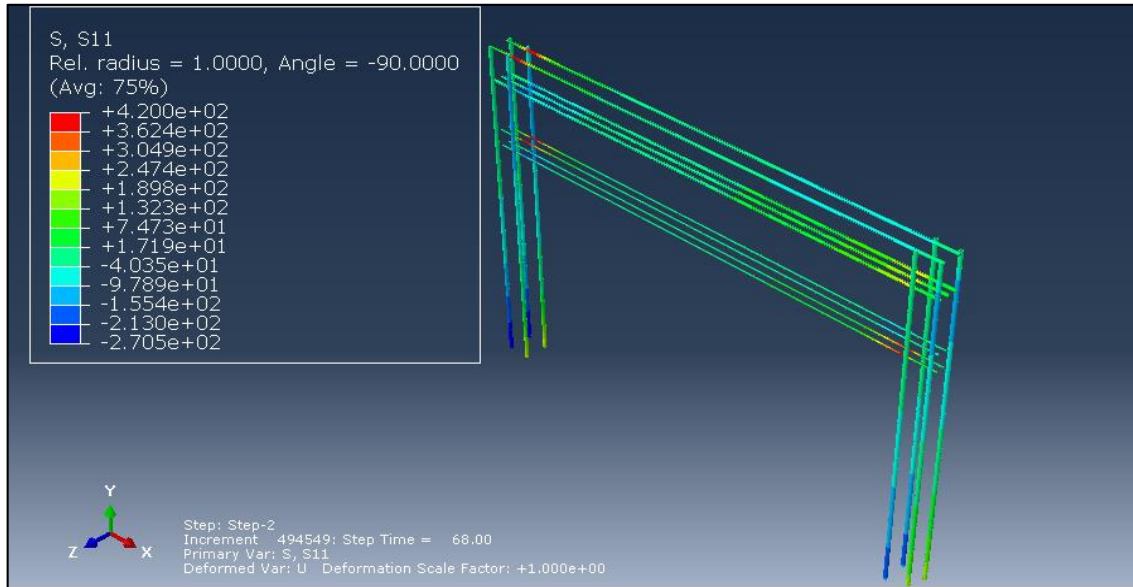


**Figure (5.18):** First yield occurred in frame W4 C30, as obtained from ABAQUS

As an example from Figure (5.18), it can be observed that the top reinforcement in the beam yields first.

In each model, the three failure stages is observed at different time step, and also at different loading value. This is summarized in Table 5.1

**Table (5. 1):** Stiffness values for all models, obtained by means of ABAQUS

Model	Load at cracking(kN)	Load at slipping(kN)	Load at yielding(kN)
W4 C30	27.8	137.9	147.17
W4 C50	79.87	297.75	344.91
W4 C75	188.3	1007.71	1195.6
W5 C30	23.05	139.07	176.46
W5 C50	40.81	402.29	453.15
W5 C75	133.6	1113.17	1181.79
W7 C30	41.16	210.74	231.81
W7 C50	82.8	400.02	443.25
W7 C75	199.5	1193.26	1302.81

## 5.4 Results and discussion

In this research, 18 models are studied in order to estimate the stiffness of the brick wall. This stiffness is estimated by determining the difference between stiffness of the frame with brick wall and the bare frame at a certain point during loading. This point is chosen to be the point at first yielding that occurs either in beam or column reinforcement. The results are summarized in Table (5.2).

**Table (5. 2): Stiffness values for all models, obtained by means of ABAQUS**

<b>Model</b>	<b>K-with (kN/mm)</b>	<b>K-without (kN/mm)</b>	<b>K-brick (kN/mm)</b>
W4 C30	10.779	8.743	2.04
W4 C50	35.832	33.968	1.86
W4 C75	82.947	82.58	0.37
W5 C30	6.699	4.596	2.1
W5 C50	24.129	21.982	2.15
W5 C75	84.195	83.565	0.63
W7 C30	10.5	7.657	2.84
W7 C50	43.92	41.322	2.6
W7 C75	98.099	96.653	1.45

Terms used in Table (5.2) are illustrated below:

K-with: Stiffness of the frame with brick wall.

K-without: Stiffness of the bare frame.

K-brick: Stiffness of the brick wall.

As shown in Table 5.1 and that is discussed earlier, that the stiffness of brick walls increases by increasing the frame wall length and decreasing

the column size in the surrounding frame. It is shown that the maximum value of brick wall stiffness is for model W7 C30 which is equal to 2.84 kN/mm, and the minimum value is for model W4 C75 which is equal to 0.37 kN/mm.

### Equivalent strut model:

After obtaining the stiffness values of the brick wall, and after they are verified, they can be used in developing an equivalent strut model consistent with static equilibrium principles (Equations (5.1 - 5.7)). The dimensions involved in developing the strut model are sketched in Figure (5.19).

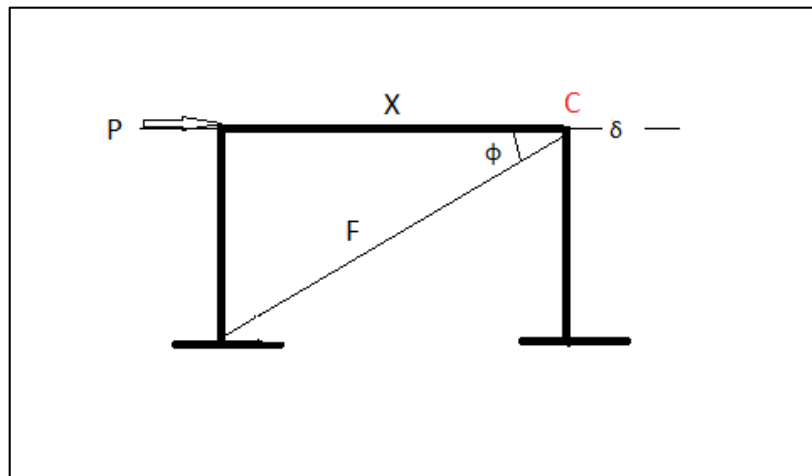


**Figure (5. 19):** Simple representation of a frame with a brick-wall-equivalent strut

The stiffness of the strut can be computed by the following equations (5.1 – 5.7).

$$P = F \cos(\phi) \quad (5.1)$$

$$F = K_s \delta \cos(\phi) \quad (5.2)$$

$$P = K_s \delta \cos^2(\phi) \quad (5.3)$$

$$\frac{P}{\delta} = K_s \cos^2(\phi) \quad K_s = \frac{EA}{L}, X = L \cos(\phi) \quad (5.4)$$

$$K_b = \frac{EA \cos^3(\phi)}{X} \quad A = bh \quad (5.5)$$

$$K_b = \frac{E bh \cos^3(\phi)}{X} \quad (5.6)$$

$$b = \frac{K_b X}{Eh \cos^3(\phi)} \quad (5.7)$$

Where:

$P$ : Laterat force applied to the wall.

$F$ : Internal force developed in the strut.

$K_b$ : Stiffness of the brick wall that is taken from F.E method.

$K_s$ : stiffness of the strut.

$b$ : Equivalent strut width.

$h$ : Equivalent strut depth.

$E$  : Modulus of elasticity of the strut material (which is considered identical to that of the brick wall).

$X$ : Wall length.

$\delta$ : Horizontal displacement of the frame when subjected to the lateral force ( $P$ ).

Based on equations (5.1 – 5.7), the stiffness of brick wall ( $K_b$ ) is replaced by stiffness of equivalent strut ( $K_s$ ). The strut width is expressed as function of ( $K_b$ ) and the wall length ( $X$ ). The strut width for each of the nine micro models are calculated and summarized in Table (5.3).

**Table (5.3): Equivalent strut width values for all models**

<b>Model</b>	<b><math>X</math> (mm)</b>	<b><math>K_b</math> (kN/mm)</b>	<b><math>b</math> (mm)</b>
W4 C30	4180	2.04	677
W5 C30	5270	2.1	700
W7 C30	7120	2.84	1041
W4 C50	4180	1.86	618
W5 C50	5270	2.15	716
W7 C50	7120	2.6	953
W4 C75	4180	0.37	123
W5 C75	5270	0.63	210
W7 C75	7120	1.44	528

### **Discussion:**

The results reveal that the stiffness of the brick wall is influenced by two factors – the brick wall length and the column size in the surrounding frame. Increasing the wall length increases the stiffness of the brick wall. In contrast, increasing the column size decreases the contribution of the brick in the lateral stiffness. This is because of the slipping that occurs between bricks when the stiffness of the surrounding frame increases. In other words, the equivalent strut width has the largest value for the frame of maximum

length and minimum column size, as observed through the values in Table (5.2). Data in Table (5.2) is correlated by a simple and practical equation as illustrated in the next section.

### **Data fitting:**

One of the main purposes of this research is to obtain a simple and practical equation that predicts the strut dimensions equivalent to a brick wall. After conducting the previous simulations and confirming the reasonability of the results, it becomes possible to develop the equation. MATLAB software is used to develop such an equation using the multivariable fitting tool. The procedure that is used in the fitting goes through some steps. First, a data set containing results from the parametric study is used to fit the equation by minimizing the norm of error between the equation and data points. The equation is then simplified. Afterwards, another set of independent F.E. simulation data are used to verify the fitted equation. The primary independent variables in the equation are selected to be the wall length ( $L_w$ ), and column size of the surrounding frame ( $A_c$ ) as shown in Table (5.4).

**Table (5.4): List of the models data used to fit the equivalent strut dimensions equation**

<b>Model</b>	<b>L<sub>w</sub> (mm)</b>	<b>A<sub>c</sub> (mm<sup>2</sup>)</b>	<b>b (mm)</b>
W4C30	4180	90000	677
W5C30	5270	90000	700
W7C30	7120	90000	1041
W4C50	4180	250000	618
W5C50	5270	250000	716
W7C50	7120	250000	953
W4C75	4180	562500	123
W5C75	5270	562500	210
W7C75	7120	562500	528

Generally, multivariable fitting is carried out in MATLAB, and a bilinear equation is applied to fit the data. The result is represented by Equation (5.8).

$$b = 76.8 + 0.12 L + 0.0005 A_c + 1.4 e^{-8 L A_c} - 2.4 e^{-9 A_c^2} \quad (5.8)$$

Where:

$b$  = Strut width in (mm).

$L$  = Wall length in (mm).

$A_c$  = Gross sectional area of the column section in the surrounding frame in (mm<sup>2</sup>).

It should be noted that Equation (5.8) is valid for wall lengths within the range (4000 mm <  $L$  < 7000 mm) and column cross sectional areas within the range (900 mm<sup>2</sup> <  $A_c$  < 5625 mm<sup>2</sup>). These ranges are specified in this

manner because they represent the domain of ( $L$  and  $A_c$ ) used to develop Equation (5.8).

The error distribution for Equation (5.8) is plotted in the Figures (5.20) and (5.21). It can be observed that the relative error is randomly distributed with respect to any of the independent variables of Equation (5.8). This means that the fit optimally provides random errors in values. The relation between strut width obtained by means of ABAQUS and that obtained from Equation (5.8) is shown in Table (5.4). The table shows that the maximum percent of error is 19%.

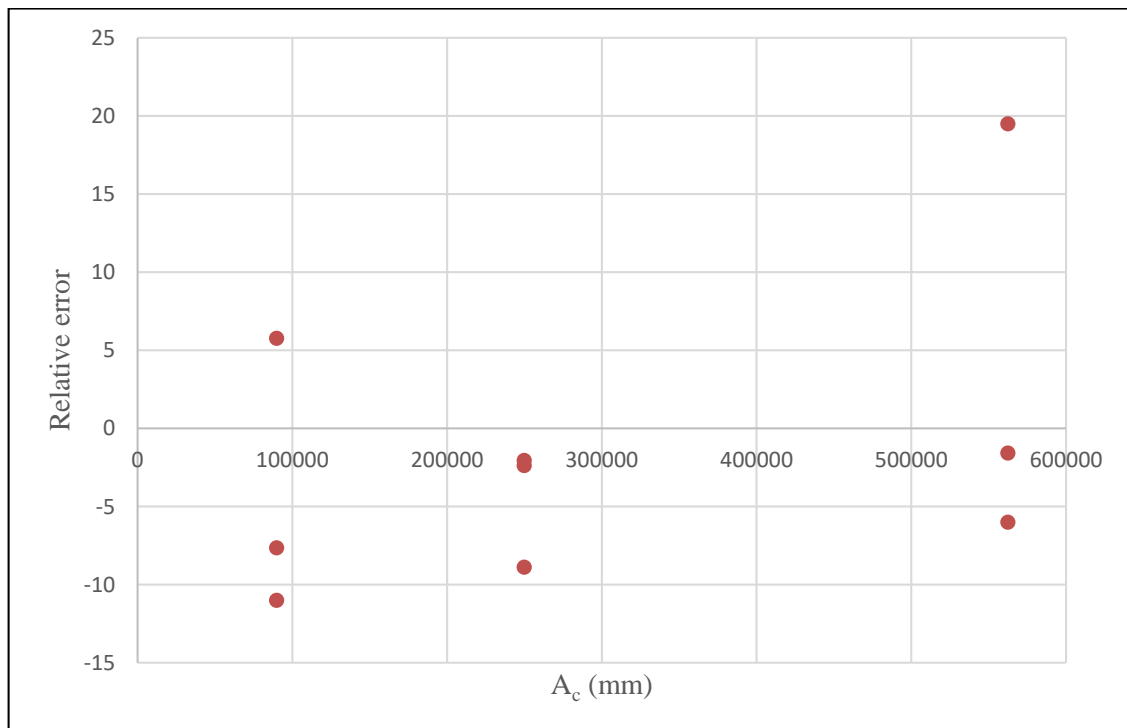


**Figure (5. 20):** Error distribution with respect to column size ( $A_c$ ) for the bilinear equation

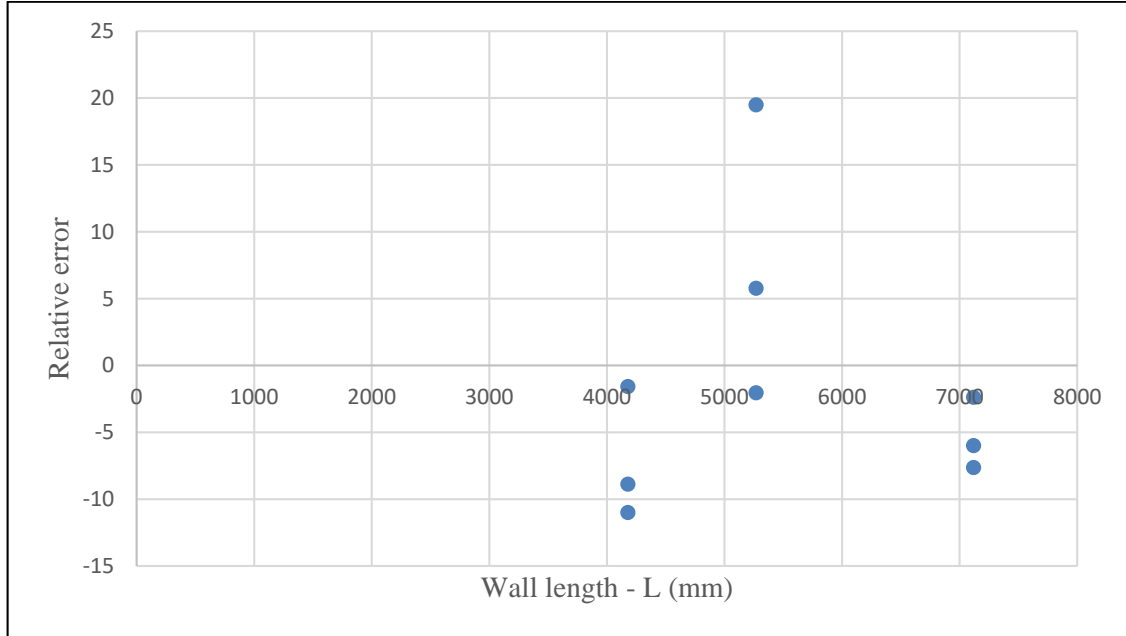


**Figure (5. 21):** Error distribution with respect to wall length ( $L$ ) for the bilinear equation

Equation (5.8) is simplified to a linear equation as given in Equation (5.9).

$$b = \frac{L}{8} - \frac{A_c}{1000} + 235 \quad (5.9)$$

Where  $L$  in mm and  $A_c$  in  $\text{mm}^2$

The simplified equation (Equation (5.9)) does not reflect significant changes in the randomness of the regression error, as shown in Figures (5.22) and (5.23). Verification of Equation (5.9) is presented in the following section.

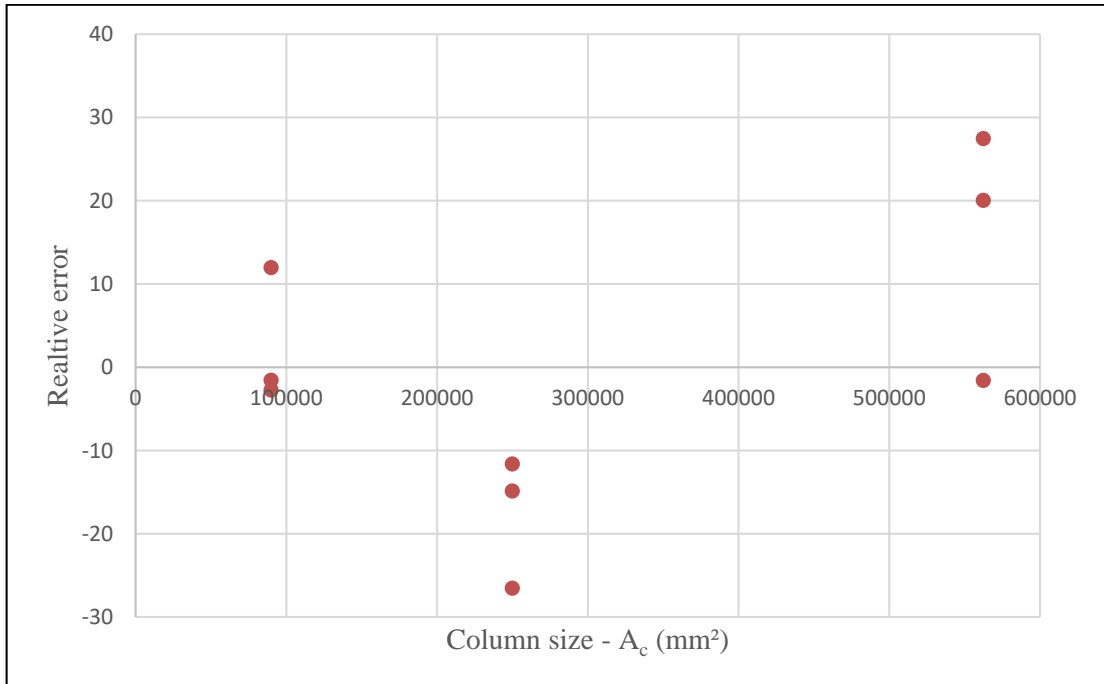


**Figure (5. 22):** Error distribution with respect to column size ( $A_c$ ) for the linear equation

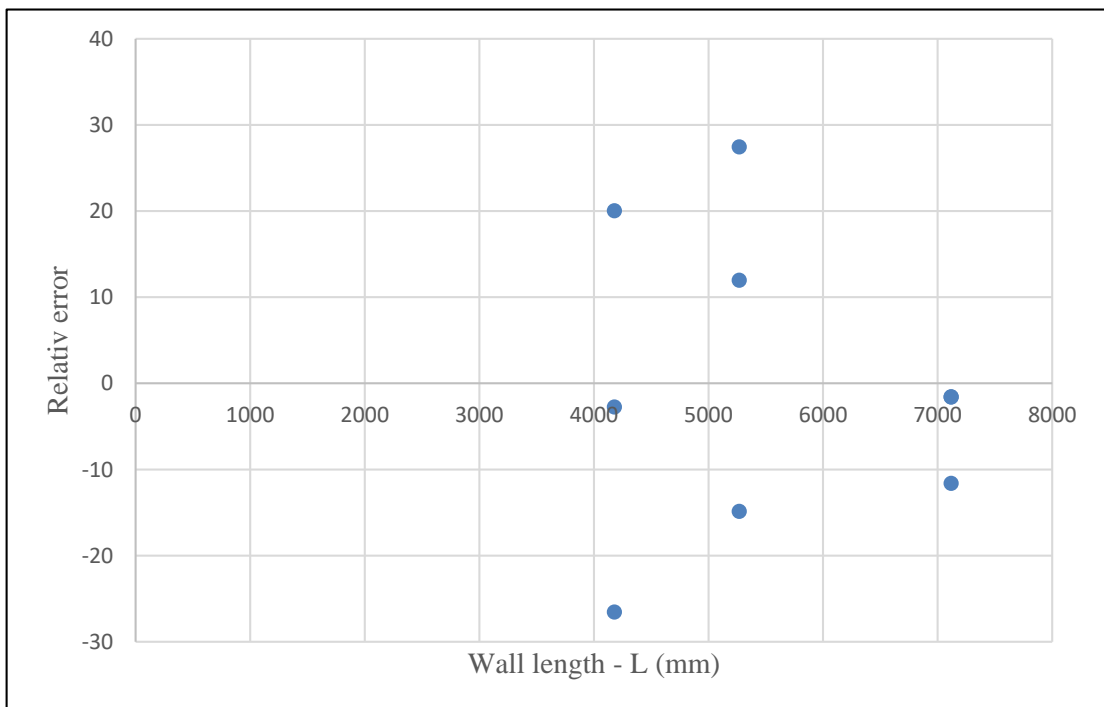


**Figure (5. 23):** Error distribution with respect to wall length ( $L$ ) for the linear equation

## 5.5 Verification of the results

For further verification, four extra models are analyzed using ABAQUS, and the results are compared to those obtained from Equation (5.9). Table (5.5) summarizes the properties of the four models and compares between results obtained both from Equation (5.9) and based on the ABAQUS analysis.

**Table (5. 5): Characteristics of the verified models and equivalent strut, with their stiffness values**

<b>Models</b>	<b>L (mm)</b>	<b>A<sub>c</sub> (mm<sup>2</sup>)</b>	<b>b<sub>s</sub></b>	<b>K<sub>s</sub></b>	<b>K<sub>ABA</sub></b>	<b>% error</b>
W6 C40	6000	160000	810	2.48	2.6	5
W6 C80	6000	640000	295	0.9	0.9	4.3
W4.5 C40	4500	160000	624	2.06	2.07	0.4
W4.5 C80	4500	640000	109	0.36	0.35	1.9

Terms used in Table (5.5) are illustrated below:

- W6 C40: Name of the model that consists of a 6m long brick wall and columns of 0.4\*0.4m cross section in the surrounding frame.
- b<sub>s</sub>: Equivalent strut width calculated using the linear equation (Equation (5.9)).
- K<sub>s</sub>: Stiffness of the brick wall calculated based on b<sub>s</sub>, by following Equations (5.1 – 5.7).
- K<sub>ABA</sub>: Stiffness of the brick wall computed from the load deflection curve that resulted from micro modeling.
- % error: the relative error in stiffness values between K<sub>ABA</sub> and K<sub>eq</sub>.

Figure (5.25) shows the relation between relative error VS. both K<sub>ABA</sub> (which was verified earlier) and K<sub>eq</sub> (which is derived based on Equations (5.1 –

5.7). This relation forms a random distribution, which means that the fitting process optimally produces random errors in values. The relation between stiffness obtained based on analysis in ABAQUS and stiffness obtained from Equation (5.9) is shown in Table (5.5).

As shown in Figure (5.25) that the relation between relative error and each of the derived  $K$  ( $K_{eq}$  given by Equation (5.9)) and verified  $K$  ( $K_{ABA}$  based on ABAQUS results) has a random distribution. This means that the fit optimally provides random errors in values. The relation between stiffness from ABAQUS and stiffness from Equation (5.9) is shown in Table (5.4). Figure (5.25) shows the maximum percentage of error is 5%.

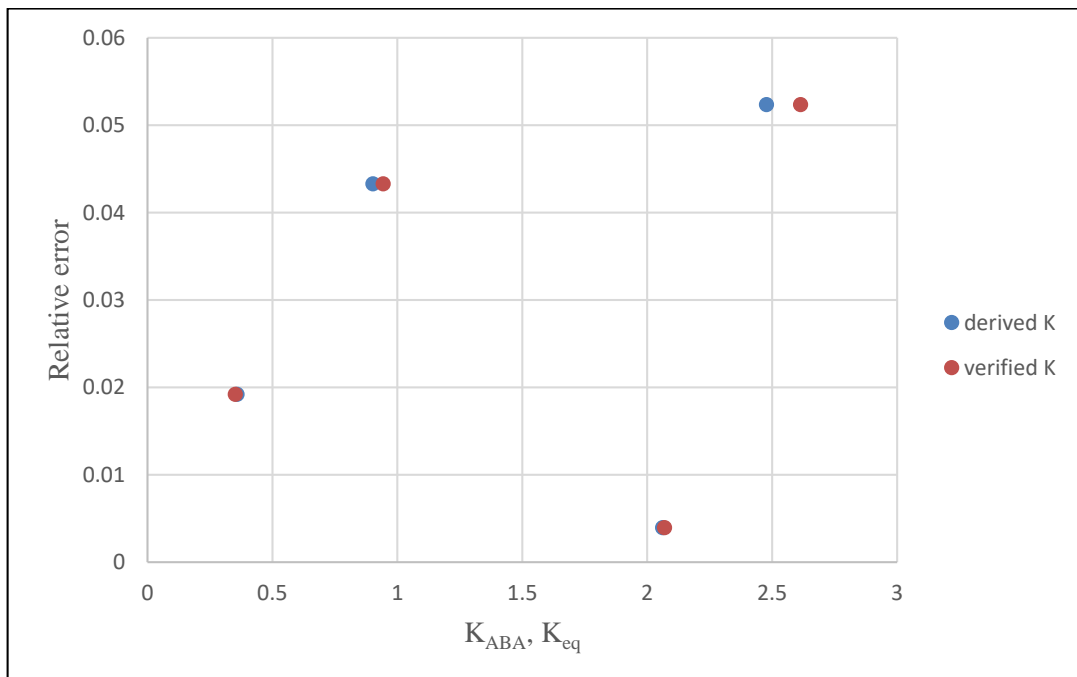


**Figure 5.25:** Relative error between derived and verified model.

Limitations:

It should be noted that the linear equation used to determine the equivalent strut width (Equation (5.9)) can be used under the following limitations:

- 1- Type of brick wall that can be represented by a strut and tie, should be hollow brick which is commonly used for interior partitions of thickness 100 mm. In addition, partition wall length should lie within the range of 4m to 7m.
- 2- The columns in the surrounding frame should be square with their sectional areas lie within  $0.3^2$ - $0.8^2$  m<sup>2</sup>.
- 3- Flexural steel ratio for beams and columns should be 1%.
- 4- The axial load in the beam should be ignored.
- 5- Axial load on column should equal  $0.25A_g \hat{f}_c$ .

## Chapter 6

### Macro Modeling and Results

#### 6.1 General

The main purpose of this thesis is to study the effect of various patterns of brick wall partitions on the fundamental period of framed structures. After conducting micro modeling of brick wall and developing a simple equation of the equivalent strut width, it is important to perform the second modeling stage of this thesis, which involves the study of the effect of brick wall partitions on the fundamental period of reinforced concrete (RC) framed structures through macro modeling. Therefore, this chapter introduces several patterns of partitions. The partition distribution is assumed to be random vertically, i.e. partitions are randomly distributed between stories while keeping their configuration unified among all stories in which partitions are placed. The factors considered are: the density of partitions distribution in the structure, the location of partitions, variations in panel lengths, and also variations in columns sizes in the structure.

#### 6.2 Model description

The framed structure used for analysis purposes is modeled using SAP2000 software, as shown in Figure (6.1). Properties of this structure are listed in Table (6.1).

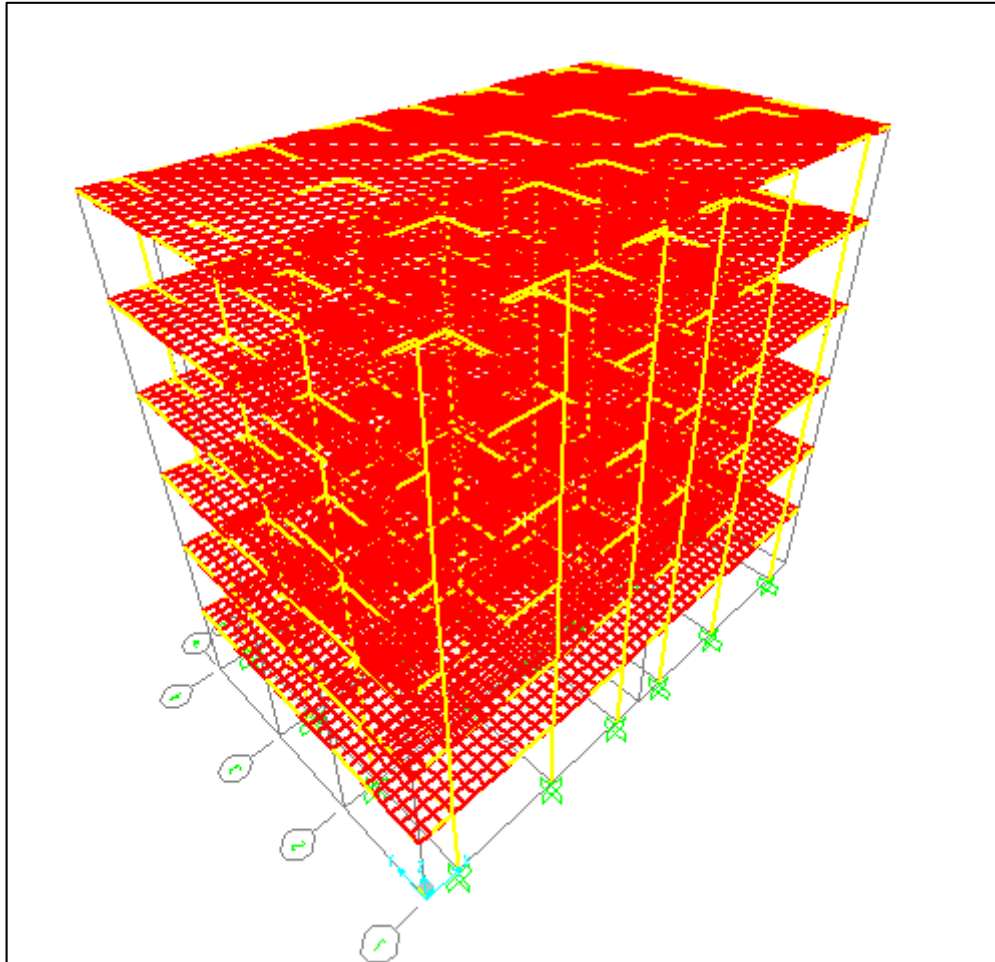


**Figure (6.1):** SAP2000 Model of the RC framed structure, prepared for macro modeling analysis

**Table (6.1):** General properties of the RC framed structure used in macro modeling

Number of stories	6
Total area of building	2088m <sup>2</sup>
Floor height	3.7m
Number of columns	24
Number of pays in X direction	5
Number of pays in Y direction	3

The plan of the RC framed structure is shown in Figure (6.2). As the plan shows, there are three different lengths of partition walls and, therefore, three types of struts are used in analysis. The strut types are explained in the following section.

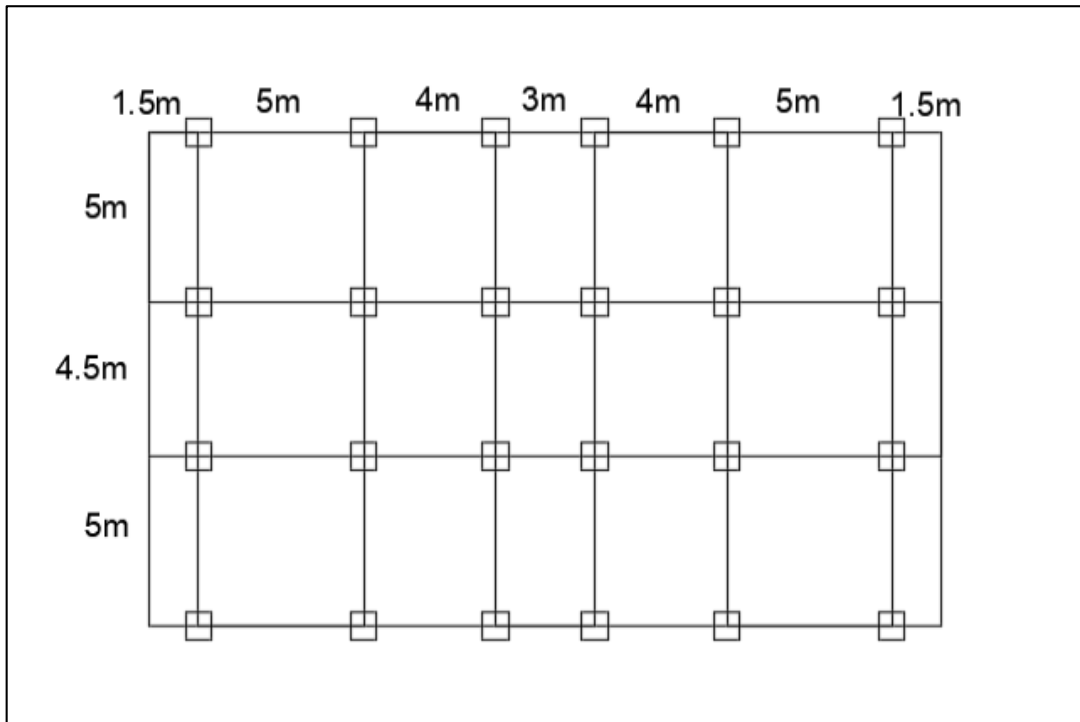


**Figure (6.2):** Plan of the RC frames structure showing the different partitions dimensions

It should be noted that the partition wall of length 3m that is shown in Figure (6.2) is not considered in the analysis, because its length lies out of the range over which Equation (5.9) is valid. In fact, this equation is valid for wall lengths within the range of  $(4m < L < 7m)$ , and column cross sectional areas within the range of  $(0.09m^2 < A_c < 0.5625m^2)$ .

### 6.2.1 Materials and sections

The main materials that are used in the modeling are: reinforced concrete which is used to build beams and columns, and brick material which is used to build wall partitions.

#### **Reinforced Concrete (RC):**

RC is a very common construction material that is used in different types of construction. If “economically designed and worked”, it becomes a competitive structural material (Hassoun and Al-Manaseer, 2015). Plain concrete has a relatively high compressive strength, and low strength in tension. Therefore, it is primarily reinforced with steel in a form of rounded bars to compensate for its weakness in tension. This final product called RC and has a unit weight ( $\rho_c$ ) of 25 kN/m<sup>3</sup> according to (IBC, 2006). Two main mechanical properties of plain concrete and steel, namely, compressive strength of concrete ( $f_c$ ), and yielding stress of steel ( $F_y$ ) are necessary to be identified for modeling. In the macro models considered in this thesis,  $f_c$  of 25MPa, and  $F_y$  is assumed to be 420MPa.

In the model, gravity loads are distributed and carried by 18 cm thick, two-way solid slab sitting on rectangular dropped continuous beams run in both directions, and set centrally on columns.

Main beams have rectangular cross sections with 45cm width and 60cm depth, while secondary beams have rectangular cross sections of 25cm width and 32cm depth.

Columns are of square cross sections that vary from case to case. It should be noted that all the assumed dimensions are selected and designed according to ACI-318 (2014).

### **Brick material:**

Hollow brick material's properties are explained in details in Chapter 3. They are used in defining the equivalent strut for partitions. Brick walls have a unit mass ( $\gamma_b$ ) of 1650 kg/m<sup>3</sup>, modulus of elasticity ( $E$ ) of 260 MPa. The analysis involved a variety of walls lengths and column sizes in the structure. Due to this variation, different struts with different properties are resulted and used to model the structure. Properties of the resulted strut types are given in Table (6.2).

**Table (6.2): Properties of the struts used in the RC framed structure**

Case No.	$L_w$ (mm)	$A_c$ (mm <sup>2</sup> )	$L_s$ (mm)	$b_s$ (mm)	$\gamma_s$ (Kg/m <sup>3</sup> )
1	5000	450x450	6220	635	3865
2	4000	450x450	5450	510	4390
3	4500	450x450	5800	573	4136
4	5000	300x300	6220	759	3235
5	4000	300x300	5450	634	3533
6	4500	300x300	5800	696	3401
7	5000	750x750	6220	239	10273
8	4000	750x750	5450	114	19592
9	4500	750x750	5800	177	13411

Where:

- $L_w$ : Wall length in (mm).
- $A_c$ : Cross sectional area of columns in (mm<sup>2</sup>).
- $b_s$ : Strut width in (mm), it is computed according to Equation (5.9). It should be noted that strut depth (d) is given a constant value of 100mm.
- $L_s$ : Strut length in (mm).
- $\gamma_s$ : Unit mass of the equivalent strut (kg/m<sup>3</sup>). This value is computed according to Equation (6.1).

$$\gamma_b \times L_w \times h \times d = 2 \gamma_s \times L_s \times d \times b_s \quad (6.1)$$

It should be noted that number 2 in Equation (6.1) is multiplied by the strut properties only for the purpose of equivalence, i.e. to indicate that both a strut and tie are considered in place of (or equivalent to) a brick wall.

During the analysis stage, the structure's configuration is changed three times through the following three steps:

Step 1: In this step the, the structure has six floors, and all columns in the structure have a cross sectional area of 45 x 45cm<sup>2</sup>.

Step 2: In this step, the first four floors have columns of cross sectional area of 45 x 45cm<sup>2</sup>, and 30 x 30cm<sup>2</sup> for the last two floors.

Step three: In this step, the structure has ten floors, with columns cross sectional area of 75 x 75cm<sup>2</sup> for the first four floors, 45 x 45cm<sup>2</sup> for the next four floors, and 30 x 30cm<sup>2</sup> for the last two floors.

## 6.2.2 Loads and boundary conditions

### Loads:

Dead loads (DL) and live loads (LL) in addition to super imposed dead load (SIDL) are considered during the analysis and design of the models. Dead load is taken as the weight of the structure itself, plus the superimposed dead load. The weight of the structure is found by the predetermined dimensions of structural members and their unit weights. The structural components of the models consist of RC members and brick wall. Superimposed dead load is that part of the dead load which represents the weight of partition walls, tiles and accessories, and building utilities (water pipes, air conditioning ducts, etc.) (Leet and Uang, 2005). Some of these parts are shown in Figure (6.3).

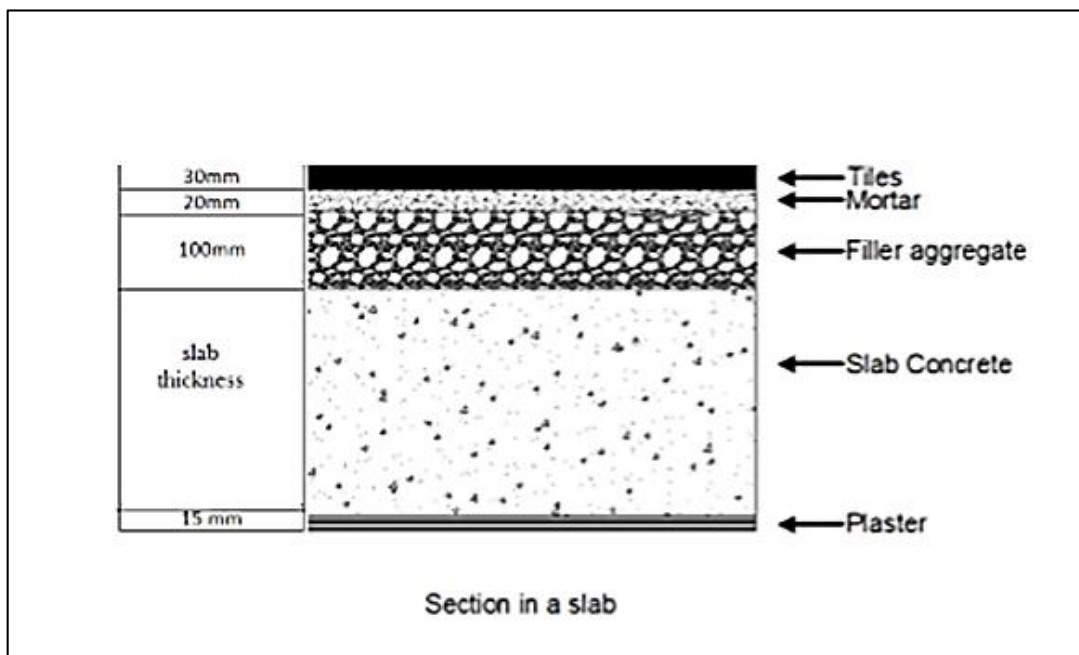


**Figure (6. 3):** Section in a slab showing some components of the super imposed dead load .

Superimposed dead load is computed by adding the weights of the layers indicated in Figure (6.3) and the other components mentioned previously, and found to be 3.4 kN/m<sup>2</sup>.

Live loads are those produced by the occupants of the building. Generally, ASCE suggests 4.8kN/m<sup>2</sup> as the live load in commercial buildings.

### **Boundary conditions:**

In seismic analysis, the ground motion is not influenced by the response of structure. In other words, except for the case of very flexible soil, the soil foundation can be assumed rigid (Chopra 2012). Based on this assumption, the model studied in this thesis is assumed constructed on rigid soil, and thereby the boundary condition is assumed to be fixed support.

### **6.2.3 Validation of the model**

Validation of the model aims to insure the used software works correctly. “Whichever analysis method is adopted during design, it must always be controlled by the designer, i.e. not a computer!” McKenzie (2013) said. Thus, the studied model is validated through three main checks as illustrated below:

- 1- Compatibility check: Through this check, elements are insured jointed at shared nodes, lines, and edges before loading. In addition, deformation after loading shall be free of splits or overlaps at the shared lines (Logan, 2012). Figure (6.4) shows the compatible

elements of the structure as taken from SAP2000 at some moment during animation of the deformed model.

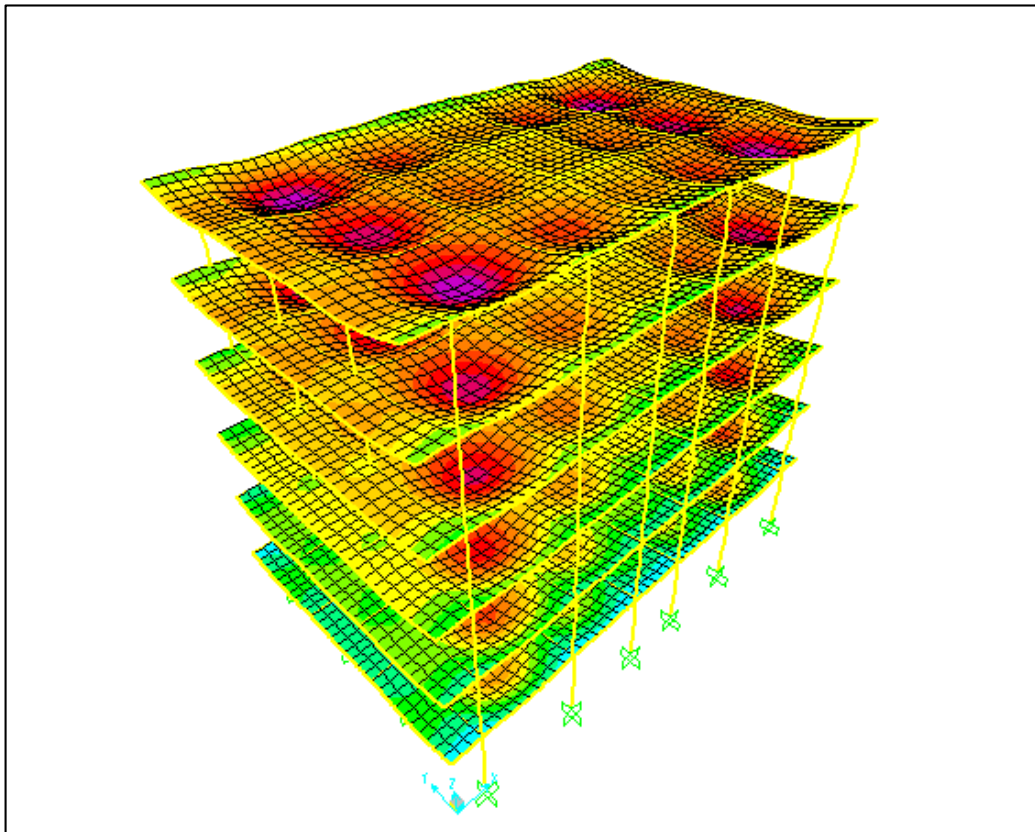


**Figure (6. 4):** Deformed shape of the structure showing compatibility of the structure, as taken from SAP2000

2- Equilibrium check: Through this check, it is insured that the summation of all forces in either horizontal or vertical directions are equal to zero. This is done by checking equality of input loads in some direction with their relevant reactions obtained by SAP2000 in the same direction. Dead loads, live loads and superimposed dead loads

are severally checked and their outcomes are summarized in Tables (6.3) and (6.4).

**Table (6. 3): Dead loads calculation both by hand and by SAP2000**

Structural elements	Length (m)	Width (m)	Depth (m)	Number of structural elements	g (kN/m <sup>3</sup> )	Weight (kN)	
Slab	24	14.5	0.18	6	25	9396	
Main beams	14.5	0.45	0.6	36	25	2466.45	
Secondary beams type (1)	24	0.45	0.6	24	25	2721.6	
Secondary beams type (2)	14.5	0.25	0.32	12	25	2260.337	
Columns	22.2	0.45	0.45	24	25	152.424	
						Manu al total (kN)	16996.81
						SAP2 000 total reactio n (kN)	16966.81
						% error	0%

**Table (6. 4): Live loads and superimposed dead loads calculations both by hand and by SAP2000**

Load case	Slab length (m)	Slab width (m)	Number of slabs	Load (kN/m <sup>2</sup> )	Manual total (kN)	SAP total reaction (kN)	% error
LL	24	14.5	6	4.8	10022.4	1022.4	0%
SIDL	24	14.5	6	3.4	7099.2	7099.2	0%

3- Internal moment check: This check is intended to verify accuracy of SAP2000 in calculating internal forces.

In this check, Direct Design Method (DDM) is adopted as the manual method to compute moments at critical sections.

In the (DDM), according to ACI-318, slabs are divided into frames in both directions, with the frame width extending between successive mid-panels, and thereby enclosing a row of columns running along its centerline. Each frame is divided into a column strip (CS) and a middle strip (MS) as shown in Figure (6.5). Moments are then found for each component of the frame as briefly illustrated below in a sample of calculation presented for the Internal moment check.

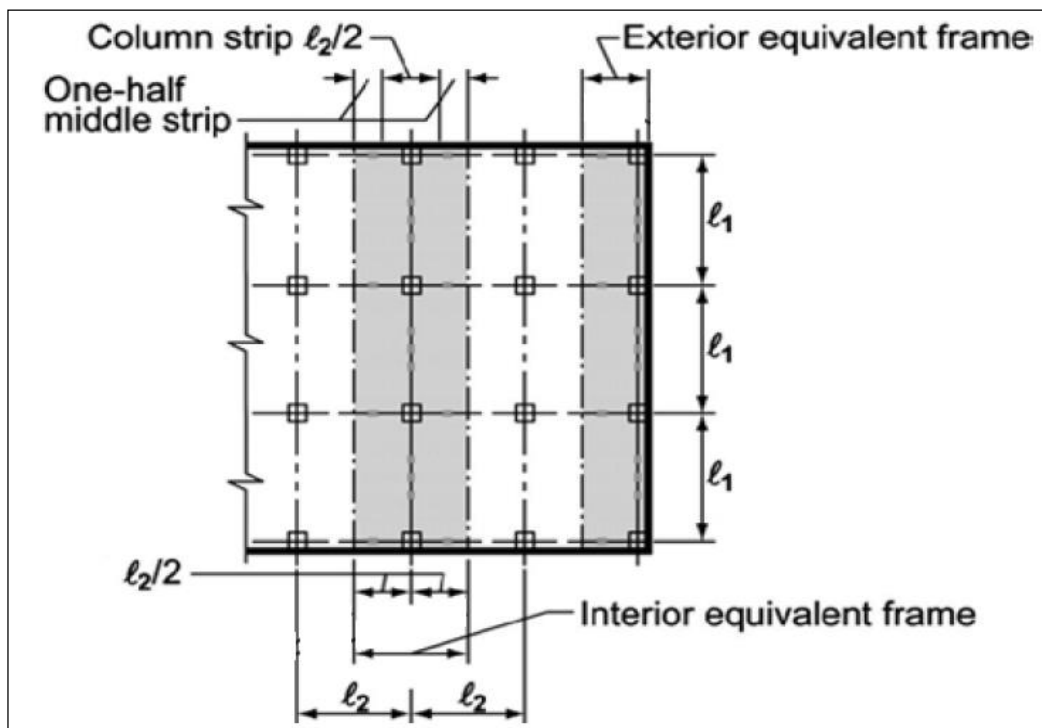


Figure (6. 5): MS and CS Definition

For the purpose of Internal moment check, an internal panel in the third floor is considered based on the effect of the load combination ( $1.2 DL + 1.6 LL$ ). Moments of this panel are calculated manually for both the middle and column strips based on the (DDM) and compared with those found by SAP2000. A sample of calculation which explains how column strip moments are found is provided below:

Parameters needed in the (DDM) calculations are shown in Figure (6.5) where ( $l_2 = 5\text{m}$ ,  $l_1 = 5\text{m}$ ,  $M_S$  width =  $5\text{m}$ ,  $C_S$  width =  $2.5\text{m}$ ,  $l_{n1} = 4.55\text{m}$ ). Effective width of beam =  $0.45\text{m}$ .

Ultimate load based on the combination ( $1.2 DL + 1.6 LL$ ) is calculated below:

$$\begin{aligned} q_u &= 1.2(3.4 + (0.18 \times 25)) + 1.6 \times 4.8 \\ &= 17.16 \text{ kN/m}^2 \end{aligned}$$

According to (ACI 318-14, section 8.10.3.2), for each span of the frame, the total static factored moment ( $M_o$ ) is computed below:

$$\begin{aligned} M_o &= \frac{q_u l_2 l_{n1}^2}{8} \\ &= 222.03 \text{ kN.m} \end{aligned}$$

According to (ACI 318-14, section 8.10.4.2),  $M_o$  is redistributed such that negative and positive moments equal some fractions of  $M_o$ . These fractions

are computed by multiplying  $M_o$  with specific coefficients that differ according to the location of the span in the frame. For the interior span, moment coefficients are (0.65 for negative moments and 0.35 for positive moment). Therefore, negative and positive moment values are:

$$\begin{aligned} M_{+ive} &= 0.35 \times 222.03 \text{ KN.m} \\ &= 77.7 \text{ kN.m} \end{aligned}$$

$$\begin{aligned} M_{-ive} &= 0.65 \times 222.03 \text{ KN.m} \\ &= 144.3 \text{ kN.m} \end{aligned}$$

According to (ACI 318-14, sections 8.10.5.1 and 8.10.5.5), negative and positive moments are then distributed to the column strip and middle strip based on specific factors. The factor used to obtain the column strip moment is 0.75. According to (ACI 318-14, section 8.10.5.7.1), as the column strip includes a beam and part of the slab, its moment is shared between these two components. The factor used to find the slab share of moment is  $(1 - 0.18 = 0.15)$ . Calculations are presented below.

$$M_{+ve (CS slab)} = \frac{77.7 \times 0.75 \times 0.15}{(2.5 - 0.45)}$$

$$= 4.26 \text{ kN.m}$$

$$M_{-ve (CS slab)} = \frac{144.3 \times 0.75 \times 0.15}{(2.5 - 0.45)}$$

$$= 7.92 \text{ kN.m}$$

If the slab part of the CS is treated as simply supported, then its total positive  $M_u$  based on the (DDM) and SAP2000 results is:

$$M_u = \frac{2 \times 7.92}{2} + 4.26$$

$$= 12.18 \text{ kN.m} \quad \text{Manually based on the (DDM)}$$

$$M_u = 10.36 \text{ kN.m} \quad \text{By SAP2000}$$

The percentage of error between  $M_u$  based on the (DDM) and that from SAP2000 is 15% (< 25%) which is an acceptable error.

### 6.3 Parametric study

For the purpose of studying the effects of brick wall partitions' properties on the fundamental period of the structure, a parametric study is conducted, in which, 73 cases of partitions are implemented for three types of models. In all these cases random partition distribution is assumed. Partitions are replaced by their equivalent struts in modeling, to take the effect of their stiffness in addition to their masses. The studied cases can be categorized under three model types – Model type (1), Model type (2) and Model type (3). These models vary in terms of number of stories as well as column sizes and their distributions throughout the stories, as clarified by Table (6.5).

**Table (6.5): Model types used in the parametric study**

<b>Floor (10)</b>			Columns	<b>Floor (10)</b>	
<b>Floor (9)</b>			(0.3 x 0.3m)	<b>Floor (9)</b>	
<b>Floor (8)</b>			Columns	<b>Floor (8)</b>	
<b>Floor (7)</b>				<b>Floor (7)</b>	
<b>Floor (6)</b>	Columns (0.45 x 0.45m)	Columns	(0.45 x 0.45m)	<b>Floor (6)</b>	
<b>Floor (5)</b>		(0.3 x 0.3m)		<b>Floor (5)</b>	
<b>Floor (4)</b>			Columns	<b>Floor (4)</b>	
<b>Floor (3)</b>		Columns		Columns	<b>Floor (3)</b>
<b>Floor (2)</b>			(0.45 x 0.45m)	(0.75 x 0.75m)	<b>Floor (2)</b>
<b>Floor (1)</b>					<b>Floor (1)</b>
	<b>Model type (1):</b>	<b>Model type (2):</b>	<b>Model type (3):</b>		
	<b>6 floors</b>	<b>6 floors</b>	<b>10 floors</b>		

Because engineer's community in Palestine neglect the effect of stiffness of partitions and only consider their masses, an extra model is developed and named (Model type (4)) to test the effect of neglecting partitions' stiffness. In this model partitions' stiffness is totally neglected by excluding partitions or their equivalent struts. At the same time, only masses of partitions are added as uniform mass to the slabs (in case the whole structure is partitioned). As the structure has its main mode in the Y-direction, the partitioning procedure is applied only along this direction.

Through the aforementioned cases, the fundamental period values are studied in case of neglecting the masses and stiffness of partitions, neglecting

the stiffness of the partitions and considering their masses, and considering the stiffness and masses of the partitions. Results are introduced in the following section.

## **6.4 Final results and verification**

### **6.4.1 Final results**

Every case is given a random distribution of partitions in order to study their effect on the fundamental period of the structure. The results of all random patterns of partitions distribution are summarized below for each model type:

Model type (1): The whole structure includes one type of columns.

The results of this model are shown in Tables (A.1) and (A.2) in Appendix A.

Model type (2): The structure includes two types of columns.

The results of this model are shown in Table (A.3) in Appendix A.

Model type (3): The structure includes three types of columns.

The results of this model are shown in Table (A.4) in Appendix A.

Model type (4): In this model, stiffness of partitions is neglected but their masses are considered, as they are usually treated in Palestinian engineering communities. This is considered in the macro modeling in order to compare it with the previous cases. The results of this model are shown in Table (A.5)

Results of the model types (1, 2 and 3) shown in Appendix (A), are subjected to regression analysis to develop simple equation that can predict the fundamental period of the frame structure with brick wall partitions, as a function of the fundamental period of the bare frame.

#### 6.4.2 Verification

The fundamental period values obtained in the previous section are verified analytically, by a procedure known as Rayleigh Method. With respect to Anderson and Naeim (2012) and (Sucuoglu, 2015), the relationship of this approximate procedure is given by Equation (6.2) and is employed, herein, to verify ( $T$ ) values computed by SAP2000.

$$T_1 = 2\pi \sqrt{\frac{\sum_{i=1}^n w_i \delta_i^2}{g \sum_{i=1}^n P_i \delta_i}} \quad (6.2)$$

Where:

$T_1$ : Time period of the structure in (mm).

$n$ : The number of stories above the base.

$w_i$ : The seismic weight of story (i) in(kN).

$\delta_i$ : The static lateral deflection at level (i) in (m).

$P_i$ : The resultant of the static distributed forces over each level in the intended direction (kN).

The frame used for verification is taken from Model type (1). It consists of 6 floors, and all its column have cross sectional area of 45 x 45cm. Table (6.6) includes calculations of all components contained in the effective seismic weight of every story in this frame.

**Table (6. 6): Seismic dead load of stories for the frame taken from Model type (1), and used for time period verification**

Types of elements in a single story	$\gamma$ (KN/m <sup>3</sup> )	Dimensions			Mass and Weight modifier	Number of elements in a single story	Weight of elements (KN) in single story
		Length (m)	Width (m)	Depth (m)			
Slab panels	25	24	14.5	0.18	1	1	1566
Main beams	25	14.5	0.45	0.6	0.7	6	411.1
Secondary beams (1)	25	24	0.45	0.6	0.7	4	453.6
Secondary beams (2)	25	14.5	0.25	0.32	0.438	2	25.4
Columns	25	3.7	0.45	0.45	0.838	24	376.7
<b>Seismic dead load (KN) for the 6th- story</b>							2644.4
<b>Seismic dead load (KN) for any other story</b>							2832.8

As for the (SIDL) and (LL) for the slab in any story, they are computed as below, followed by Equation (6.3) which gives the seismic weight of any story.

$$\begin{aligned} \text{Seismic (SIDL) for the slab in any story} &= 24 \times 14.5 \times 3.4 \\ &= 1183.2 \text{ KN} \end{aligned}$$

$$\begin{aligned} \text{Seismic (LL) for the slab in any story} &= 24 \times 14.5 \times 4.8 \times 0.25 \\ &= 417.6 \text{ KN} \end{aligned}$$

*Seismic weight of any story*

$$= \text{Seismic DL} + \text{Seismic SIDL} \quad (6.3) \\ + \text{Seismic LL}$$

It should be noted that all terms in Equation (6.3) are computed for only the story under consideration.

Table (6.7) includes the values of the terms needed for Rayleigh method.

**Table (6. 7): Values of the terms used in Rayleigh method to compute time periods**

Level	$w_i$ (KN)	$P_i$ (KN/m <sup>2</sup> )	Floor area (m <sup>2</sup> )	$P_i$ (KN)	$\delta_i$	$w_i \delta_i^2$	$P_i \delta_i$
6	4245.2	10	348	3480	0.4748	957	1652.3
5	4433.6	10	348	3480	0.4476	888.2	1557.6
4	4433.6	10	348	3480	0.3965	697	1379.8
3	4433.6	10	348	3480	0.3211	457.1	1117.4
2	4433.6	10	348	3480	0.2216	217.7	771.2
1	4433.6	10	348	3480	0.1012	45.4	352.2
<b>Sum</b>						3262.5	6830.5

By applying Rayleigh Method, and substituting the needed values from Table (6.7) in Equation (6.2). The fundamental period of the frame for Model type (1) in the X-direction is:

$$T_X (\text{Rayleigh}) = 1.385 \text{ sec}$$

$$T_X (\text{SAP}) = 1.395 \text{ sec}$$

*Percentage of error = 0.7% (acceptable error)* 6.5 Discussion of Results

From the previous results, several points are noted in the analysis procedure and discussed below:

- 1- The fundamental period of the structure is affected not only by how dense partitions are distributed, but also by the location of partitions. It can be observed from Tables (A.1 – A.3) in Appendix (A) that for the same density of partitioning, the fundamental period of the structure is at its smallest when partitions are added to the first and second floors. In contrast, the fundamental period is at its largest when partitions are added to the last floor. This means that the partitions in the first floors affect the structure in terms of stiffness more than mass. On the other hand, the partitions in the last floors affect the structure in terms of mass more than stiffness.
- 2- The fundamental period of the structure decreases with the increase in the amount of partitions. This is because as the number of partitions increases, stiffness of the structure increases, causes the fundamental period to decrease. This result is consistent with Equation (6.4) which gives the natural period of an object of mass (m) and stiffness (k).

$$T = 2\pi \sqrt{\frac{m}{k}} \quad (6.4)$$

- 3- When the mass of partitions is considered while their stiffness is neglected, the fundamental period of the structure, in this case, has the

largest value. This can be observed in Table (A.4) in Appendix (A). In fact, this case is very common practice by Palestinian engineers.

- 4- The column size, density of partitions distribution, and the location of partitions have small effects on the fundamental period. As can be noted from the results that the difference between the fundamental period with and without partitions, does not exceed 5% at most, except for a few cases in which the difference reaches 7%. Hence, it is possible to fit these random points, in order to have a simple equation of determining the fundamental period of structure according to the density of partitions distribution in this structure.

**Data fitting:**

According to the random fundamental time period values shown in Figure (6.6), their most suitable fitting is shown in the same figure. The equation resulted from fitting is given by Equation (6.5).

$$T = T_0 (1 - 0.08 P) \quad (6.5)$$

Where:

$T$ : The fundamental period of the structure with brick wall partitions in (sec).

$T_0$ : The fundamental period of the structure without brick wall partitions in (sec).

$P$ : The length percentage of the density of partition distribution. It is computed as shown by Equation (6.6).

$$P = \frac{(\text{Strut length}) \times (\text{Number of the struts and ties in the frame})}{(\text{Wall perimeter}) \times (\text{Number of walls in the frame})} \quad (6.6)$$

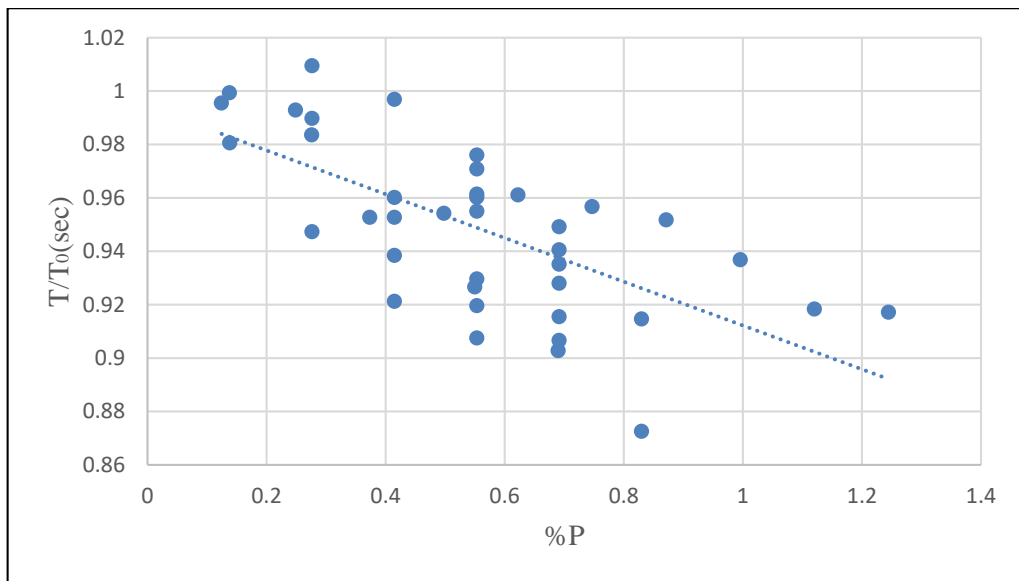


**Figure (6. 6):** Fitting of the fundamental period values in cases of variation in the amount of partitions

In order to validate Equation (6.5), this equation is applied for some of the cases associated with Model type (1). The resulting errors are plotted in Figure (6.7).

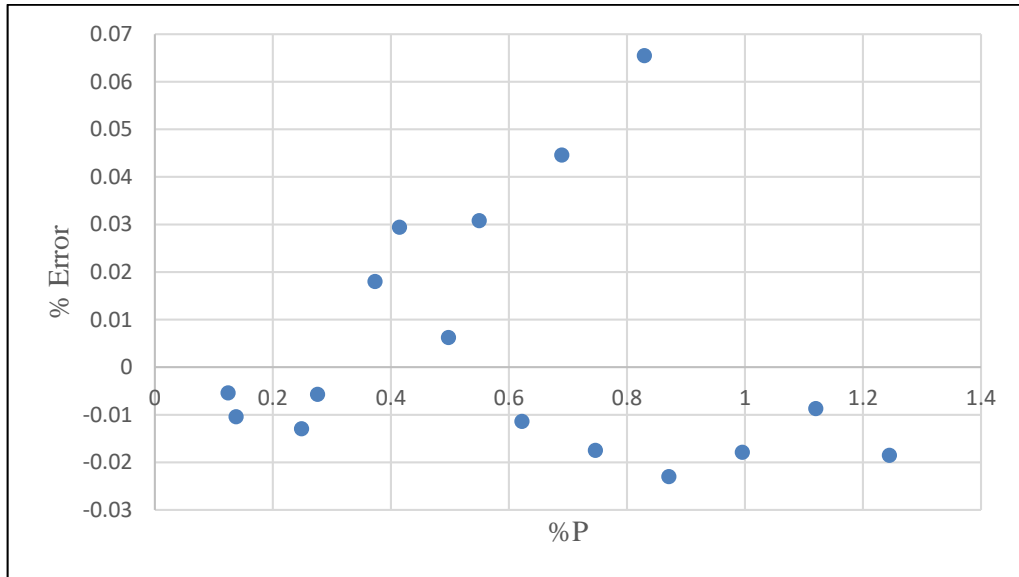


**Figure (6.7):** Error distribution that results from using the proposed equation of determining the fundamental period of partitioned structure (Equation (6.5))

From Figure (6.7), it can be observed that the error distribution is not random, and that is due to several factors that affect the fundamental period in addition to the density of the partitions distribution. These factors are mentioned earlier, such as the location of the partition and the length of the brick wall partitions.

In summary, it is acceptable to use the simple equation (Equation (6.5)) in determining the fundamental period of the partitioned structure which takes into account the partitions, instead of ignoring them.

## 6.6 Modification to Rayleigh method

As mentioned previously, the fundamental period of framed structure can be estimated using Rayleigh method (Sucuoglu (2015)). This method is used for bare frame without partitions. Therefore, simple linear equation was proposed in the previous section in order to find the fundamental period of the frame with partitions. However, this equation is approximate and has some limitations that is mentioned previously, such as the brick type and the surrounding frame.

In this section, another theoretical equation is suggested to find the fundamental period of the framed structure, when it has partitions, by modifying Rayleigh method. The following Eq.6.7 is suggested:

$$T^* = 2\pi \sqrt{\frac{\sum_{i=1}^n w^* \delta_i^2}{g \sum_{i=1}^n P^* \delta_i}} \quad (6.7)$$

Where:

$T^*$ : the fundamental period of the framed structure with partitions according to modified Rayleigh method.

$w^*$ : the modified seismic weight of the frame with partitions it can be calculated according to Eq.6.8:

$$w^* = W_i + W_p \quad (6.8)$$

Where:

$W_i$ : the seismic weight of the bare frame.in kN.

$W_p$ : the weight of the partitions in the frame, it is equal to (No. of struts and ties x dimensions of each strut and tie x unit weight of the strut and tie) in kN.

$P^*_i$ : the lateral load applied to the partitioned wall in each floor, in kN, it can be calculated as following Eq. 6.9:

$$P^* = V^*_{i-1} - V_i$$

$$V^* = V_i + K^* \delta_{i+1} - \delta_i$$

Where  $K^*$  is the stiffness of strut and ties that can be found from Eq.5.7

This equation (Eq.6.7) is applied for case one in the macro modeling, in order to find the fundamental period of the frame with partitions in each X and Y direction, and compared with those periods in SAP. As shown in Table 6.8 and Table 6.9.

**Table (6. 8): Values of the terms used in modified Rayleigh method to compute time periods in X direction.**

Level	$W_i$ (kN)	$W_p$ (kN)	$W^*$ (kN)	$P_i$ (kN/m <sup>2</sup> )	floor area (m <sup>2</sup> )	$P_i$ (kN)	$\delta_i$ (m)	$V_i$ (kN)	Drift (m)	$K^*$ (kN/m)	$V^*$ (kN)	$P^*$ (kN)	$W_i \cdot \delta_i^2$	$P^* \cdot \delta_i$
1	4433.6	562.54	4996.14	10	348	3480	0.101	20880	0.1012	23.84	20881.2	3480.3	51.168	352.2
2	4433.6	562.54	4996.14	10	348	3480	0.222	17400	0.1204	23.84	17401.4	3480.3	245.34	771.2
3	4433.6	562.54	4996.14	10	348	3480	0.321	13920	0.0995	23.84	13921.2	3480.3	515.13	1117.5
4	4433.6	562.54	4996.14	10	348	3480	0.396	10440	0.0754	23.84	10440.9	3480.3	785.45	1379.9
5	4433.6	562.54	4996.14	10	348	3480	0.448	6960	0.0511	23.84	6960.6	3480.3	1000.96	1557.8
6	4245.2	562.54	4807.74	10	348	3480	0.475	3480	0.0272	23.84	3480.3	3480.3	1083.83	1652.5
Sum												3681.88	6831.13	

The results show that :

$T_x=1.472$  sec ( modified Rayleigh method)

$T_x=1.395$  sec (SAP)

The percent of error is equal to 5.2% which is acceptable.

**Table (6. 8): Values of the terms used in modified Rayleigh method to compute time periods in Y direction.**

<i>Level</i>	<i>W<sub>i</sub></i> (kN)	<i>W<sub>p</sub></i> (kN)	<i>W*</i> (kN)	<i>P<sub>i</sub></i> (kN/m <sup>2</sup> )	<i>floor area</i> (m <sup>2</sup> )	<i>P<sub>i</sub></i> (KN)	<i>δ<sub>i</sub></i> (m)	<i>V<sub>i</sub></i> (kN)	<i>Drift</i> (m)	<i>K*</i> (kN/m)	<i>V*</i> (kN)	<i>P*</i> (kN)	<i>W<sub>i</sub>*δ<sub>i</sub></i>	<i>P*δ<sub>i</sub></i>
1	4433.6	562.54	4996.14	10	348	3480	0.101	20880	0.1012	39.14	20884	3481	51.168	352.2
2	4433.6	562.54	4996.14	10	348	3480	0.222	17400	0.1204	39.14	17404.7	3481	245.34	771.4
3	4433.6	562.54	4996.14	10	348	3480	0.321	13920	0.0995	39.14	13924	3481	515.13	1117.7
4	4433.6	562.54	4996.14	10	348	3480	0.396	10440	0.0754	39.14	10443	3481	785.45	1380.2
5	4433.6	562.54	4996.14	10	348	3480	0.448	6960	0.0511	39.14	6962	3481	1000.96	1558.1
6	4245.2	562.54	4807.74	10	348	3480	0.475	3480	0.0272	39.14	3481.1	3481	1083.83	1652.8
Sum													3681.88	6832. 5

The results show that:

$T_y=1.472$  sec (modified Rayleigh method)

$T_y=1.469$  sec (SAP)

The percent of error is equal to 0.2% which is acceptable.

From the previous results, it is recommended to use the modified Rayleigh method to find the fundamental period of the frame with partitions.

## Chapter 7

### Conclusions and Recommendations

#### 7.1 Overview

In this thesis, three-dimensional (3-D) non-linear finite element (F.E.) models of brick wall are used to study its stiffness in order to replace the brick wall with an equivalent strut. Experimental tests of brick wall are conducted to use some parameters in the modeling. As a result, a simplified equation to predict the strut width is proposed. Furthermore, macro modeling of reinforced concrete (RC) framed structure is conducted to study the effect of several patterns of brick wall partitions on the fundamental period of the structure. Another simplified equation to predict the fundamental period of the structure with partitions is also proposed. A summary of the main findings and results of the study is presented in the following section.

#### 7.2 Conclusions

Based on the study, the following conclusions are made:

- 1- The brick wall stiffness is affected by two main parameters – length of brick walls and size of columns in the surrounding frame. Increasing frame length increases the stiffness of the brick wall inside, while increasing column size of the surrounding frame decreases the stiffness of brick wall inside.

- 2- Results show that, failure in the brick wall in the linear stage is actually a slipping failure in the bricks.
- 3- Failure criteria at which the yielding in steel reinforcement occurs, either in beams or columns, is the criteria adopted in the results.
- 4- The fundamental period of the structure decreases with increasing the amount of brick wall partitions.
- 5- The fundamental period of the structure is also affected by the vertical location of partitioning walls. The structure has a small fundamental period when partitions are located in the lower floors.
- 6- Considering the mass of partition, and neglecting its stiffness in design, increases the fundamental period of the structure.

### 7.3 Proposed equations

Two simplified equations (Equations (7.1) and (7.2)) can be used to predict the strut width and the fundamental period of the structure considering brick wall partitions. These equations are developed by using statistical regression and fitting data generated by ABAQUS F.E models as well as SAP000 models. These equations are subjected to some limitations are illustrated below:

$$b = \frac{L}{8} - \frac{Ac}{1000} + 235 \quad (7.1)$$

Where:

*b*: Strut width in (mm).

$L$ : Frame length in (mm).

$A_c$ : Cross sectional area of column in (mm<sup>2</sup>).

Limitations of Equation (6.7):

- 1- The strut is equivalent to hollow brick wall with the following properties:

Dimensions: 400 x 100 x 200 mm<sup>3</sup>.

Modulus of elasticity ( $E$ ) = 260.23 MPa.

Poisson ratio ( $\nu$ ) = 0.2.

- 2- The equation is generated for squared columns, whose cross sectional area lie within the range ranges ( $0.09 \text{ m}^2 < A_c < 0.5625 \text{ m}^2$ ).
- 3- The range of ( $L$ ) used in the equation is ( $4\text{m} < L < 7\text{m}$ ).
- 4- No axial load on beams.
- 5- Axial load on column ( $p$ ) =  $0.25 Agf'c$ .
- 6- Flexural steel ratio for beams and columns is 1%.

$$T = T_0(1 - 0.08 P) \quad (7.2)$$

Where:

$T$ : Fundamental period of the structure considering partitions, in (sec).

$T_0$ : Fundamental period of the structure ignoring partitions, in (sec).

$P$ : Percentage of strut length to wall length.

The limitations of the time period equation (Equation (7.2)) are similar to those of the strut width equation (Equation (7.1)).

Another theoretical equation is developed in this thesis, which is modified Rayleigh method. It is shown in Eq. 7.3 below:

$$T^* = 2\pi \sqrt{\frac{\sum_{i=1}^n w^* \delta_i^2}{g \sum_{i=1}^n P^* \delta_i}} \quad (7.3)$$

Where:

$T^*$ : the fundamental period of the framed structure with partitions according to modified Rayleigh method.

$w^*$ : the modified seismic weight of the frame with partitions it can be calculated according to Eq.6.8:

$$W^* = W_i + W_p \quad (7.4)$$

Where:

$W_i$ : the seismic weight of the bare frame.in kN.

$W_p$ : the weight of the partitions in the frame, it is equal to (No. of struts and ties x dimensions of each strut and tie x unit weight of the strut and tie) in kN.

$P^*_i$ : the lateral load applied to the partitioned wall in each floor, in kN, it can be calculated as following Eq. 6.9:

$$P^* = V^*_{i-1} - V_i$$

$$V^* = V_i + K^* \delta_{i+1} - \delta_i$$

Where  $K^*$  is the stiffness of strut and ties that can be found from Eq.5.7

#### **7.4 Recommendations and Future studies**

Based on the results of this study, there are main important recommendations given below:

- 1- The masonry walls have to be modeled, to predict their effect on the structure. Most of the Palestinian buildings, with reference to the Palestinian Central Bureau of Statistics, are masonry structures. Therefore, it is important to simplify the masonry walls into equivalent strut, in order to facilitate their consideration in design.
- 2- What the engineering community does in design (As referred to the engineer's syndicate), by neglecting the partitions stiffness and considering their mass only, is rejected. This custom has to be modified, by starting considering the stiffness of brick wall partitions in design, as it affects the fundamental period of the structure.
- 3- It can be expected that in case of shear wall structures, and when the structures have high stiffness, the effect of brick walls can be ignored. Their effect on the fundamental period of the structure may be small to the degree that it can be neglected.
- 4- Further studies may be added in this area, in order to find guidelines to our offices, when they can neglect bricks in lateral consideration.
- 5- In order to exploit the benefits of infills in a rational manner, more methodologies should be produced.

## References

- 1 AA Chaker, A Cherifati, (1999). *Influence of masonry infill panels on the vibration and stiffness characteristics of R/C frame building*. earthquake engineering and structure.
- 2 ABAQUS version 6.13. (2013). [Computer software]. *Assault Systems*. Waltham. MA.
- 3 ABAQUS: ABAQUS Analysis User's Manual Version 6.13. (2013). *Assault Systems*.
- 4 ACI (2008). *Building Code Requirements for Structural Concrete. Committee report 318-08*, American Concrete Institute, Detroit, Michigan, 473 pages.
- 5 A. Masi M. Vona, *Experimental and numerical evaluation of the fundamental period of undamaged and damaged RC framed buildings*, Bulletin of Earthquake Engineering, 2010.
- 6 American Concrete Institute (1984), *Earthquake Effects on Reinforced Concrete Structures, Publication SP-84, US-Japan Research*, American Concrete Institute, Detroit.
- 7 ASCE 2010. *Minimum design loads for buildings and other structures*, Reston, Va., American Society of Civil Engineers: Structural Engineering Institute.
- 8 ANDERSON, J. C. & NAEIM, F. 2012. Basic structural dynamics, *John Wiley & Sons*. ARAKERE, A. C. & DOSHI, T. D. 2015. *COMPARISON OF MULTI-STOREY BUILDING WITH NORMAL BEAMS AND*

- CONCEALED BEAMS. International Research Journal of Engineering and Technology (IRJET), 02.**
- 9 Asran, G., EL-Esnawi, H., and Fayed, S. (2016). *Numerical Investigation of RC Exterior Beam Colum Connections under Monotonic Loads. Journal of Mechanical and Civil Engineering*, Vol .13, No. 1, pp. 60-67.
  - 10 Chopra and Goel, (2000). **Building Period Formulas for Estimating Seismic Displacements**, Earthquake Spectra.
  - 11 CHOPRA, A. K. 2012. **Dynamics of structures: theory and applications to earthquake engineering**, Upper Saddle River, NJ, Prentice Hall.
  - 12 Crowley and Pinho, (2006). *Simplified equation for estimating the period of vibration of existing buildings*, First European Conference on Earthquake Engineering and Seismology.
  - 13 C.V.R. Murly et al. (2012). *Some Concepts of Earthquake Behavior of Buildings*, Gujarat State Disaster Management Authority.
  - 14 El-Dakhakhni WW, Elgaaly M, Hamid AA. (2003). *Three-strut model for concrete masonry-infilled steel frames. Journal of Structural Engineering.*
  - 15 Federal Emergency Management Agency FEMA 450, (2004). **Recommended Provisions for Seismic Regulations for New Buildings and Other Structures.**
  - 16 **HASSOUN, M. N. & AL-MANASEER, A. A. 2015. Structural concrete: theory and design** [Online]. Available:

<http://catalogimages.wiley.com/images/db/jimages/9781118767818.jpg>.

- 17 Holmes M. Steel frames with brickwork and concrete infilling. Proceedings of the Institution of Civil Engineers 1961.
- 18 INTERNATIONAL CODE COUNCIL 2014. International building code 2015, Country Club Hills, Ill., ICC.
- 19 Juan Rodriguez, February 22,2017. 5 Common Used Bricks Types: *Classifications and Uses*.
- 20 K. Guler E. Yuksel and A. Kocak, (2008). *Estimation of the Fundamental Vibration Period of Existing RC Buildings in Turkey Utilizing Ambient Vibration Records*, **Journal of Earthquake Engineering**.
- 21 Kmiecik, P., and Kamiński, M. (2011). *Modeling of reinforced concrete structures and composite structures with concrete strength degradation taken into consideration*. **Archives of civil and mechanical engineering Journal**, Vol. 11, No. 3, pp. 623–636.
- 22 Lee, J., and Fenves, G. L. (1998). *Plastic-Damage Model for Cyclic Loading of Concrete Structures*. **Journal of engineering mechanics**, Vol. 124, No. 8, pp. 892–900.
- 23 LEET, K. & UANG, C.-M. (2005). **Fundamentals of structural analysis**, Boston, McGraw-Hill.
- 24 LOGAN, D. L. 2012. *A first course in the finite element method*, Stamford, Cengage Learning.

- 25 Lubliner, J., Oliver, J., Oller, S., and Onate, E. (1989). *A Plastic-Damage Model for Concrete*. **International Journal of solids and structures**, Vol. 25, No. 3, pp. 299–326.
- 26 Lu, X. Z., Teng, J. G., Ye, L. P., and Jiang, J. J. (2005). *Bond–Slip Models for FRP Sheets/Plates Bonded to Concrete*. **Journal of Engineering structures**, Vol. 27, No. 6, pp. 920–937.
- 27 Maidiawati, Yasushi Sanada,(2016), *R/C frame–infill interaction model and its application to Indonesian buildings, earthquake engineering and structural dynamics*.
- 28 Mainstone R.J. (1971), *Summary of paper 7360 On the stiffness and strength of infilled frames*. **Proceedings of the Institution of Civil Engineers**.
- 29 Mander, J. B., Priestley, M. J., and Park, R. (1988). *Theoretical Stress-Strain Model for Confined Concrete*. **Journal of structural engineering**, Vol. 114, No. 8, pp. 1804-1826.
- 30 MCKENZIE, W. M. 2013. **Examples in structural analysis**, CRC Press.
- 31 M. Kose, *Parameters affecting the fundamental period of RC buildings with infill walls*, Engineering Structures, 2009.
- 32 Monti, M., Renzelli, M., and Luciani, P. (2003). *FRP Adhesion in Uncracked and Cracked Concrete Zones*. In **Fiber-Reinforced Polymer Reinforcement for Concrete Structures: (in 2 Volumes)** pp. 183-192.

- 33 Nakaba, K., Kanakubo, T., Furuta, T., and Yoshizawa, H. (2001). ***Bond Behavior Between Fiber-Reinforced Polymer Laminates and Concrete. Structural Journal***, Vol. 98, No. 3, pp. 359–367.
- 34 Neubauer, U., and Rostasy, F. S. (1999). **Bond Failure of Concrete Fiber Reinforced Polymer Plates at Inclined Cracks—Experiments and Fracture Mechanics Model. Proc., 4<sup>th</sup> Int. Symp. on Fiber-Reinforced Polymer Reinforcement for Reinforced Concrete Structures, SP-188, American Concrete Institute, Farmington Hills, Mich., pp. 369–382.**
- 35 P. Asteris et al. (2015), **Parameters affecting the fundamental period of infilled RC frame structures**, Earthquakes and structures.
- 36 Paulay T, Priestley MJN. (1992), ***Seismic Design of Reinforced Concrete and Masonry Buildings. John Wiley & Sons: New York.***
- 37 R. K. Goel A. K. Chopra, (1997), ***"Period formulas for moment-resisting frame buildings"*** *Journal of Structural Engineering*.
- 38 R. K. Goel A. K. Chopra, (1998), ***"Period formulas for concrete shear wall buildings"*** *Journal of Structural Engineering*.
- 39 Saenz, L. P. (1964). ***Equation for the Stress-Strain Curve of Concrete. ACI Journal***, Vol. 61, No. 9, pp. 1229–1235.
- 40 Savoia, M., Ferracuti, B., and Mazzotti, C. (2003). **Nonlinear Bond-Slip Law for FRP-Concrete Interface. In Proc. of 6<sup>th</sup> international symposium on FRP reinforcement for concrete structures, Singapore: World Scientific Publications.**

- 41 Sharif, A. M., Samaaneh, M. A., Azad, A. K., and Baluch, M. H. (2015). *Use of CFRP to Maintain Composite Action for Continuous Steel–Concrete Composite Girders*. **Journal of Composites for Construction**, Vol. 20, No. 4.
- 42 Smith BS. (1967), **Methods for predicting the lateral stiffness and strength of multi-story infilled frames**. Building Science.
- 43 Smith BS, Carter C. (1969), *A method of analysis for infilled frames*. **Proceedings of the Institution of Civil Engineers**.
- 44 S Sattar, AB Liel ,(2010), **Seismic performance of reinforced concrete frame structures with and without masonry infill walls**, 9th US National and 10th Canadian conference.
- 45 SUCUOGLU, H. (2015). **Basic earthquake engineering from seismology and seismic analysis to design principles**, Cham, Springer.
- 46 Wahalathantri, B. L., Thambiratnam, D. P., Chan, T. H. T., and Fawzia, S. (2011). *Material Model for Flexural Crack Simulation in Reinforced Concrete Elements Using ABAQUS*. **In Proceedings of the First International Conference on Engineering, Designing and Developing the Built Environment for Sustainable Wellbeing**, pp. 260-264.
- 47 WILLAM, K. J. (1975). *Constitutive Model for the Triaxial Behavior of Concrete*. **International association for bridge and structural engineering proceedings**, Vol. 19, pp. 1-30.
- 48 Y Sanada et al. (2011), *Seismic performance of nonstructural brick walls used in Indonesian R/C buildings*, **Journal of Asian Architecture and Building Engineering**.

- 49 Yong, Y. K., Nour, M. G., and Nawy, E. G. (1988). *Behavior of Laterally Confined High-Strength Concrete Under Axial Loads*. **Journal of Structural Engineering**, Vol. 114, No.2, pp.332-351.

## Appendix A

*Table (A. 1): Fundamental period, in Y-direction, for Model type (1)*

<b>Fundamental period in Y-direction</b>							
<b>% P</b>	<b>Case</b>	<b>Floor Number</b>	<b>H (m)</b>	<b>Presence of struts</b>	<b>T<sub>y</sub> (sec)</b>	<b>T<sub>0</sub> (sec)</b>	<b>Normalized value</b>
0.83	All	1	3.7	Yes	1.3433	1.4688	0.9146
		2	7.4	Yes			
		3	11.1	Yes			
		4	14.8	Yes			
		5	18.5	Yes			
		6	22.2	Yes			
0.692	case 1	1	3.7	No	1.3734	1.4688	0.9351
		2	7.4	Yes			
		3	11.1	Yes			
		4	14.8	Yes			
		5	18.5	Yes			
		6	22.2	Yes			
0.692	case 2	1	3.7	Yes	1.3941	1.4688	0.9491
		2	7.4	No			
		3	11.1	Yes			
		4	14.8	Yes			
		5	18.5	Yes			
		6	22.2	Yes			
0.692	case 3	1	3.7	Yes	1.3814	1.4688	0.9405
		2	7.4	Yes			
		3	11.1	No			
		4	14.8	Yes			
		5	18.5	Yes			

		6	22.2	Yes			
0.692	case 4	1	3.7	Yes	1.363	1.4688	0.928
		2	7.4	Yes			
		3	11.1	Yes			
		4	14.8	No			
		5	18.5	Yes			
		6	22.2	Yes			
0.692	case 5	1	3.7	Yes	1.34463	1.4688	0.9155
		2	7.4	Yes			
		3	11.1	Yes			
		4	14.8	Yes			
		5	18.5	No			
		6	22.2	Yes			
0.692	case 6	1	3.7	Yes	1.3316	1.4688	0.9066
		2	7.4	Yes			
		3	11.1	Yes			
		4	14.8	Yes			
		5	18.5	Yes			
		6	22.2	No			
0.553	case1	1	3.7	No	1.4258	1.4688	0.9707
		2	7.4	No			
		3	11.1	Yes			
		4	14.8	Yes			
		5	18.5	Yes			
		6	22.2	Yes			
0.5533	case 2	1	3.7	Yes	1.4335	1.4688	0.976
		2	7.4	No			
		3	11.1	No			
		4	14.8	Yes			

		5	18.5	Yes			
		6	22.2	Yes			
0.553	case 3	1	3.7	Yes	1.4026	1.4688	0.955
		2	7.4	Yes			
		3	11.1	No			
		4	14.8	No			
		5	18.5	Yes			
		6	22.2	Yes			
0.553	case 4	1	3.7	Yes	1.3654	1.4688	0.9296
		2	7.4	Yes			
		3	11.1	Yes			
		4	14.8	No			
		5	18.5	No			
		6	22.2	Yes			
0.553	case 5	1	3.7	Yes	1.3329	1.4688	0.9075
		2	7.4	Yes			
		3	11.1	Yes			
		4	14.8	Yes			
		5	18.5	No			
		6	22.2	No			
0.553	case 6	1	3.7	Yes	1.3507	1.4688	0.9196
		2	7.4	Yes			
		3	11.1	Yes			
		4	14.8	No			
		5	18.5	Yes			
		6	22.2	No			
0.553	case 7	1	3.7	Yes	1.4121	1.4688	0.9614
		2	7.4	No			
		3	11.1	Yes			

		4	14.8	No			
		5	18.5	Yes			
		6	22.2	Yes			
0.553	case 8	1	3.7	No	1.4103	1.4688	0.9601
		2	7.4	Yes			
		3	11.1	No			
		4	14.8	Yes			
		5	18.5	Yes			
		6	22.2	Yes			
0.415	case 1	1	3.7	No	1.4641	1.4688	0.997
		2	7.4	No			
		3	11.1	No			
		4	14.8	Yes			
		5	18.5	Yes			
		6	22.2	Yes			
0.415	case 2	1	3.7	Yes	1.353	1.4688	0.9212
		2	7.4	Yes			
		3	11.1	Yes			
		4	14.8	No			
		5	18.5	No			
		6	22.2	No			
0.415	case 3	1	3.7	No	1.4102	1.4688	0.9601
		2	7.4	Yes			
		3	11.1	No			
		4	14.8	Yes			
		5	18.5	No			
		6	22.2	Yes			
0.415	case 4	1	3.7	Yes	1.3993	1.4688	0.9527
		2	7.4	No			

		3	11.1	Yes			
		4	14.8	No			
		5	18.5	Yes			
		6	22.2	No			
0.277	case1	1	3.7	No	1.483	1.4688	1.01
		2	7.4	No			
		3	11.1	No			
		4	14.8	No			
		5	18.5	Yes			
		6	22.2	Yes			
0.277	case2	1	3.7	Yes	1.454	1.4688	0.99
		2	7.4	No			
		3	11.1	No			
		4	14.8	No			
		5	18.5	No			
		6	22.2	Yes			
0.277	case3	1	3.7	Yes	1.391	1.4688	0.9473
		2	7.4	Yes			
		3	11.1	No			
		4	14.8	No			
		5	18.5	No			
		6	22.2	No			
0.139	case 1	1	3.7	Yes	1.44	1.4688	0.981
		2	7.4	Yes	1.418	1.4688	0.961
		3	11.1	Yes	1.431	1.4688	0.974
		4	14.8	Yes	1.45	1.4688	0.987
		5	18.5	Yes	1.469	1.4688	1
		6	22.2	Yes	1.482	1.4688	1.01

**Table (A. 2): Fundamental period, in X-direction, for Model type (1)**

<b>Fundamental period in X-direction</b>							
<b>% P</b>	<b>Cas e</b>	<b>Floor Numbe r</b>	<b>H (m)</b>	<b>Presenc e of struts</b>	<b>T<sub>x</sub> (sec)</b>	<b>T<sub>0</sub> (sec)</b>	<b>Normalize d value</b>
0.505	case 1	1	3.7	Yes	1.325	1.3955	0.95
		2	7.4	Yes			
		3	11.1	Yes			
		4	14.8	Yes			
		5	18.5	Yes			
		6	22.2	Yes			
0.421	case 1	1	3.7	No	1.343	1.3955	0.963
		2	7.4	Yes			
		3	11.1	Yes			
		4	14.8	Yes			
		5	18.5	Yes			
		6	22.2	Yes			
0.421	case 2	1	3.7	Yes	1.354	1.3955	0.97
		2	7.4	No			
		3	11.1	Yes			
		4	14.8	Yes			
		5	18.5	Yes			
		6	22.2	Yes			

0.421	case 3	1	3.7	Yes	1.347	1.3955	0.965
		2	7.4	Yes			
		3	11.1	No			
		4	14.8	Yes			
		5	18.5	Yes			
		6	22.2	Yes			
0.421	case 4	1	3.7	Yes	1.336	1.3955	0.958
		2	7.4	Yes			
		3	11.1	Yes			
		4	14.8	No			
		5	18.5	Yes			
		6	22.2	Yes			
0.421	case 5	1	3.7	Yes	1.325 6	1.3955	0.95
		2	7.4	Yes			
		3	11.1	Yes			
		4	14.8	Yes			
		5	18.5	No			
		6	22.2	Yes			
0.421	case 6	1	3.7	Yes	1.318	1.3955	0.945
		2	7.4	Yes			
		3	11.1	Yes			
		4	14.8	Yes			
		5	18.5	Yes			
		6	22.2	No			

0.337	case 1	1	3.7	No	1.373	1.3955	0.984
		2	7.4	No			
		3	11.1	Yes			
		4	14.8	Yes			
		5	18.5	Yes			
		6	22.2	Yes			
0.337	case 2	1	3.7	Yes	1.376	1.3955	0.986
		2	7.4	No			
		3	11.1	No			
		4	14.8	Yes			
		5	18.5	Yes			
		6	22.2	Yes			
0.337	case 3	1	3.7	Yes	1.358	1.3955	0.973
		2	7.4	Yes			
		3	11.1	No			
		4	14.8	No			
		5	18.5	Yes			
		6	22.2	Yes			
0.337	case 4	1	3.7	Yes	1.337	1.3955	0.958
		2	7.4	Yes			
		3	11.1	Yes			
		4	14.8	No			
		5	18.5	No			
		6	22.2	Yes			

0.337	case 5	1	3.7	Yes	1.318	1.3955	0.945
		2	7.4	Yes			
		3	11.1	Yes			
		4	14.8	Yes			
		5	18.5	No			
		6	22.2	No			
0.337	case 6	1	3.7	Yes	1.329	1.3955	0.952
		2	7.4	Yes			
		3	11.1	Yes			
		4	14.8	No			
		5	18.5	Yes			
		6	22.2	No			
0.337	case 7	1	3.7	Yes	1.364	1.3955	0.978
		2	7.4	No			
		3	11.1	Yes			
		4	14.8	No			
		5	18.5	Yes			
		6	22.2	Yes			
0.337	case 8	1	3.7	No	1.364	1.3955	0.978
		2	7.4	Yes			
		3	11.1	No			
		4	14.8	Yes			
		5	18.5	Yes			
		6	22.2	Yes			

0.252	case 1	1	3.7	No	1.394	1.3955	0.999
		2	7.4	No			
		3	11.1	No			
		4	14.8	Yes			
		5	18.5	Yes			
		6	22.2	Yes			
0.252	case 2	1	3.7	No	1.329	1.3955	0.952
		2	7.4	Yes			
		3	11.1	Yes			
		4	14.8	No			
		5	18.5	No			
		6	22.2	No			
0.252	case 3	1	3.7	No	1.364	1.3955	0.977
		2	7.4	Yes			
		3	11.1	No			
		4	14.8	Yes			
		5	18.5	No			
		6	22.2	Yes			
0.252	case 4	1	3.7	Yes	1.356	1.3955	0.972
		2	7.4	No			
		3	11.1	Yes			
		4	14.8	No			
		5	18.5	Yes			
		6	22.2	No			

0.168	case 1	1	3.7	No	1.404	1.3955	1.006
		2	7.4	No			
		3	11.1	No			
		4	14.8	No			
		5	18.5	Yes			
		6	22.2	Yes			
0.168	case 2	1	3.7	Yes	1.386	1.3955	0.993
		2	7.4	No			
		3	11.1	No			
		4	14.8	No			
		5	18.5	No			
		6	22.2	Yes			
0.168	case 3	1	3.7	Yes	1.35	1.3955	0.9675
		2	7.4	Yes			
		3	11.1	No			
		4	14.8	No			
		5	18.5	No			
		6	22.2	No			
0.168	case 4	1	3.7	No	1.364	1.3955	0.978
		2	7.4	No			
		3	11.1	Yes			
		4	14.8	Yes			
		5	18.5	No			
		6	22.2	No			

0.084	case 1	1	3.7	Yes	1.378	1.3955	0.9877
0.084	case 2	2	7.4	Yes	1.367	1.3955	0.98
0.084	case 3	3	11.1	Yes	1.374	1.3955	0.985
0.084	case 4	4	14.8	Yes	1.385	1.3955	0.993
0.084	case 5	5	18.5	Yes	1.395 9	1.3955	1
0.084	case 6	6	22.2	Yes	1.404	1.3955	1.006

Symbols and terms in Tables (A.1) and (A.2) are explained below:

- % P: The length percentage of partitions. It is computed based on Equation (A.1).

$$\%P = \frac{(Struts\ length) \times (Number\ of\ struts\ and\ ties\ in\ the\ case)}{(Wall\ perimeter) \times (Number\ of\ walls\ in\ the\ case)} \quad (0.1)$$

- H: floor height in (m).

- Presence of struts: It is indicating strut and tie existence in some floor. (Yes) means the struts and ties exist in the floor, (No) means no struts are in the floor.
- T: fundamental period of the structure in (sec), in the case mass and stiffness of the strut and tie are considered.
- T<sub>0</sub>: Fundamental period of the structure in (sec), when neither mass nor stiffness is considered.
- Normalized value = T / T<sub>0</sub>.

**Table (A. 3):** Fundamental period of the structure, in each X and Y-directions, for Model type (2)

<b>Fundamental period for two columns (C30 &amp; C45)</b>								
<b>Case</b>	<b>T<sub>y</sub> (sec)</b>	<b>T<sub>0y</sub> (sec)</b>	<b>Normalized value</b>	<b>% P<sub>y</sub></b>	<b>T<sub>0x</sub> (sec)</b>	<b>T<sub>x</sub> (sec)</b>	<b>Normalized value</b>	<b>% P<sub>x</sub></b>
1	1.3738	1.5745	0.8725	0.83	1.50786	1.3789	0.9145	0.505
2	1.4214	1.5745	0.9027	0.69	1.50786	1.4049	0.9317	0.421
3	1.4589	1.5745	0.9266	0.55	1.50786	1.4583	0.9671	0.336
4	1.4776	1.5745	0.9384	0.415	1.50786	1.4775	0.9799	0.252
5	1.5486	1.5745	0.9835	0.276	1.50786	1.4891	0.9876	0.168
6	1.5734	1.5745	0.9993	0.138	1.50786	1.5037	0.9973	0.084

**Table (A. 4):** Fundamental period of the structure, in each X and Y-directions, for Model type (3)

<b>Fundamental period for the three columns of Model type (3)</b>								
<b>Case</b>	<b>T<sub>0y</sub> (sec)</b>	<b>T<sub>y</sub></b>	<b>Normalized value</b>	<b>% P<sub>y</sub></b>	<b>T<sub>0x</sub> (sec)</b>	<b>T<sub>x</sub> (sec)</b>	<b>Normalized value</b>	<b>% P<sub>x</sub></b>
1	2.078	1.906	0.917	1.245	1.948	1.865	0.957	0.5052
2	2.078	1.908	0.919	1.121	1.948	1.867	0.959	0.455
3	2.078	1.947	0.937	0.996	1.948	1.869	0.959	0.4042
4	2.078	1.978	0.952	0.872	1.948	1.866	0.958	0.354
5	2.078	1.988	0.957	0.747	1.948	1.869	0.959	0.303
6	2.078	1.997	0.961	0.623	1.948	1.869	0.959	0.2526
7	2.078	1.983	0.954	0.498	1.948	1.895	0.973	0.202
8	2.078	1.98	0.953	0.374	1.948	1.918	0.985	0.1516
9	2.078	2.06	0.993	0.249	1.948	1.935	0.993	0.101
10	2.078	2.069	0.995	0.125	1.948	1.945	0.999	0.0505

**Table (A. 5):** Fundamental period of the structure in Y-direction for Model type (4).

<b>Case</b>	<b>T<sub>0y</sub> (sec)</b>	<b>T<sub>y</sub> (sec)</b>	<b>T (sec)</b>
1	1.4688	1.3433	1.527
2	1.5745	1.3738	1.6391

Where:

T<sub>0y</sub>: Fundamental period of Model type (4) in (sec) without partitions.

T<sub>y</sub>: Fundamental period of Model type (4) in (sec) with considering mass and stiffness of partitions.

T: Fundamental period of Model type (4) in (sec) with considering only mass of partitions.

جامعة النجاح الوطنية

كلية الدراسات العليا

تأثير الانماط المختلفة للتقطيعات الداخلية على الزمن  
الدوري لإطارات المباني الخرسانية المسلحة- دراسة  
مخبرية ونمذجة محدودة

اعداد

علا محسن قاروط

اشراف

د. منذر دويكات

د. محمود دويكات

قدمت هذه الأطروحة استكمالاً لمتطلبات الحصول على درجة الماجستير في هندسة الإنشاءات  
بكلية الدراسات العليا في جامعة النجاح الوطنية، نابلس - فلسطين.

2018

ب

تأثير الانماط المختلفة للتقطيعات الداخلية على الزمن الدوري لإطارات المباني الخرسانية

المسلحة- دراسة مخبرية ونمذجة محدودة

اعداد

علا محسن قاروط

اشراف

د. منذر دويكات

د. محمود دويكات

## الملخص

ان المباني الخرسانية المسلحة التي تتشكل من واجهات الطوب هي الاكثر شيوعا في فلسطين ,وقد يكون لهذه الواجهات اثر مهم على التصرف الزلزالي للمنشأ بسبب مساهمتها في صلابه و كتلة المنشأ ,هذان العاملان يشكلان اساسا لحساب الزمن الدوري الاساسي للمنشأ.

نظرا لأهمية هذا الموضوع , تم اقتراح العديد من النماذج من قبل مختلف الباحثين للتنبؤ بالتصرف الزلزالي لمباني الطوب, وايضا لدراسة اثرها على الزمن الدوري الاساسي للمبنى , لكن ما ينقص هذه البحوث انها لا تتلاءم مع خصائص مباني الطوب الفلسطينية .و لهذا السبب , يقدم هذا البحث دراسة حول التنبؤ بصلابه واجهات الطوب من خلال تحليل باستخدام طريقة العناصر المحدودة لنموذج غير خطي ثلاثي الابعاد. اضافه الى ذلك , تم الحصول على بعض المتغيرات اللازمة لعملية النمذجة من خلال اجراء بعض الفحوصات العملية اللازمة لعينات الطوب المستخدمة في فلسطين .

نتائج عملية تحليل واجهه الطوب تم استخدامها لتطوير نموذج استبدال واجهه الطوب بركائز تسهل عليه تحليل المباني. اضافه الى ذلك تم دراسة اثر التقطيعات الداخلية المتشكلة من الطوب على الزمن الدوري الاساسي للمبنى , من خلال القيام بتحليل اخر لاطار منشأ خرساني ثلاثي الابعاد , و دراسة اثر هذه الحالات المتعددة من الركائز على الزمن الدوري الاساسي للمنشأ .

تم تبسيط نتائج هذا البحث بمعادتين تتصف كل منهما بالبساطة وسهولة الاستخدام . احدى هاتين المعادلتين تتبأ بأبعاد الركيزة المستخدمة كبديل مناسب لواجهة الطوب , وتعتمد الركيزة بشكل اساسي على طول واجهه الطوب وابعاد الأعمدة المحيطة بها . والمعادلة الثانية تستخدم للتنبؤ بالزمن الدوري الاساسي للمنشأ الذي يتشكل من واجهات طوب , هذا الزمن الدوري يعتمد بشكل اساسي على كميته واجهات الطوب الموجودة في المنشأ .